

**NIST-GCR-98-742**

---

# **FIRE PROTECTION FOAM THERMAL PHYSICAL PROPERTIES**

---

A.M. Tafreshi, M. di Marzo,  
R. Floyd, and S. Wang

University of Maryland  
Department of Mechanical Engineering  
College Park, MD 20742



**United States Department of Commerce**  
**Technology Administration**  
National Institute of Standards and Technology

# **FIRE PROTECTION FOAM THERMAL PHYSICAL PROPERTIES**

---

**Prepared for**

U.S. Department of Commerce  
Building and Fire Research Laboratory  
National Institute of Standards and Technology  
Gaithersburg, MD 20899

**By**

A.M. Tafreshi, M. di Marzo,  
R. Floyd, and S. Wang

University of Maryland  
Department of Mechanical Engineering  
College Park, MD 20742

**Issued March 1998**



### Notice

This report was prepared for the Building and Fire Research Laboratory of the National Institute of Standards and Technology under grant number 60NANB6D0073. The statement and conclusions contained in this report are those of the authors and do not necessarily reflect the views of the National Institute of Standards and Technology or the Building and Fire Research Laboratory.

# **FIRE PROTECTION FOAM THERMAL PHYSICAL PROPERTIES**

A.M. Tafreshi, M. di Marzo, R. Floyd, S. Wang  
Department of Mechanical Engineering  
University of Maryland College Park, Maryland 20742

## FORWARD

This report describes the research performed during the period of June 1996 - July 1997 under a joint research program between the Mechanical Engineering Department of the University of Maryland at College Park and the Building and Fire Research Laboratory of the National Institute of Standards and Technology. The research was conducted in the laboratories of the BFRL by Mr. Robert Floyd and Ms. Shirley Wang, Graduate Research Assistants of the ME Department at the time, under the supervision of Drs. Marino di Marzo and Ali Tafreshi (ME Dept. - UMCP). This reports summaries result of the masters thesis of Mr. Floyd and Ms. Wang which were defended in 1997.

## EXECUTIVE SUMMARY

BACKGROUND	1
1. FOAM GENERATION	2
1.1 Design Considerations	2
1.2 Apparatus Design	3
1.3 Experimental Procedure	12
1.4 Foam Generation Consistency	16
2. FOAM STRUCTURE	25
2.1 Bubble Size and Distribution	25
3. FOAM PROPERTIES	28
3.1 Thermal Expansion	28
3.2 Radiation Absorption	32
3.3 Thermal Diffusivity	38
4. SUMMARY AND CONCLUSIONS	53
Appendix A Selected Photographs of Foam Used in the Analysis	55
Appendix B Radiation Absorption Data	64
Appendix C Thermal Diffusivity Data	69
Appendix D Fortran Programs	90
REFERENCES	99

## EXECUTIVE SUMMARY

This document contains the results of work performed to evaluate properties of foams used for fire exposure protection. The scope of this effort is to establish a testing procedure to evaluate the relevant properties of fire exposure protection foams. There are many different types of foams on the market. Most of the foams are used for fire suppression, but this study focusses on those intended to be used for fire exposure protection. Five foams were selected, all commercially available. Each comes in a concentrated liquid which is diluted in water and mixed with air to form a protective coating. Four of the foams chosen are synthetic hydrocarbon based. The fifth is a protein based foam manufactured from raw animal protein sources. All five foams are generated and tested in identical manners to observe their individual fire exposure protection characteristics. The four synthetic foams are identified as Foams A, B, C, and D and the protein based foam is identified as E.

This study has systematically addressed the evaluation of the parameters that effect the foam performance. The progression of these efforts is outlined hereafter.

- Design and construction of a lab sized foam generator
  - Operating parameters
  - Maintenance requirements
  - Effect of various parameters on the output foam
- Detailed study of the foam physical characteristics
  - Characterization of bubbles structure in the foam
  - Study of bubble structure dependence on the foam generating conditions
- Experimental Measurement of thermal properties of foam
  - Thermal expansion coefficient
  - Thermal diffusivity
  - Radiation absorption

A foam generating system has been designed and build, capable of generating up to 10 liters of foam solution. The foam generator is capable of generating foam with the expansion ratio ranging from 15 to 35 times its initial liquid volume. The expansion ratio is a measure of how much the foam solution has expanded by addition of air. The foam generated by this system is used for all the experiments. Various options have been considered on how to generate a consistent and continuous flow stream of foam. The best results are achieved by using a pressurized foam solution tank with low static head. The low static head is required to generate a relatively constant flow of foam solution. A coaxial mixing chamber has been used to mix the foam solution with air. This mixture consequently passes through a packed-bed bead mixing tube. Several variations on the mixing tube have been experimented with, but the packed-bed bead provides the best foam output.

The effect of fouling on the system performance has been investigated and it is recommended that the system be cleaned and maintained continuously such that repeatable foam can be generated.

Once a consistent and repeatable foam characteristics are obtained the physical structure of the foam is evaluated. Foam consists of small air bubbles separated by a thin layer of water. Photographs of the foam have been taken under a microscope. Foams contain bubbles of various sizes ranging from 300-1200 micron. Different foam generator operating parameters have been studied to determine their effect on the foam structure. It was found that same expansion ratio foams, generated at higher system pressure, had a larger amount of small bubbles than foams generated at a lower pressure. These observations have been made under constant temperature conditions. The variation of the bubble size and distribution in the foams as the temperature changes has not yet been characterized.

Thermal expansion of the foam has been studied. Foams with various expansion ratios have been placed in a convection oven and allowed to expand at constant pressure. The results indicate that high expansion ratio foams have a lower thermal expansion than low expansion ratio foams. Qualitative explanation for this phenomenon is that high expansion ratio foams contain bubbles with thinner walls than the lower expansion ratio foams. As the foam is heated, it is easier to burst these bubbles, hence the foam expands less because the gases escape from it.

Thermal diffusivity of the foam has been evaluated experimentally. This is accomplished by measuring the heat up transient thermal response of foam. The test apparatus is designed such that one dimensional heat transfer can be assumed. Temperature variations in the direction of the applied heat flux are measured in a large foam sample which approximates a semi-infinite solid. These data are used to solve a transient one dimensional heat transfer conduction equation with thermal diffusivity as a parameter. Relatively small temperature increase in the foam ( $\Delta T < 6^\circ\text{C}$ ) are considered. Larger temperature increase would cause a major change in the foam characterization. The data indicates a thermal diffusivity of  $5\text{E-}7 \text{ m}^2/\text{s}$  for all the foams.

A test apparatus has been built to measure the foam radiant extinction coefficient. This is accomplished by exposing foam samples to a radiative heat source and measuring the transmitted radiation by a total heat flux gage. The data from various thicknesses of foam is then used to calculate the extinction coefficient. From the analysis of the data a quantity has been termed Reflection and Scattering Coefficient (RSC) which represents the total energy that is not absorbed nor transmitted by the foam. The results of these measurements are summarized in the table 1.

In performing the thermal diffusivity and radiation absorption experiments a range of expansion ratios have been used. Additional insight into the foam behavior can be gained by considering the test matrices. Since not all the foams in the range of expansion ratios



exhibited sufficient structural properties to carry out the measurements. The test matrices are shown in tables 2 and 3. The numbers in each column indicates the number of tests performed for each expansion ratio.

Table 1 Summary of the radiation absorption experimental results

Foam Type	Absorptivity $\text{cm}^{-1}$	% RSC for test expansion ratios
Foam A	0.65	95-93
Foam B	0.65	90
Foam C	0.65	84
Foam D	0.65	79
Foam E	$0.5 \pm 0.2$	92-96

Table 2 Thermal Diffusivity Test Matrix

Thermal Diffusivity	XP = 15	XP = 20	XP = 25	XP = 30
Foam A	untestable	1	1	0
Foam B	untestable	2	2	0
Foam C	untestable	untestable	2	3
Foam D	untestable	untestable	2	1
Foam E	2	2	2	0

Table 3 Radiation Absorption Test Matrix

Radiation Absorption	XP=15	XP=20	XP=25	XP=30
Foam A	untestable	3	3	0
Foam B	untestable	2	2	0
Foam C	untestable	untestable	2	2
Foam D	untestable	untestable	2	2
Foam E	3	4	4	1

## BACKGROUND

Modern fire-protection techniques aim at guarding people and their property from destruction by fire. Large fires have been responsible for major loss of life and property in early 20th century U.S. [1]. Large industrial fires, large building fires, and large wildfires are the three most dangerous and destructive kinds of fire.

In 1911, a large industrial fire at the Triangle Shirtwaist Factory in New York City claimed 145 lives. Large industrial fires, especially in the oil-refinery and chemical industries, can be dangerously destructive and costly. A 1976 joint report prepared by the Philadelphia police and fire department and the Gulf Oil Company describes an August 1975 fire in Philadelphia that killed eight firefighters and caused damage estimated at \$13 million to the Gulf Oil Company-U.S. refinery [2].

Although lives are lost in fires at industrial and storage properties, the major loss of life results from fires in theaters, night clubs, schools, institutions, hotels, and similar properties. Large domestic fires in the early 20th century U.S. include those at the 1903 Rhoades Opera House in Boyertown, Pennsylvania, which claimed 170 lives; the Iroquois Theater in Chicago, which claimed 602 lives; and the Lakeview Grammar School in Collinwood, Ohio, which claimed 175 lives.

Forest vegetation when exposed to hot winds after a long dry spell is highly flammable and the resulting fires over large areas are difficult to suppress. Each year, thousands of acres of forest are lost to forest fire, which can race through vegetation at very high speed.

Fire-protection precautions can reduce the vulnerability of buildings and structure to heat and fire, and can ultimately save both lives and property. Since the first documented attempts in about 300 B.C. to control fire devastation in Rome, fire-protection regulations and fire-protection methods have been developed worldwide.

Different types of fire require different kinds of fire-protection technologies. Industrial and domestic fire protection has depended principally on sophisticated fire-detection and alarm systems, and on installation of fire-extinguishing equipment. Large supplies of water and foam are generally used to cool structures and to provide coating against the fire. Water, though it is the agent most commonly used to protect structures and to suppress fires, can also damage properties and structures. It has other disadvantages in fire protection, in that it can not affect petroleum or chemical fire, and that its effectiveness depends on the availability of large quantities of it. In large fires that involve volatile petroleum or chemical products in storage tanks, foam has proven effective for both fire protection and fire suppression.

Fire-protection foams are highly structured fluids with complex rheological behavior [3]. In physical appearance, fire-protection foam resembles shaving or whipped cream, as it consists of numerous small bubbles separated by thin layers of liquid. Like fire-suppression foam, fire-protection foam is a combination of air, a comparatively small amount of water, and foaming agent. Unlike the flowing fire-suppression foam, the fire-protection foam, after it is generated, usually does not flow (by design), has slow or no liquid drainage.

Fire-protection foams are normally used on structures in or near fire, where they can form a protective shield on such structures in situations like large forest fires, or spill fires due to volatile petroleum or chemical products, where other methods are not practicable. Buildings in wild land area are vulnerable to fast-spreading wildfire. In such situations, where supplies of water are usually scarce, coating the exterior of a structure with fire-protection foam may save it even in the path of the fire.

For industries that handle flammable material, fire protection foam is used to protect storage structures from nearby fire. For example, in case of fire in an oil refinery, a coating of fire-protection foam can keep adjacent storage tanks cool and prevent the fire from spreading. Fire-protection foam can serve as a temporary shield to block out heat from a fire. The process of making fire-protection foam uses air, a foaming agent, and a small amount of water. Because air is the major component of the fire-protection foam, which has low thermal conductivity, the foam is able to protect as insulation.

## **1. FOAM GENERATION**

### **Purpose of the Design**

Basic design requirements of the lab sized compressed air foam (CAF) generator is to supply controlled and reproducible foam for the experiments. Commercially available CAF equipment produces fire-protection foam on much larger scale: generation of foam in great quantity is not suitable for lab research, not only because of the amount of product that must be handled but also because the foam characteristics are hard to control and replicate. A lab-scale foam generator, on the other hand, provides freely made and manageable amounts of controlled and reproducible foam for each experiments.

### **1.1 Design Considerations**

To ensure proper handling of the foam, it is important to be aware of its basic physical nature (e.g. its storage stability). Identifying physical properties (e.g. appearance of the foam such as foam-bubble sizes) are needed to describe the foam after it is generated. Foam E concentrate is a two-phase colloidal solution consisting of solid protein particle dispersed in a liquid medium. Studies show that these protein particles are

surrounded by an electric charge to suspends and disperses them in the concentrate liquid [4]. When foam E concentrate is exposed to air, for example, the electric charge drops, precipitating the protein particles and shortening the concentrates's storage life. Foam E concentrate, shares the physical nature of other protein-based foam concentrate in that it deteriorates easily by forming visible and measurable proteinaceous precipitate. In addition, on the surface exposed to air and /or heat in a container, the protein based foam concentrate loses moisture and forms a hard crust quickly; it therefore requires special handling to maintain freshness. Foam E concentrate looks black and has a faint odor because of its protein base. The foam product itself appears white. The protein based 3% foam, which contains mostly air, is very light in weight.

Foam E can be identified by its expansion ratio and by the distribution of air-bubble size in the foam. Varying expansion ratios and air-bubble size distribution in foam E can be controlled by adjusting the foam solution and air value and the system air pressure. The expansion ratio is the ratio between the volume of foam produced, and the volume of the foam solution used in its production. The foam is generated by trapping air inside the foam solution and expanding the volume of the foam solution: hence, the term expansion ratio. Figure 1 is a schematic of the foam generator that produces the fire-protection foam by mechanically mixing air, water, and the foaming agent (the foam concentrate). Generation of expansion ratio with specific sizes and distributions of air bubbles in the foam is made possible by adjusting the Cv value and the air-system pressure. The overall

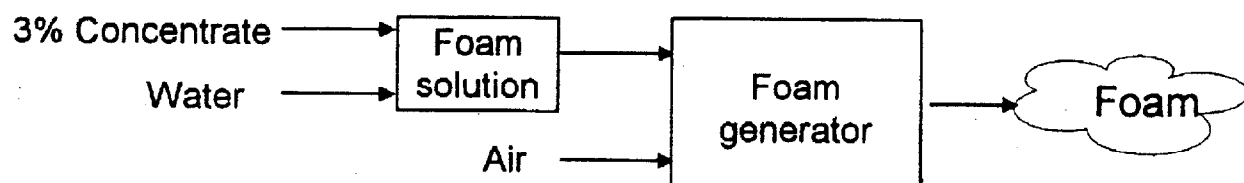


**Figure 1** Schematic of the Foam Generator

design requirement is to produce a stable amount of foam, with desired foam expansion and bubble sizes, by constructing a foam generator equipped with adjustable system air pressure and simple maintenance so that its generation of foam can be easily monitored.

## 1.2 Apparatus Design

Figure 2 shows the process of foam generation. The foam generator is a combination of ready-made and specially designed parts whose core elements are:

1. Solution reservoir
2. Air and liquid feed
3. Coaxial blending
4. Stationary packed-bed bead mixer
5. Foam delivery

The entire foam generator setup, built on a cart, allows the foam generator to be easily moved around and carried to different labs if needed.

### Solution Reservoir

Choosing a tank with a low-aspect-ratio geometry as the foam-solution reservoir that will contain the water/foam-concentrate solution serves to reduce the effect of variations in the liquid head on the feed-flow rate. Choice of the size and position of the solution reservoir depends on operational requirements, especially its ability to withstand any pressure needed to generate the foam. The size of the solution reservoir depends on the manufacturer-suggested foam-expansion ratio and the requirements of the lab experiment. Assuming the need to generate a foam with an expansion ratio of 10, and assuming also that the reservoir must be able to hold at least 10 liters of foam solution for

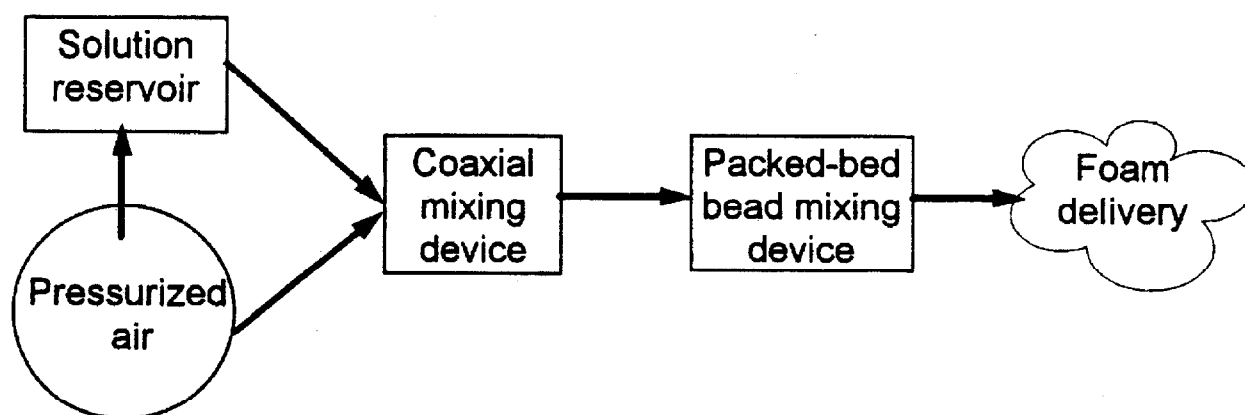


**Figure 2** Process of CAF Generation

a typical experiment needing 100 liters of foam; the maximum necessary size of the reservoir would correspond to the maximum amount of foam needed in the studies. The solution reservoir for this study is a pancake-shaped tank with storage capacity of 16 liters. Positioning the solution reservoir at the top of the other components; facilitates loading of the water/foam-concentrate solution and simplifies draining loading and flushing procedures between batches of foam generation. A clear PVC tube used as a sight tube permits observation of the amount of solution remaining in the tank. Figure 3 is a schematic of the solution reservoir.

## Air Feed

A standard high-pressure air bottle supplies air through flexible PVC tube to both the solution reservoir and the coaxial mixing device. Air supplied to the solution reservoir is the force pushing the solution out of the reservoir; air supplied to the coaxial mixing device mixes with the solution and is trapped within the foam bubbles. A needle valve on the air supply controls the Cv value in the mixing device.

## Coaxial Mixing Device

The coaxial mixing device, whose role is to combine the air and the foam solution, pushes the two streams in the same direction, with solution stream fed in the center and the air stream fed in a surrounding ring. Figure 4 is a coaxial schematic of the mixing.

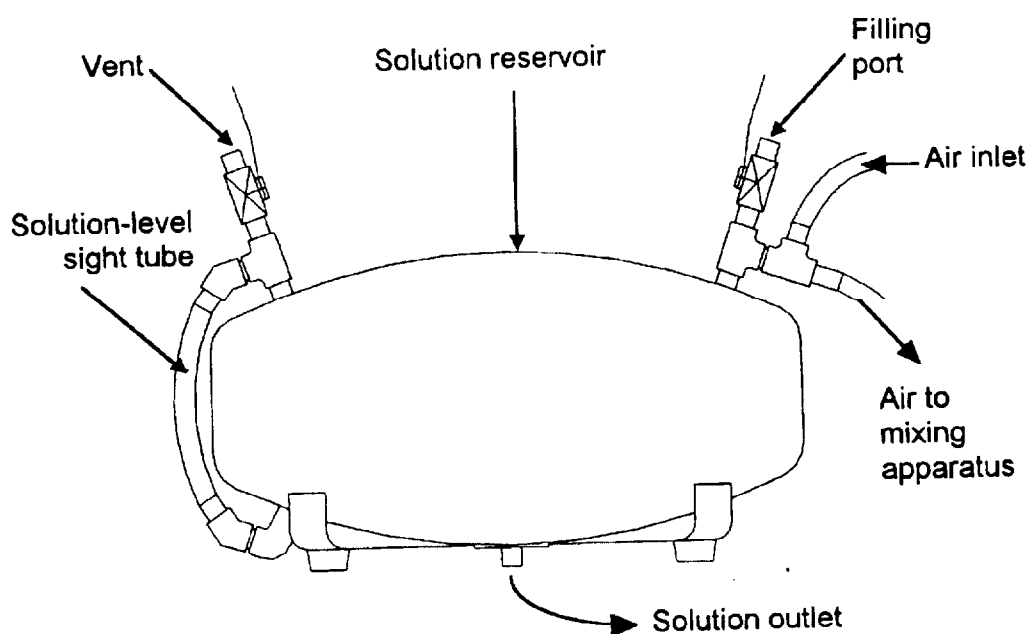


**Figure 3**      Solution Reservoir

Coaxial mixing has applications in various fields such as medical science and aeronautics [15,16]. Compared to other mixing arrangements, coaxial mixing generally provides a more steady mix of two streams [17,18]. The product of the original mixing arrangements, which used a simple T-shaped joint to combine the air stream and solution

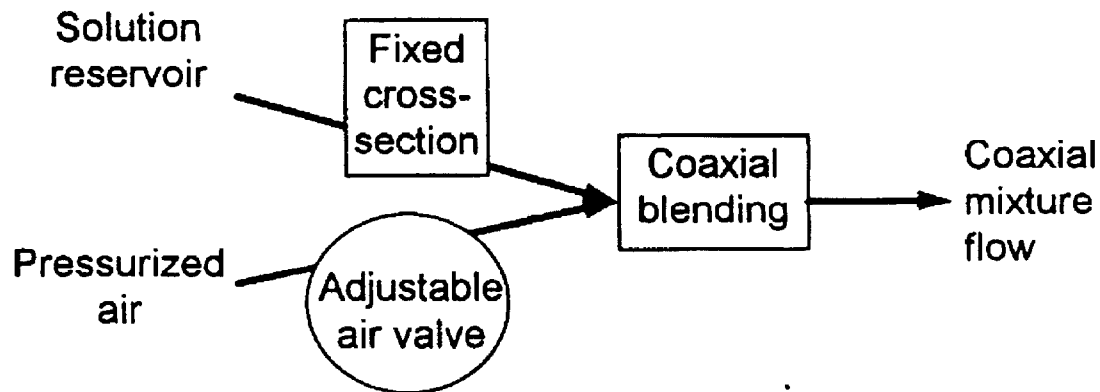


**Figure 4** Coaxial Schematic of the Mixing Arrangement

stream at a 90° angle, was not uniform because of the impact of the intermittent air flow on the foam-solution liquid, as shown in Figure 5. By use of a coaxial mixing arrangement, however, the air stream surrounds the solution stream, resulting in a more steady mix of the two streams. Locating the coaxial mixing device vertically serves to eliminate the effect of gravity, which would stratify the air/liquid flow. Figure 6 illustrates the process of coaxial mixing. The coaxial mixing device used in the foam generator consists of two blocks of

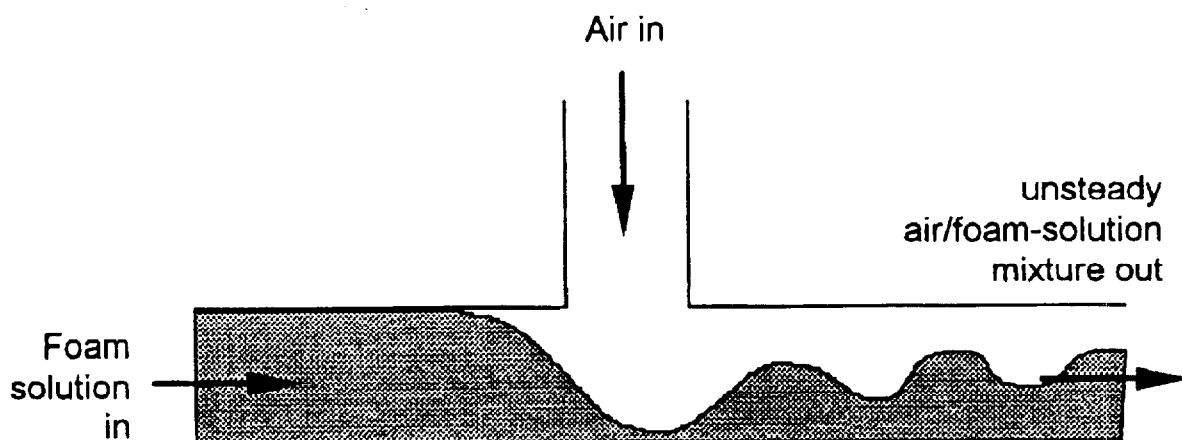


**Figure 5** T-Shaped Joint Mixing Arrangement Yields Unstable Mixture

aluminum, a plug connected to a small tube, a rubber o-ring, two inlet connectors, a mixture outlet connector, and four hex-head screws. The foam solution flows through the small tube, which has a 0.132 cm (0.052") inner tube diameter and is 7.62 cm (3") in length. The two aluminum blocks are screwed together with four hex-head screws, with the o-ring placed between the two blocks to prevent leakage. The mixture-outlet connector, positioned at the bottom block, serves to connect the coaxial mixing device with the packed-bed bead mixer.

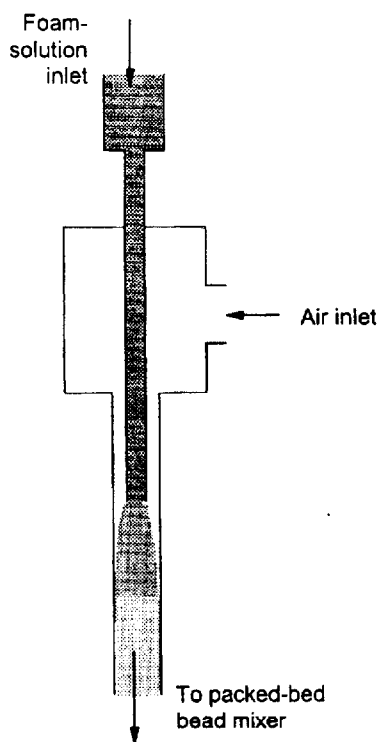


**Figure 6** Coaxial Mixing Process

### **Stationary Packed-Bed Bead-Mixing System**

The packed-bed bead mixer, a section of tube containing small spherical particles, constitutes the foam generator's stationary mixer. The packed-bed bead mixer provides a better mixing output than other static mixers that have the same mixing length and radius with twisting inserts. Early design stages used static mixing tube with twisted inserts as the mixer; unfortunately, a generator with static mixing tubes does not produce foam steadily, and the foam output is not easily controllable. The static mixing tubes are therefore replaced by the packed-bed bead mixer. Although the packed-bed mixer requires more air pressure than do the static mixers, it offers a shorter mixing length and a better foam supply, and is therefore preferable to the static mixer.



Additional experiments to demonstrate the best mixing arrangements might use varied orientations of the packed-bed bead mixer and varied effective tube length with different sizes of the beads (the spherical particles in the packed-bed bead mixer). Changing the orientation of the packed-bed bead mixer changes the mixing condition and the associated pressure consumption (pressure drop): to determine which orientation of the packed-bed bead mixer would produce an uniform and steady supply of foam, the mixer can be positioned at 20.32, 30.48, 45.72 and 60.96 cm (8", 12", 18" and 24" respectively); sizes of the glass beads examined are 3 mm and 6 mm (0.12" and 0.24"). Table 1 illustrates the effect of vary the packed-bed bead mixer arrangements.

Results of these various arrangements of the mixers show that, if the air-and-solution mixture must travel against gravity, the initial output foam is dryer (lighter), the output rate is slower, and the procedure requires high pressure (i.e. great pressure drop in the mixer) to generate the foam. In this arrangement it takes longer for the foam generator to pass the initial stage of slow accumulation of foam solution in the mixing tubes and to reach the final steady state. When the packed-bed bead mixer is placed horizontally, the heavier stream tends to accumulate at the lower part of the mixer tube; on the other hand, if the packed-bed bead mixer is positioned vertically downward (allowing the air and liquid mixture to be assisted by gravity), the foam generated is more uniform. As shown in Table 1, a 20.32 cm (8") vertical tube with 3 mm glass beads gives the most satisfactory results. Hence, the packed-bed bead mixer for the foam generator should be placed vertically downward.

Although the pressure drop is not a concern in this experiment, it is necessary to define it in order to estimate the minimum pressure needed to generate foam in a steady state manner. As Table 1 shows, generating the foam using different lengths mixers and different sizes of beads each time demonstrates that the packed-bed bead mixer with mm glass beads requires greater pressure to generate the foam than does the mixer of the same length using 6 mm glass beads. The test shows that a packed-bed mixer with mm glass beads, 5.1 cm (2") inner tube diameter, and 20.32 cm (8") tube length requires a pressure of a least 1.7 bar (10 psig) to produce a steady and uniform output of foam.

The foam-generating process shows that , the longer the mixer, the higher the pressure needed to push the air-and-solution mixture through the mixer; also, above the minimum pressure, the higher the pressure, the faster the output. Although pressure does not significantly affect the condition of the output mixture, high pressure is not desirable because the foam is output too rapidly and becomes uncontrollable. This is because the mixing tube requires only a fixed (minimum) amount of pressure for the mixing process. Excess pressure becomes the drive that increases the foam-output rate. Furthermore, because not all of the air goes into the foam, the excess air is accumulated and forms larger and pressurized air pockets. These air pockets have a higher pressure and tend to spit out of foam rapidly before the release of the air pockets. As a result, a higher foam-generating pressure produces higher pressure pockets and uncontrollable foam. The

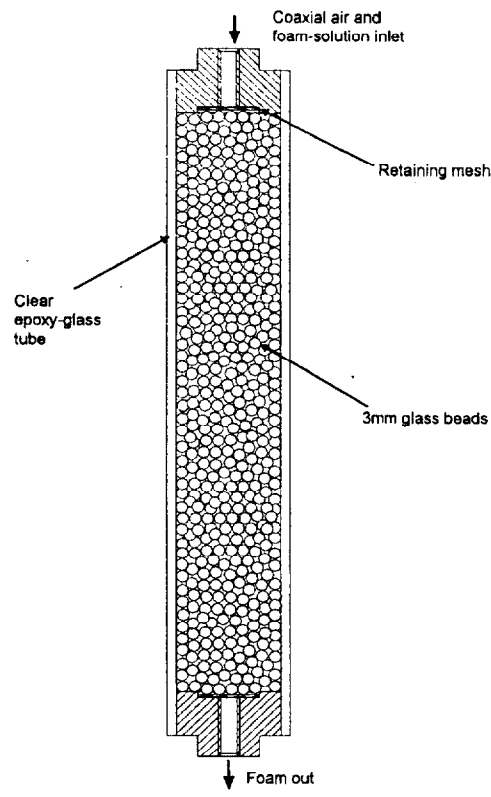
experiment shows that the Cv value control using an air pressure of 25 psig or above is ineffective and that the foam is harder to collect.

Table 1 Arrangement of Mixing Tubes

Tube Direction	No. of Tubes	Tube Length (cm)	Bead Sizes (mm)	Foam Output from a Single Mixer or a Combination of Mixers
Horizontal	1	30.48 (12")	6	The air-and-solution mixture appears to separate and the liquid settled at the bottom part of the mixer. The foam output has large air pockets and is mixed inadequately
Horizontal	2	45.72 (18")	6	The-air-solution mixture appears to separate and the liquid settled at the bottom part of the first mixer. The output mixture is more uniform than the output from the static mixer, but is still not satisfactory.
Vertical	2	60.96 (24")	6	With the Mixers connected side-by-side vertical in a U-shape, the foam solution appears to accumulate at the bottom of the U (the bottom outlet of the first mixer and the bottom inlet of the second mixer). This combination requires more air pressure to generate the foam, and the initial foam output appear dryer (lighter) and has a slower output rate than other foam outputs.
Vertical/ Horizontal	2	20.32 (8") 45.72 (18")	6	When the 8" vertical mixer is connected to an 18" horizontal mixer, the foam mixture is good but has many large air pockets.
Vertical/ Horizontal	2	20.32 (8") 30.48 (12")	6/3	When the 8" vertical mixer is connected to a 12" horizontal mixer, the foam is dryer (lighter) than other produces and requires much greater system air pressure.
Vertical	1	20.32 (8")	3	The output foam reaches steady state in a short time, and the foam mixture is fairly uniform. Small air pockets still exist in the output, but are evenly distributed.

The packed-bed bead mixer consists of several components, the principal ones being the mixing tube and the mixing beads, whose parameters (i.e., diameters and length of the mixing tube, size of the mixing beads) determine the uniformity of output and pressure drop in the mixer. Test show that the quality of the foam output from a shorter packed-bed bead mixer with 3 mm glass beads is similar to that of the foam output from a longer packed-bed bead mixer with 6 mm glass beads.

The water/foam-concentrate solution is dark brown in color, and the resulting foam is white. Therefore, to establish the optimum length of the mixer, the process (mixing the air with the foam solution to produce foam) can be easily observed through a clear plexy-glass tube used at the container of the mixer. Air and foam solution are rapidly mixed in the first three inches from the mixture inlet of a vertical 5.08 cm (2") inner-diameter tube with 0.3 cm (0.12") glass beads. From about three inches down, foam begins to form with large air pockets, the color of the mixture becoming lighter. Between three and six inches, the beads seem to break down the large air pockets to smaller size. From six inches down, the mixture (now mostly foam) turns white. Although a packed-bed bead mixer with 6 mm glass beads in a longer tube might produce a similar output mixture, the 20.32 cm (8") tube mixer with 3 mm glass beads is preferable because of its compactness. Figure 7 is a detailed schematic of the packed-bed bead mixer.



**Figure 7** Packed-Bed Bead Mixer

## Foam-Delivery System

The foam emerges from the packed-bed bead mixer through a 5-foot-long tube, which contributes to stabilize the foam output and to ease the delivery of the foam to various testing surfaces. Figure 8 is a schematic of the final setup of the foam generator.

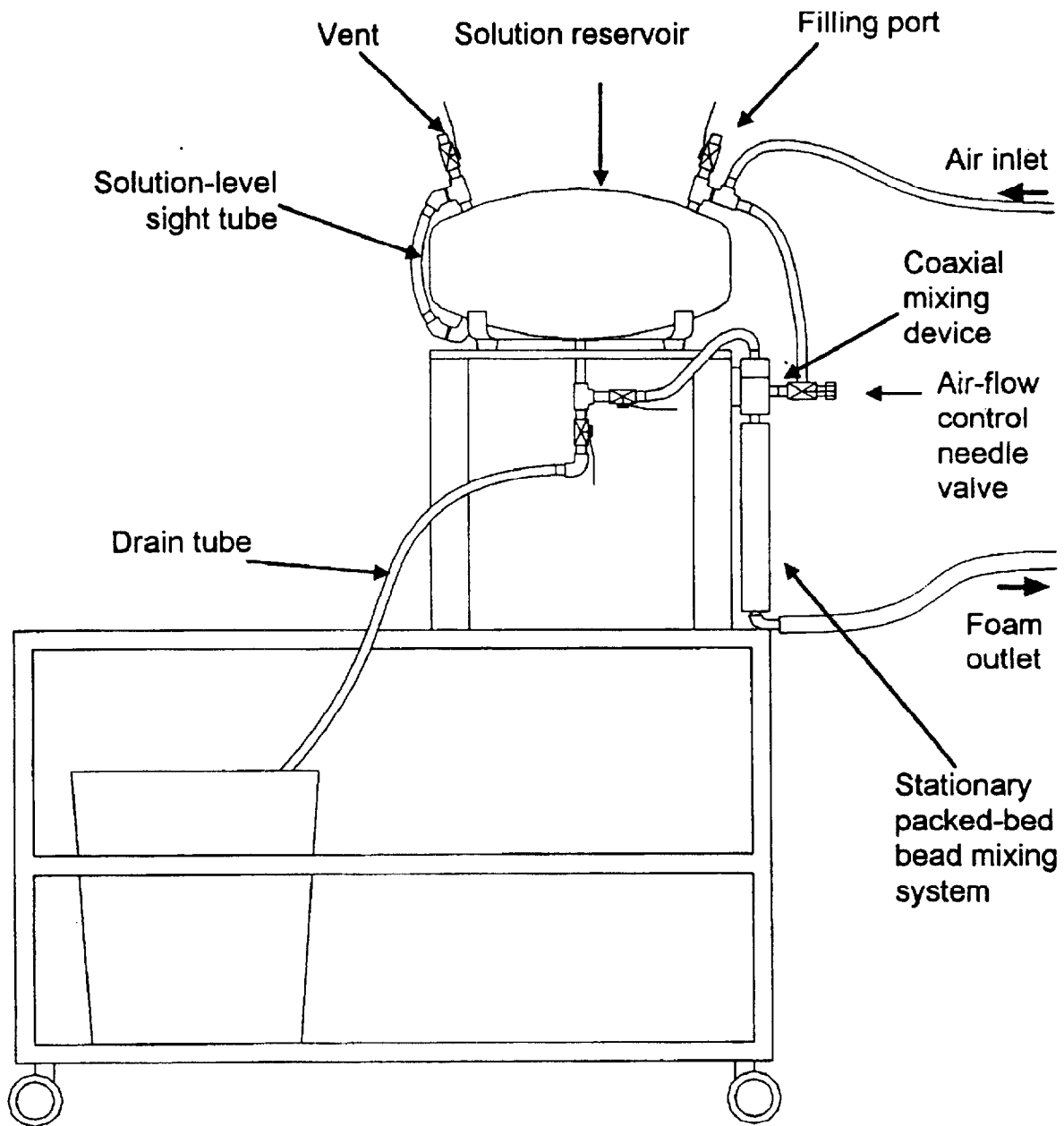


**Figure 8** Foam Generator

### **1.3 Experimental Procedures**

Experimental procedures established to ensure accountable and repeatable results are :

1. storage of the foam concentrate
2. maintenance of the foam generator
3. preparation of the foam solution
4. generation of the foam.

#### **Storage and Handling of the Concentrate**

As recommended by the manufacturer, the foam concentrate is stored in a room at constant temperature. Heavier particles in the foam concentrate slowly settle to the bottom of the container, and the concentrate forms a layer of dried crust where it comes in contact with air. It is therefore necessary to homogenize the foam concentrate, originally showed in a 20 liter container, by stirring it before opening its shipping container and transferring it immediately into smaller bottles (250 ml, 500 ml and 1000 ml containers) to minimize air contact and easier handling in the lab.

#### **Maintenance of Foam Generator Components**

At the end of each experiment, it is necessary to drain any remaining solution from the foam generator reservoir and immediately clear all foam generator components. The solution reservoir and the packed-bed bead mixer are two major components requiring thorough cleaning to ensure repeatable results. As any foam residue dries into a hard deposit, clogging the foam-solution passage, the foam generator must be thoroughly flushed with water and drained to eliminate any residue. Performance of the packed-bed bead mixer also depends on the cleanliness of the mixer. Cleaning the foam generator includes:

1. Removing of the packed-bed bead mixer from the foam generator.
2. Flushing and draining the foam-generator components.
3. Disassembling the packed-bed bead mixer.
4. Collecting and cleaning the mm glass beads.
5. Filtering the mm glass beads and reassembling the packed-bed bead mixer.
6. Reattaching the packed-bed bead mixer to the foam generator.

#### **Preparation of the 3% Foam Solution**

Equipment needed to prepare the foam solution include a 150 ml beaker, a stirring rod, a fine mesh filter, and a 4 liter plastic container. The fine-mesh filter serves to eliminate large lumps or chunks or dried particles, if any, from the foam concentrate. The

marked plastic container is used to measure desirable amounts of foam solution. The procedure for preparing four liters of the 3% foam solution is:

1. Measure 120 ml of foam concentrate into the beaker.
2. Measure 3 liters of water into the plastic container.
3. Pour the foam concentrate through the filter into the container.
4. While rinsing the beaker, fill the container with water to the 4-liter mark.
5. Stir the solution gently to avoid formation of bubbles. (Formation of bubbles will create crust that may clog the foam solution passage when generating the foam).

Three percent is the foam concentration recommended by the manufacturer. Preliminary test results show that foam made from slightly varying percentages of concentration do not differ significantly if the concentrate used in different trials are from the same batch of foam concentrate. For instance, foam resulting from 2% concentrate foam solution does not visibly differ from foams made from a 3% or 4% concentrate of the same content. However, when the concentration of the solution is above 5%, the output foam is wetter and heavier, and exhibits inadequate mixing. As the output foam is not significantly different using 2%, 3% or 4% concentration, and the manufacturer recommends the 3% concentration, all the experiments reported here use foam produced from 3% concentration for easy comparison of results.

### **Foam Generating Procedure**

The foam used in these experiments is generated from freshly made and well-mixed water/foam-concentrate solution. Use of the same consistency of water/foam-concentrate solution and the same operating settings means that foam generated at varying times and under varying conditions should exhibit repeatable characteristics. To generate foam with given parameters:

1. Close the drain valve and the liquid to coaxial mixing fixture valve.
2. Open the fill valve and pressure-relief valve on the solution reservoir.
3. Using a funnel with a fine mesh filter, pour the solution into the solution tank. The filter should prevent bubbles and sludge, if any, generated in the foam preparation process from getting into the tank.
4. Close the fill valve and the pressure-relief valve on the solution tank.
5. Open the air valve on the pressured air tank.
6. Regulate the air to a set pressure.
7. Adjust the needle air valve to a set opening to obtain desired air flow rate.
8. Open the liquid-to-coaxial-mixing-fixture valve.

The output foam should reach steady state (i.e., steady output with same foam quality) in about two minutes. Although the minimum pressure needed to generate foam is 1.7 bar

(10 psig), several trials have shown that the foam generator provides an optimal uniform output at a system pressure of 2.05 bar (15 psig).

### **Foam Output and Effects Produced by the Variables**

Because many variables can affect the consistency of the foam, it is necessary to identify these variables and their possible impact on the production of reliable foam. Some are design variables, others are operating parameters. Conclusion of the preliminary experiments allows setting of the design variable at fixed values. Table 2 summarizes the design variables and their treatments.

Among the variables, the system air pressure and the Cv value constitute two operating parameters that can produce foam with different output rates and consistencies. System air pressure directly affects the rate of foam output and the sizes and distribution of bubbles. The Cv value, up to 0.55, is linearly related to the foam-expansion ratio. Table 3 shows operating parameters and limits.

The following sections describe the rationale and the various experiments used to define selected values for design variables and operating parameters.

Table 2 Design Variables and Their Treatments in the Experiment

Variable	Treatment	Effect
Blending Method	Foam Solution mixes with air coaxially; fixture arranged vertically in the direction of gravity	Provides steady flow to the packed-bed bead mixer
Foam-solution concentration	3% of foam concentration with 97% of water	Prevents possible variations in foam caused by different concentrations of solution (also manufacturer's recommended percentage)
Foam-solution flow	Fixed cross section of 1.32 mm (0.052") in diameter	Eases the adjustment of valve flow coefficient Cv
Solution reservoir	15 liter (4 gallon), 12-gauge steel construction pancake tank with epoxy coating inside	Contains sufficient amount of foam solution for experiment; epoxy lining keeps tank rust from polluting the foam solution
stationary mixer	3 mm glass bead, 50.8 mm (2") diameter, 20.3 cm (8") in length packed-bed bead mixer, vertical orientation; flow travels in direction of gravity	Most effective combination of tube length and bead sizes in providing steady and satisfactory foam

Table 3 Operating Parameters and Limits

Operating Parameters	Limits
System air pressure	Maximum pressure to obtain foam: 2.56 bar (22.5 psig) Minimum pressure required to generate foam 1.7 bar (10 psig)
Valve flow coefficient, CV	Maximum Cv value to obtain usable foam : 0.08 Minimum Cv value to generate the foam : 0.011



## 1.4 Foam Generation Consistency

### Physical Characterization of the Foam

Foam quality is identified by its expansion ratio, and by the sizes of air bubbles and their distribution within the foam. Studies have shown that protein-type air foams are generated from aqueous liquid concentrates with proportioned water [7]. Foam concentrate is a hydrolysis of natural protein solids and natural proteinaceous polymers derived from a chemical digestion which has high molecular weight. The polymers give elasticity, water-retention capability, and mechanical strength to the foams generated from them. Such a protein-based foam concentrate also contains dissolved polyvalent metallic salts that contribute to the bubble-strengthening capability of the natural protein polymers when the foam is exposed to heat and flame. In this study, every 1000 ml of foam solution prepared consists of 30 ml of protein based 3% foam concentrate and 970 ml of water.

Foam expansion ratio,  $\epsilon$ , is the volume ratio of the foam to the solution.

$$\epsilon = \frac{V_{foam}}{V_{solution}}$$

As the solution consists mostly of water and its density is approximately equal to that of water, the volume of the solution can be found by:

$$V_{solution} = \frac{W_{solution}}{\rho_{solution}} \approx \frac{W_{solution}}{\rho_{water}}$$

The foam expansion ratio becomes

$$\epsilon = \rho_{water} \frac{V_{foam}}{W_{solution}}$$

The weight of the foam is the combined weight of the solution and air. However, as the weight of air in foam is negligible, the weight of the foam is actually equal to the weight of the solution,  $W_{foam} = W_{solution}$ . Hence the expansion-ratio equation evolves to

$$\epsilon = \rho_{water} \frac{V_{foam}}{W_{foam}}$$

Or alternatively, as the density of the water is 1 kg/liter, one obtains

$$\epsilon = \frac{1 \left[ \frac{\text{kg}}{\text{liter}} \right]}{\rho_{\text{foam}} \left[ \frac{\text{kg}}{\text{liter}} \right]}$$

The foam expansion ratio is calculated using the following steps:

1. Clean and dry a 1000 ml container.
2. Zero the scale with the empty container.
3. Fill the container with foam and weight it.
4. Invert the weight (in kg) to obtain the foam expansion ratio.

In this study the usable range of the foam expansion ratios generated is from 10 to 35. Foams with expansion ratios lower than 10 are too watery, and foams with expansion ratios higher than 35 are too dry. Neither watery foam nor over-dried foam is suitable for experiments, because watery foam tends to accumulate foam solution at the lower portion of the foam, causing the foam to run off the test surface, and over-dried foam tends to flake off the test surface.

### Process Variable

In order to have accountable and repeatable measurements, the physical characteristics of the foam ( that is, the foam-expansion ratio) must be consistent. The foam-production process reaches steady state after 2 minutes of continuous flow. Steady-state status is defined as the output foam expansion ratios within a fluctuation range of  $\pm 5\%$  about the average. Figure 9 shows results of a typical foam generator calibration test performed to assess the consistency of a foam expansion ratio of 13.6. When the foam solution tank is nearly empty, the expansion ratio of the foam decreases dramatically, as shown in Figure 9. Fortunately, this occurs when there is only half-liter of foam solution left in the tank.

The foam-bubble size variation is observed to decrease as the valve flow coefficient (Cv) increases, at the same foam generating system pressure as discussed before. Figure 10, shows the trend for operating system pressure of 15 psig. Although the pattern of decreasing bubble size variation with increasing Cv is common to all operating system pressures, the maximum bubble size is affected by the operating system pressure: the higher the operating system pressure the smaller the bubble size variation. In general, foam generated at lower operating pressure exhibits larger variation in bubble sizes and foam generated at higher operating pressure exhibits more uniform bubble sizes. Figure 10 shows the average bubble diameter for a range of expansion ratios. Selected

photographs of actual foam used in the experiments are included in Appendix A.

### **Effect of the Valve-Flow Coefficient**

Changing the valve-flow coefficient,  $C_v$ , directly affects the output-foams's expansion ratio and , consequently, the average foam-bubble sizes. With fixed cross-section of the foam-solution flow, the  $C_v$  value is controlled by adjusting the openings of the airflow-control needled valve attached at the air inlet of the coaxial blending fixture. The  $C_v$  value is controlled simply by adjusting the airflow-control needle valve, thus provides an adjustment in the air-to solution cross-section ratio. Figure 11 shows that each air-valve opening corresponds to a valve-flow coefficient  $C_v$  [9]. Figure 12 shows the valve flow coefficient,  $C_v$ , versus the  $C_v$  valve at various system air pressures.

The foam expansion ratio is linearly related to  $C_v$  up to 0.055, for  $C_v$  greater than 0.055, the amount of air that can be trapped within the foam reaches maximum, and the foam-expansion ratio thus remains mostly constant. Untrapped air escapes in the form of large air pockets in the foam. The linear relationship does not appear in system air pressure at or lower than 1.84 bar (12 psig). Without a linear relationship between the  $C_v$  and the foam-expansion ratio, adjustment of the foam-expansion ratio is difficult. A system air pressure at, or lower than 1.88 bar (12.5 psig) produces foam at lower output rate (as shown in Figure 13) with wider bubble-size range (i.e. watery foam with inadequate mixing). Therefore, even though the minimum system air pressure required to generate the foam is 1.7 bar (10 psig), a system air pressure at or lower than 1.88 bar (12.5 psig) is not suitable for the controlled experiments.

Smaller  $C_v$  value (i.e., smaller airflow rate) produces foam with slower output rate, as shown in Figure 13, because the foam solution travels more slowly through the packed-bed bead mixer than does the air; at the same system pressure, more foam-solution must travel through the packed-bed bead mixer at smaller  $C_v$  value than at a larger  $C_v$  value.

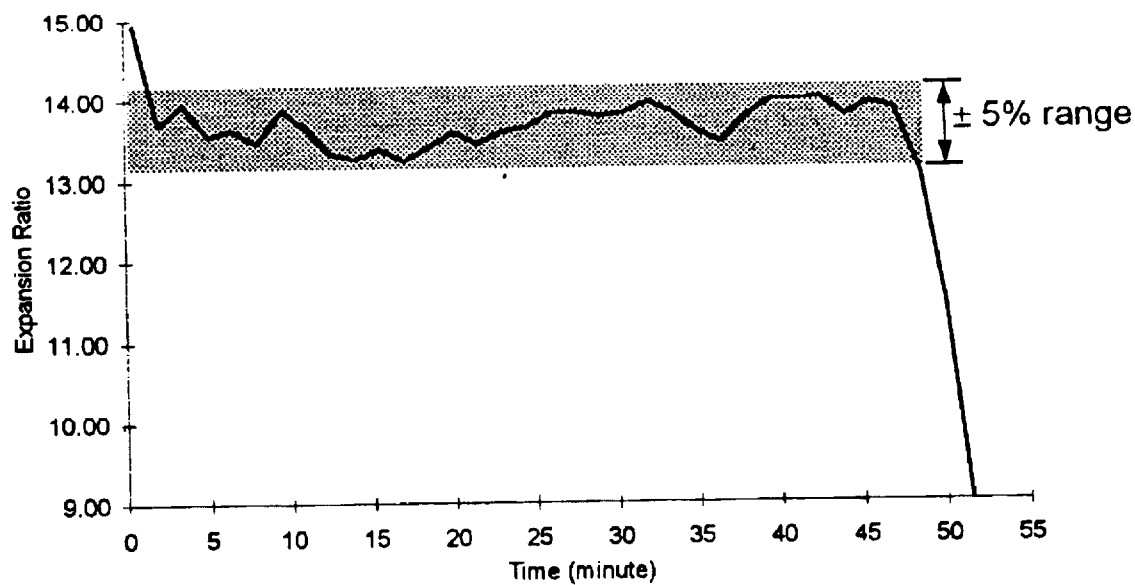


**Figure 9** Typical Foam Generator Calibration Test on Foam Expansion Consistency

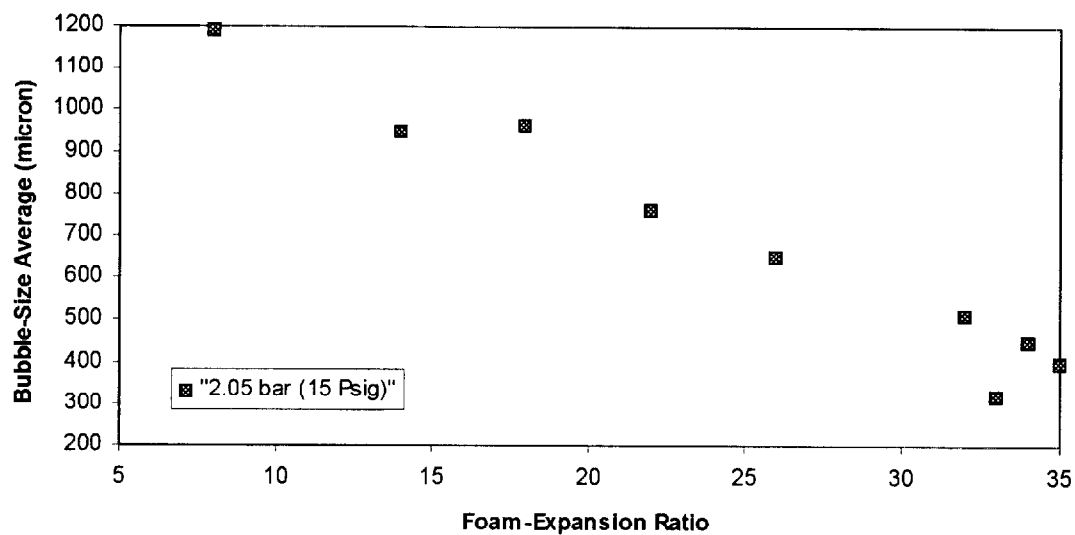


**Figure 10** Bubble Size Ranges at Different Expansion Ratios

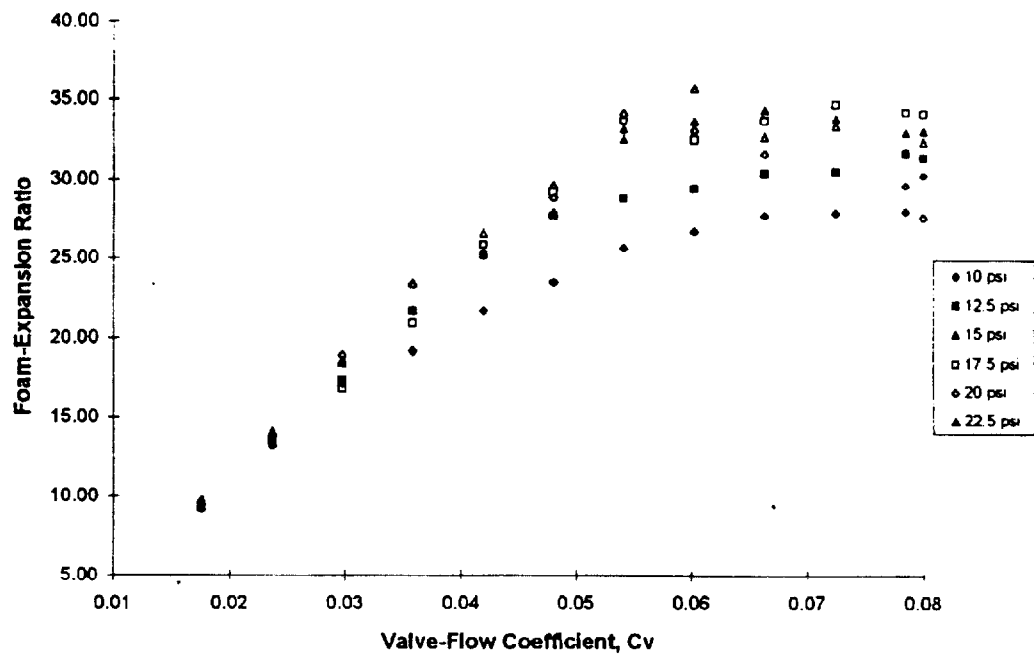


**Figure 11** Foam-Expansion Ratio and  $C_v$

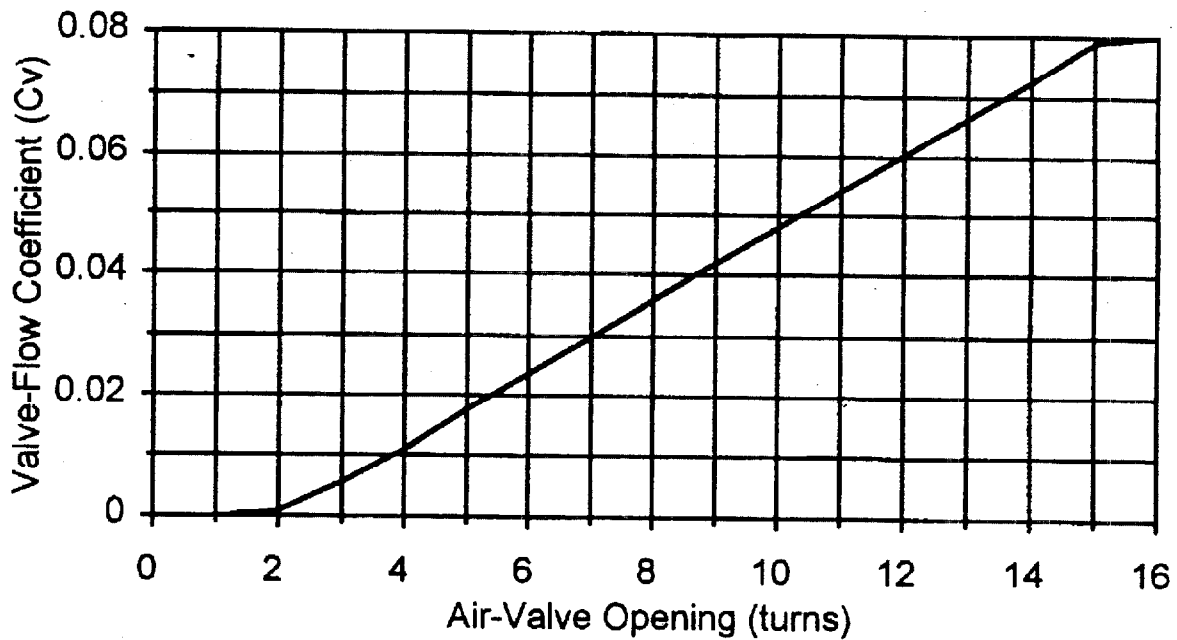


**Figure 12** Air-Valve Opening and the Correspondent Valve-Flow Coefficient  $C_v$

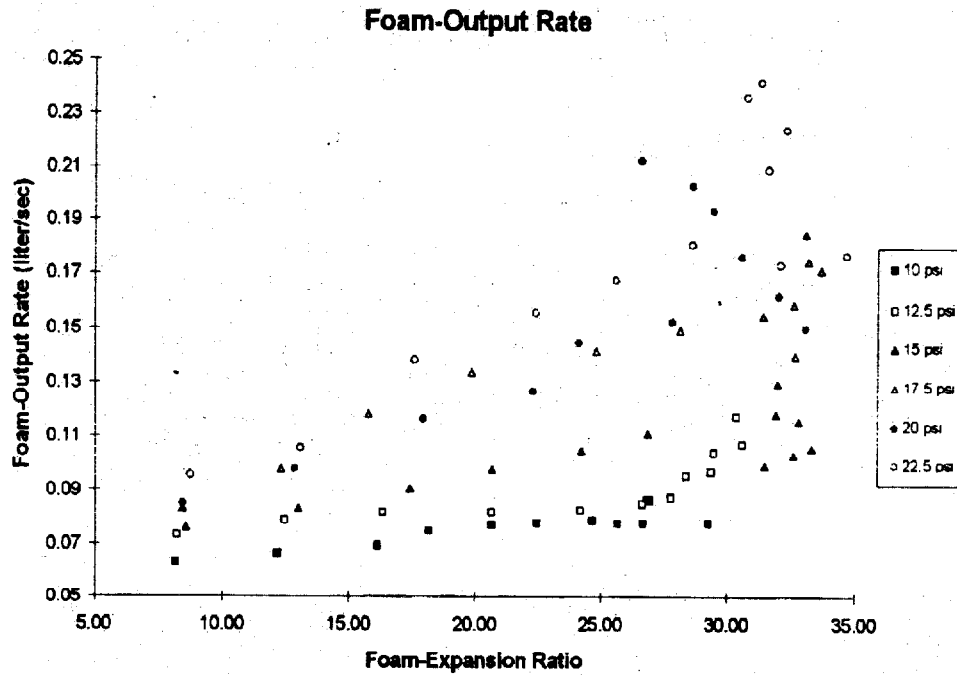


**Figure 13** Foam-Output Rate at Varying System Air Pressure

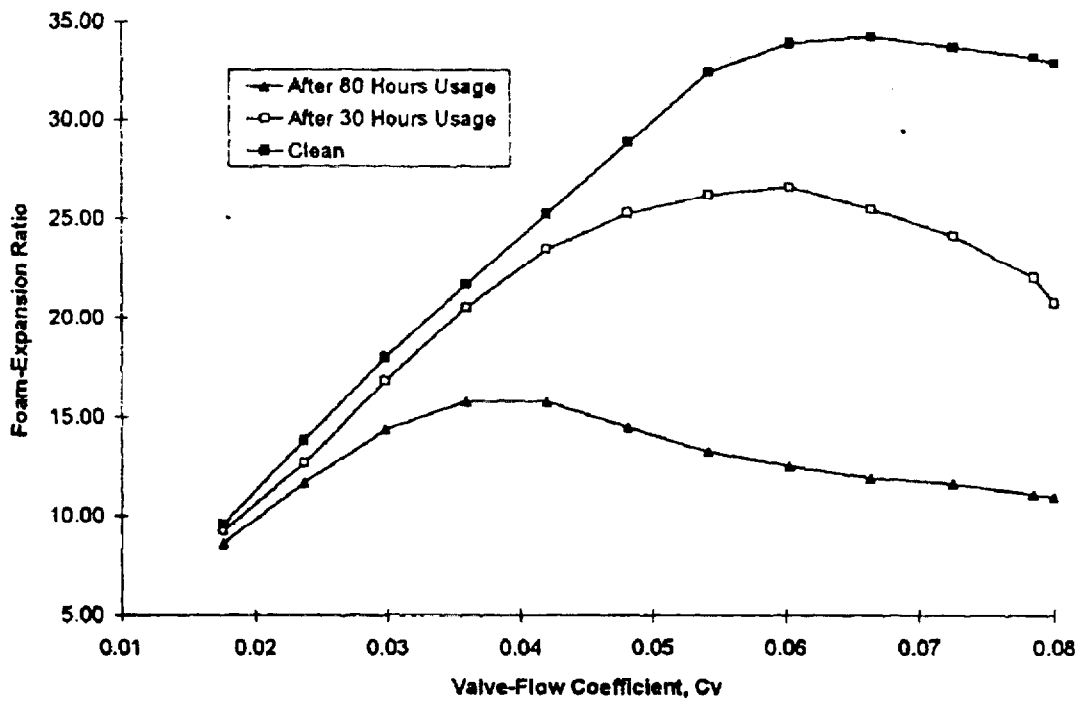


**Figure 14** Effect of Fouling on the Linearity Range of  $C_v$  Value and Foam Expansion Ratio

## Packed-Bed Bead-Mixing Tube Maintenance

Fouling of the packed-bed bead mixer dramatically affects the quality of the output foam and the maximum foam expansion. Figure 14 shows that, as the packed-bed bead mixer gets dirtier, the linear range of the foam-expansion ratio and  $C_v$  is reduced, and the maximum foam-expansion ratio achieved is lower. This results from the presence of hardened residuals of the foam solution remaining in the tube after the experiment, blocking passage within the packed-bed mixer, thereby changing the quality of the output foam. Foam produced from a fouled packed-bed bead mixer is not desirable for the experiments, being un-reproducible even though the foam produced with fouled mixing tubes exhibit smaller and more uniformly distributed bubble sizes. A fouled packed-bed bead mixer produces foam with lower expansion ratios. As shown in Figure 14 at typical system air pressure of 15 psig, at the maximum  $C_v$  values, the expansion ratio declines from 34 to 25 and 16 as the packed-bed bead mixer becomes dirtier with time. The grit-filled packed-bed bead mixing tube with fouled mixing beads produces a foam with lower expansion ratio. Fouling of the packed-bed bead mixer also affects foam bubble sizes and uniformity. A grit-filled packed-bed bead mixing tube with stained mixing beads produces

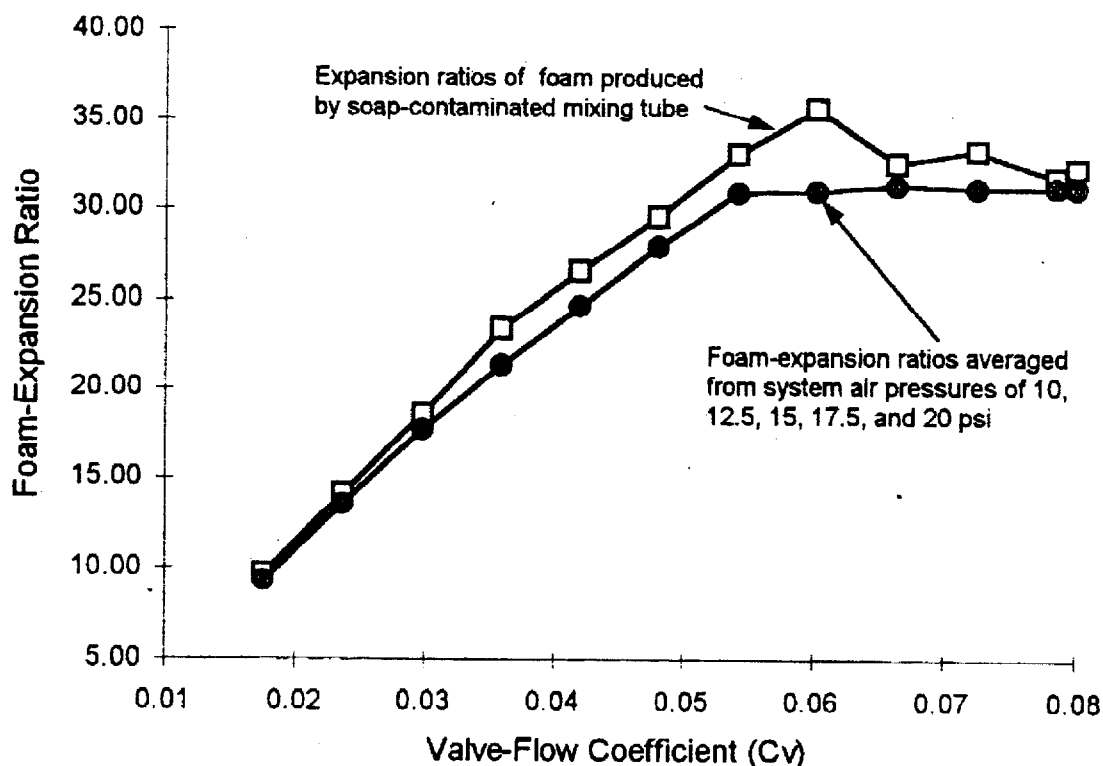


**Figure 15** Effect of Soap Contamination on Mixing Tube

foam with smaller and more uniformly distributed bubble size, apparently because the passage within the packed-bed bead mixer is further narrowed and the air and foam solution is broken down more than if it had traveled through a clean packed-bed bead

mixer. The foam generator with a fouled packed-bed bead mixer also requires a higher minimum system air pressure to generate the foam.

Different from the grit filled fouling, residue of cleaning solution in the packed-bed bead mixing tube will produce foam with much higher expansion ratio than the average. If the glass-cleaning solution is not completely rinsed off during the cleaning process, foam produced tends to have an expansion ratio higher than predicted. Figure 15 compares the expansion ratios of foam produced with soap contaminated packed-bed bead mixing tube and the average expansion ratios of foam produced with clean mixing tubes. Because of its out of ordinary creation, and with no means of repeating its production in the future, such unusually high-expansion foam is not desired for any experiment.

### **Foam-Solution Consistency**

The 3% foam E concentrate contains heavier particles that precipitate to the bottom of the container, as mentioned in section 2.2. Therefore, older foam concentrate (i.e, concentrate exposed to air for a longer period) tends to develop clumps of soft particles that do not dissolve easily in water. Like the foam generated from a fouled packed-bed bead mixer, which offers no guarantee of repeat production in the future, the foam resulting from uneven consistency in the foam solution is likewise not desired for any experiment. To maintain repeatability, the foam solution for each experiment must be made from fresh and well-stirred foam concentrate and must have an even consistency. The foam solution must be well mixed with water and used quickly to avoid settling of the heavier ingredient in the solution, which results in an inconsistent foam expansion. In this study, the foam solution is filtered twice through a mesh of 1 mm<sup>2</sup> to remove any large clumps of protein particles. Any uneven consistency of the foam solution also contributes to the fouling of the foam generator; any sudden change of the foam expansion ratio usually means that a narrow passage has been fouled up by heavier particles. If not stirred, the foam concentrate at the bottom of its manufacturing container looks thicker from the settling of heavier ingredients, and the foam concentrate flows sluggishly. Foam solution made from thicker and older foam concentrate produces foam with expansion ratios lower than predicted; as nothing can assure repeatability in the future, such foam is not desired for any experiment.

### **Effect of Contamination in the Air-Valve**

The solution flow path has a fixed cross-sectional area; hence, the only variable in Cv value is the air-flow valve, and the maintenance of their valve thus becomes important. An air valve contaminated by the foam solution will produce foam with unpredictable expansion ratios and bubble sizes. The foam generated in this manner is undesirable because its characteristics are unpredictable and not repeatable.



Furthermore, contamination of the air valve means a reduction in the cross-section of the air feed; although such a reduction may not be significant when the passage is large (i.e. at larger Cv value). When their passage is small (for generating the lower expansion foam with smaller Cv value) the contamination allows less air through the air valve, reducing the Cv value and producing foam with lower expansion than predicted. A contaminated air valve will also generate foam with fluctuation greater than  $\pm 5\%$  in the expansion ratio; foam with high fluctuation in its expansion ratio is not desirable for the experiments. Table 4 summarizes the causes of air -valve and mixing-tube contamination.

Table 4 Summary of Component Contamination

Component	Cause	Effect
Mixing tube	Grit-filled with hardened lump	Produces foam with uncontrollable low expansion ratio; linear operating range is shortened
Mixing tube	Soap residue	Produces foam with unusual and uncontrollable high expansion ratio
Air valve	Reservoir overfilled	High fluctuation of foam-expansion ratios
Air valve	Back pressure of the mixing tube	High fluctuation of foam expansion ratios

### Summary of Component Contamination

When the foam solution reservoir is overfilled, excess foam solution will contaminate the air valve, because system air is supplied to both the solution reservoir and the air valve through a T-joint, as shown in Figure 8. When the system air is turned off (while filling the foam solution to the reservoir) and if the solution reservoir is overfilled, excess foam solution will flow out to the T-joint traveling down to and contaminating the air valve. At the end of the foam-generation process, if the pressure-relief valve on top of the solution reservoir is opened too early, pressure in the packed-bed bead mixer will force the foam solution remaining in it to travel backward through the coaxial blending fixture and to contaminate the air valve.

## 2. FOAM STRUCTURE

### 2.1 Bubble Size and Distribution

Foams with the same expansion ratio may have different bubble sizes and distribution: foam generally contains small bubbles with some larger air pockets, their sizes ranging from a visible diameter of 300 micron to a diameter (virtually invisible to the naked eye ) of 2 micrometers. The weight of most foam produced in this research is carefully measured and foam bubbles sizes and distribution are captured in a close up photograph. The square area surrounded by lines is 1 cm<sup>2</sup>.

Despite the fact that a higher expansion-ratio foam traps more air, the biggest bubbles in a foam with a lower expansion ratio are generally larger, and the foam with a larger expansion ratio exhibits smaller maximum size bubbles. A wide range of bubble sizes is observed in the lower foam expansion ratio; also, a lower expansion ratio foam is more watery (i.e. exhibits inadequate mixing) than a foam with higher expansion ratios. These phenomena are common at all system air pressures. Figure 16 shows bubble-size ranges versus foam expansion ratios at two system air pressures. Selected photographs are included in Appendix A.

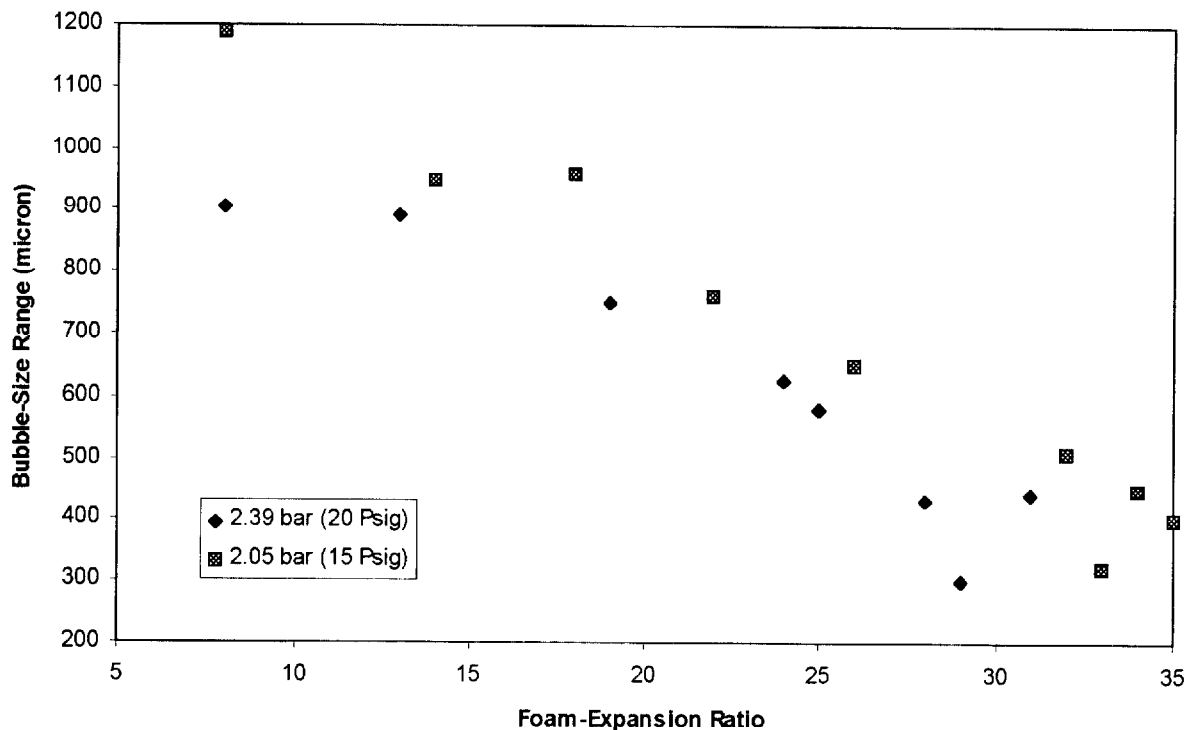


**Figure 16** Bubble Size Ranges at Different System Pressures

Supplying pressurized air with adjustable pressure to the foam generator has two purposes: to provide the air in the foam, and to apply pressure to the solution. System air pressure directly affects the output rate of the foam and its bubble sizes and distribution. System air pressure has no effect on the foam-expansion ratio: at different system air pressures, all the foam generated have the same trend of foam expansion ratio. The foam expansion ratio has linear dependency to the  $C_v$  value.

System air pressure greatly affects foam bubble size and distribution. Two different foam may have the same foam expansion ratio (i.e. The two foams hold an equal volume of air and foam solution), but the size of the bubbles and their distribution can be very different depending on the system air pressure. At higher system pressures the air bubbles are smaller and more uniformly distributed. Furthermore, at the same expansion ratio, the foam with smaller bubbles appear whiter, drier and more dense than the foam with larger bubbles. Figure 17 and 18 show two foam samples at same foam expansion ratio generated by different system pressure, which illustrates the characteristic previously described.

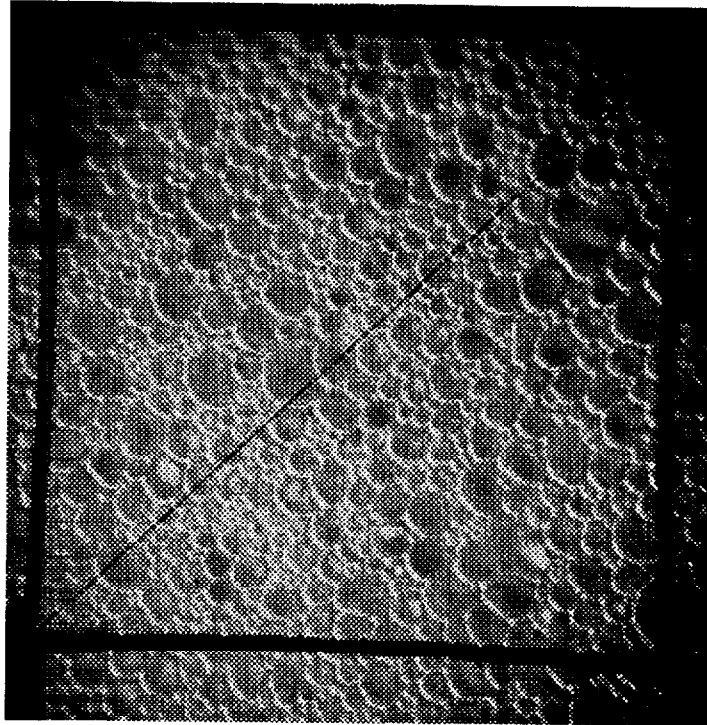


**Figure 17** Foam generated at 15 Psig, Expansion Ratio of 14

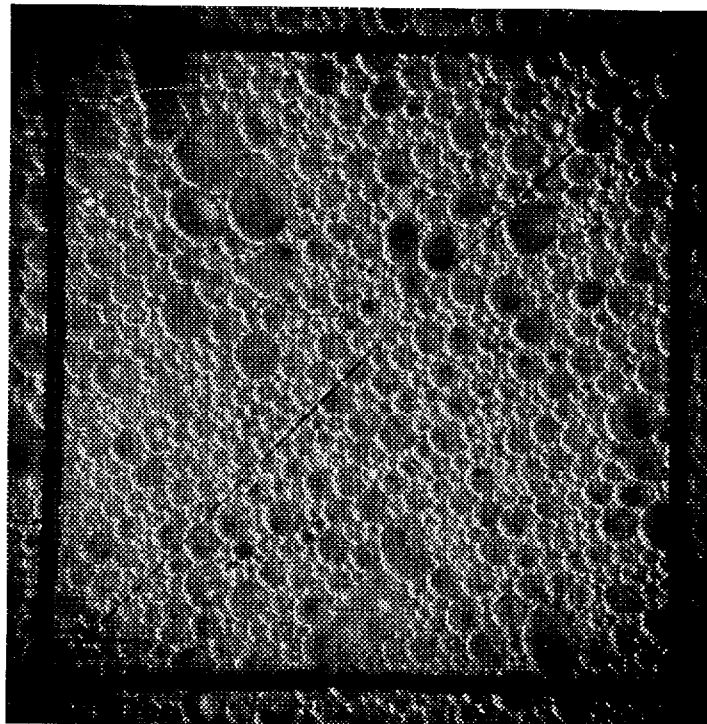


**Figure 18** Foam generated at 20 Psig, Expansion Ratio of 14

### 3. FOAM PROPERTIES

#### Purpose of the Experiment

The purpose of these experiments is to measure the thermophysical properties of protein based 3% foam, a fire protection foam. Knowing the thermophysical properties of this fire protection foam will help understand its characteristics and performance in fire protection. Thermophysical properties of protein based foam measured in these experiments are specific heat, thermal diffusivity, thermal expansion and density. In addition, the thermal conductivity of the foam is derived from these properties. The dependence of the thermophysical properties on the foam expansion ratio is demonstrated by experiments carried out in a small temperature range.

#### 3.1 Thermal Expansion

Like most objects, the foam under study expands in a heated environment. When the mass of the foam is preserved, the density change of the foam is proportional to its volume change. The volume change of the foam includes the change in the volume of air and the solution.

Thermal expansion is the amount by which density changes in response to a change in temperature at a constant pressure [8]. The volumetric thermal expansion coefficient is defined as

$$\beta = -\frac{1}{\rho} \left( \frac{\partial \rho}{\partial T} \right)_p$$

where  $\rho$ ,  $T$ , and  $P$  denote the foam density, temperature and pressure respectively. The foam density is inversely proportional to the foam expansion ratio as described previously. Because the weight of the foam is close to the weight of the solution, for 1 liter of solution weighting approximately 1 [kg], the foam density is simply the inverse of the foam expansion ratio,  $e$ .

Three foam expansion ratios 14, 20 and 27 chosen represent lower, medium, and high foam expansion serve in a test conducted in a convection oven with the foam in scale-marked test tubes. The amount by which the foam expands (i.e. density change with respect to time and temperature ) is recorded.

#### Experimental Setup

The experimental setup consists of three parts: heat source, test tube arrangement and data recording.

The heat source used in the experiment is a well-circulated convection oven preheated for the test to a desired temperature. Testing temperatures range from 20 °C (room temperature) to 90 °C (a temperature lower than the boiling point of the water).

Test tubes arranged vertically are spaced apart to ensure no interference from an adjoining test tube. Each test tube has two sections, both made of thin clear glass and open on two ends. Figure 19 shows the upper section as slightly larger than the lower section, allowing the foam to expand freely upward when heated. A plug with a pressure release plastic pin on top of the upper section preserves the moisture and minimizes pressure buildup within the test tube. The upper section of the test tube is marked alongside the tube for measurements purposes. The bottom of the lower section is sealed after the foam is inserted in the lower section. The lower section has a cross sectional area of 1.911 cm<sup>2</sup> and volume of 34.7 ml. Thermal expansion of the foam is recorded at the predetermined temperature and time. Each test uses two test tube sets and the final reading is an average of the results.

### Experimental Procedure

The thermal expansion experiment includes three procedure: preparation of the experiment, conduct of the experiment and data processing.

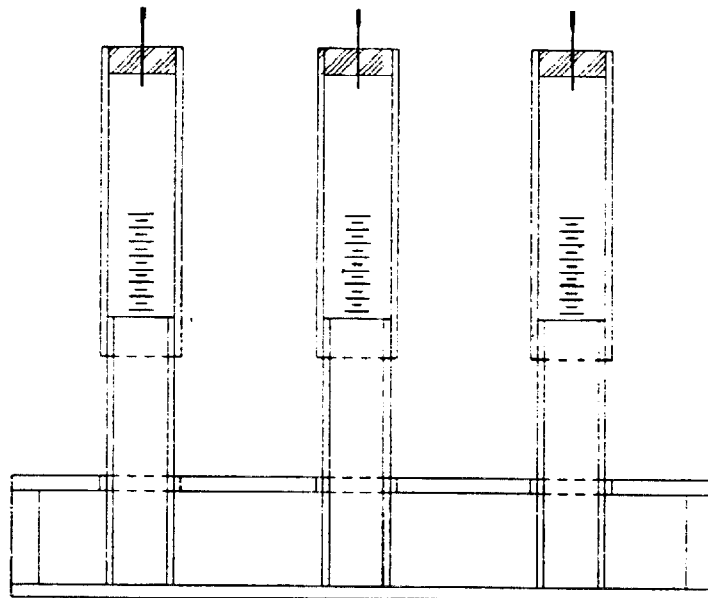


**Figure 19** Arrangement of Thermal Expansion Test Tubes

Preparation of the thermal expansion experiment includes the following steps:

1. Turn on the convection oven and set to the desired temperature.
2. Generate steady state foam with the desired expansion ratio, and fill the lower section of the test tubes.
3. Seal the bottom of the lower section of the test tubes.
4. Scrape off excess foam from the top of the test tubes (lower section)
5. Place the upper section on top of the lower section.

Conduct of the thermal expansion experiment include the following steps:

1. Place the test tubes into the oven on a rack and start the experiment.
2. Record the height of the foam expansion from periodic observations
3. Stop the experiment when the foam is no longer expanding.

The observed data from the two test tube sets are combined and plotted with the results from all other experiments.

## **Experimental Results**

To understand the thermal expansion characteristics of the foam, foams with expansion ratios of 14, 20, and 27 are first allowed to expand at an oven temperature of 45°C with respect to time . Figure 20 shows that foams of all three expansion ratios exhibit similar thermal expansion trends at various time intervals before reaching maximum thermal expansion. The foam might even show a slight reduction in the height at the end of the experiment, when the foam starts to become dry.

Different expansion ratio foams exhibit different maximum thermal expansions when reacting to the temperature. A series of experiments performed to examine this characteristic used the same expansion ratio foams (14,20 and 27) put into the oven various temperature setting, and record the maximum expansion volume of each foam. Figure 21 shows that the foam of higher expansion has a lower maximum thermal expansion.

As discussed before, higher expansion ratio foam has thinner bubble walls compared to the lower expansion ratio foam. As the foam responds to the heat and expands, the air inside the higher expansion ratio foam bubble will expand and further thin the bubble wall, which will finally break when it exceeds the limit of its surface tension. Furthermore, the lower expansion ratio foam forms thicker liquid walls between the bubbles than the higher expansion ratio foam, and this allows the air inside the lower expansion ratio foam to expand further before overstretching the bubble walls and breaking them.

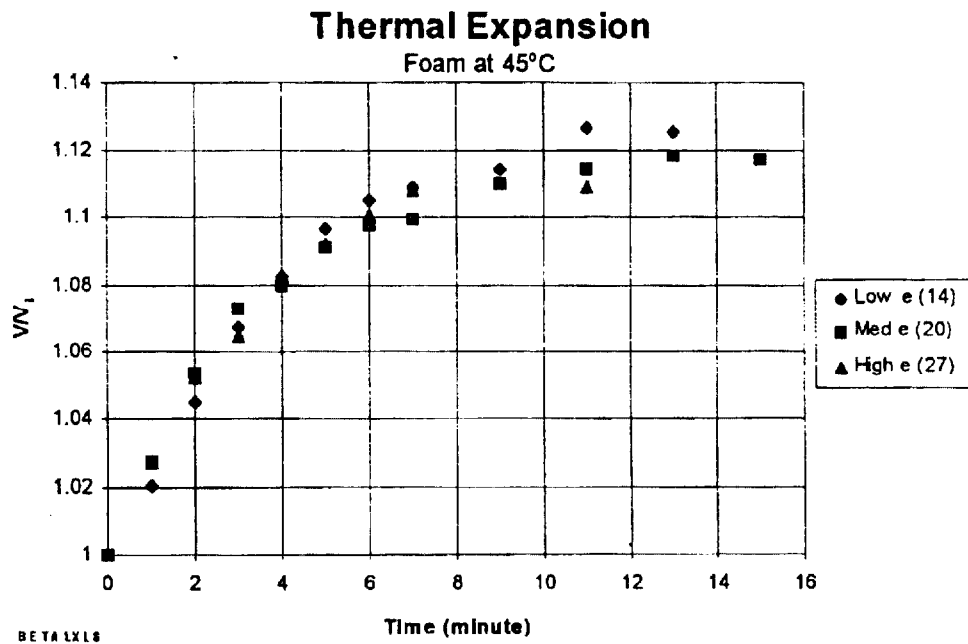


**Figure 20** Thermal Expansion of Foam with Respect to Time at 45 °C

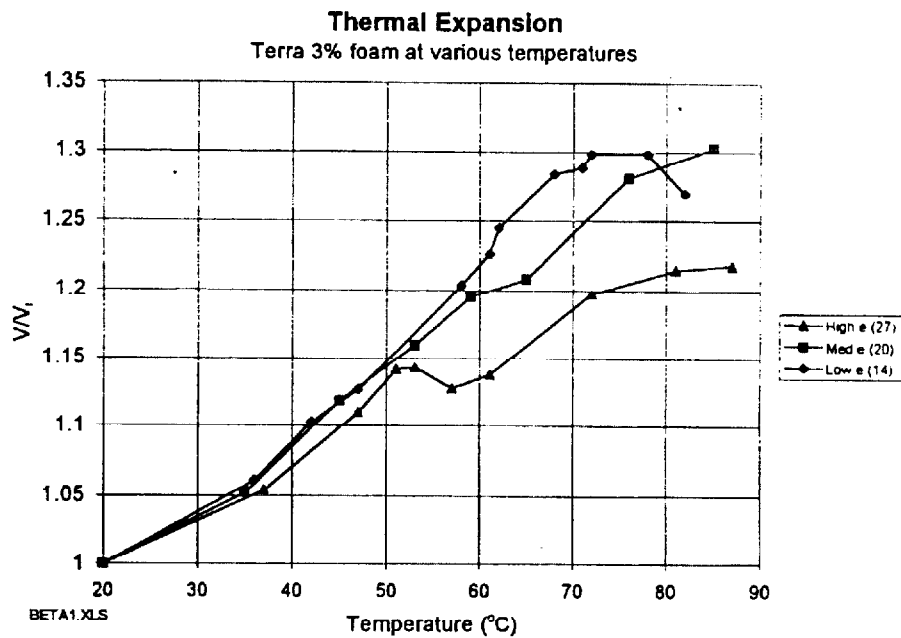


**Figure 21** Thermal Expansion of Foam at Various Temperatures



## 3.2 Radiation Absorption

Due to the unique aspects of fire protection foams, it is necessary to construct a special testing platform to evaluate the radiative properties. The primary consideration is the evaporation of the foam over time and with the application of heat. It is therefore important to create a test rig that is capable of testing foams quickly and under minimal thermal load.

### Radiation Absorption Test Rig

#### theoretical basis

Radiation energy is absorbed in a foam by the water in the foam lattice structure. The water absorbs the amount of energy that is required to change it from a liquid into a vapor. Measuring the radiation absorption directly is very difficult. It can be determined, however, by measuring the difference in the total extinction of energy through a series of foam thicknesses. The measured extinction is related to the amount absorbed.

First, consider the energy balance for the control volume in Figure 22. The incident radiation is either reflected by the surface, absorbed or scattered within the foam, or transmitted through the sample. This is represented by the equation,

$$I_o = I_r + I_a + I_s + I_t \quad (1)$$

where  $I_o$  is the incident energy,  $I_r$  is the reflected energy,  $I_a$  is the absorbed energy,  $I_s$  is the scattering energy, and  $I_t$  is the transmitted energy. From experimentation, the values for  $I_o$  and  $I_t$  can be determined directly.

The absorption and scattering terms can be functions of the expansion ratio and the thickness of the foam, while the reflection term is a surface phenomena that can only be a function of the expansion ratio. In a larger scale experiment, the scattering could be compensated by the feedback from the foam around it. In other words, the neighboring foam would scatter energy into the sample at the same rate that the sample scatters energy out. This occurs when the test section is much smaller than the total size of the foam sample. Such a case results in a one dimensional energy transfer over the test section. In the present experiment, the testing area comprises the entire foam sample and is bounded by an aluminum holder. For this case, the effects of scattering are minimized by polishing the inside surfaces of the aluminum foam holders. This more closely approximates the one-dimensional case and maximizes the scattering compensation for such a small sample of foam.

### Control Volume for Foam

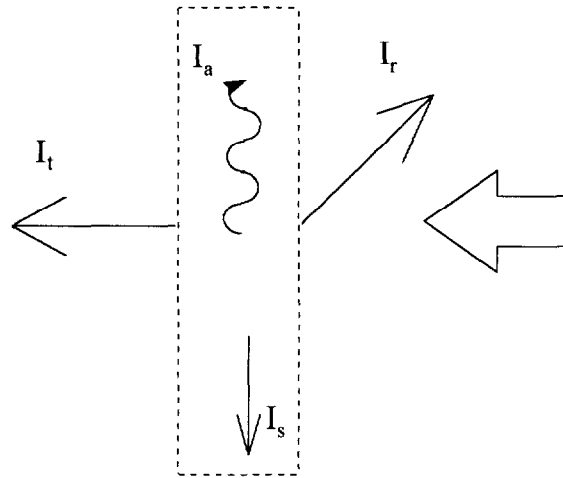


**Figure 22** Control volume for radiation absorption

Since the absorption coefficient is the primary concern of this experiment, it is necessary to combine the scattering and reflection terms. Although the dependencies of the scattering and reflection are different, combining them is the best approach possible for the given experimental setup. The scattering and reflection terms are therefore combined as follows,

$$I_{RSC} = I_s + I_r \quad (2)$$

The combined effect of reflection and scattering, as shown by  $I_{RSC}$ , will be considered a surface phenomena, and therefore will be related only to the expansion ratio of the foam. This approximation is possible because the magnitude of the scattering energy has been minimized, and is considerably smaller than the reflection energy.

Combining (1) and (2), the governing equation results in

$$I_o = I_t + I_a + I_{RSC} \quad (3)$$

This is the basis for the radiation absorption test. A measure of the scattered and reflected energy will be found by extrapolating the data to the limit where the thickness, and therefore the absorbed energy goes to zero.

To determine the radiation absorption coefficient, we must consider the decay of energy through the thickness of the foam. This relationship is modeled as an exponential decay [27],

$$I_t / (I_o - I_{RSC}) = e^{-at} \quad (4)$$

where  $a$  is the radiation absorption coefficient, and  $t$  is the thickness of foam.

Now, equation (4) is transformed by dividing by  $I_o$  and taking the natural log of each term. The resulting equation is,

$$\ln (I_t/I_o) = -a t + \ln [(I_o - I_{RSC})/I_o] \quad (5)$$

The slope of the transformed data is therefore the absorption coefficient,  $a$ .

### Special Considerations

When designing an experimental setup for measuring the radiative properties of a foam, several items must be given special consideration. First consider the nature of the foam itself. The foam evaporates at room temperature, and the evaporation rate increases at high intensities of incoming radiant input. The testing must, therefore, be done quickly to avoid evaporation effects, but also done at low temperatures to allow significant testing time for each sample without evaporating a portion of the foam. The heat source is chosen as a 375 watt infrared heat lamp. By choosing this low radiation source, it is noted that care must be taken to eliminate extraneous radiation sources and minimize convective effects [28]. Another consideration is insuring the alignment of all the test components, namely the source, the foam, and the detector. The three must be collinear and precisely measured to ensure repeatable and comparable results. The relative geometries are preserved by the use of an optical rail. As a third consideration, a single batch of foam must be tested at different thicknesses. This is accomplished by using four identical foam holders and a second optical rail positioned perpendicular to the first rail. This configuration allows each sample to be translated into the testing area in sequence. As a final consideration, the source must be as diffuse as possible to achieve accurate results. This is solved by using machined glass to diffuse the infrared light before it reaches the foam.

### Design and Setup

A test rig is designed such that all the quantities of interest can be determined through experimentation. A diagram of the test rig is shown in Figure 23. The platform consists of two optical rails from Oriel Industries mounted perpendicularly to each other and fastened horizontally to a plywood base. One rail is used to align the test equipment, while the other is used to hold several foam samples such that they can be moved into the testing area in sequence without losing the alignment of the test equipment. The foam holding rail can hold four foam holders mounted to optical carriers that slide along the rail.

The test equipment rail has several components attached rigidly to it. Starting with the source, a 375 watt, incandescent heat lamp is attached to a standard ceramic fixture and mounted to an optical holder. The front of the light bulb rests inside a steel tube. The tube is made of 0.46 mm (0.018") thick low carbon steel, rolled into an open tube and fastened together with machine screws. The tube, which is 15.24 cm (6") long and 12.7 cm (5") in diameter, is screwed onto an optical rod and rigidly mounted to the optical rail. The 375 watt light fits snugly into the tube and is directed towards the testing area. The tube helps prevent excess scattering. At the end of the tube a machined glass plate 6 inches square and 3 mm thick is mounted to the rail. This machined glass plate acts as a diffuse surface for the light to shine through. The transmitted light is considered diffuse and homogeneous, making it an ideal radiant heat source for a one-dimensional experiment. After the diffuse surface, light is incident on a 0.95 cm (3/8 inch) thick aluminum shield. The shield has a center drilled hole that is identical in size to the inside diameter of the foam holders. The foam holders, traveling on the second optical rail, pass through the testing area between the shield and detector gauge. This gauge is a 0.2 W/cm<sup>2</sup> total heat flux gauge, located at the end of the testing rail, to measure the radiation that is transmitted through the foam sample. The shield plate acts as a barrier to prevent extra radiation from leaking around the foam holders to the detector. This minimizes the error associated with the low radiation values recorded by the detector.

The foam holders are lengths of 0.318 cm (1/8 inch) thick aluminum pipe with an inside diameter of 4.45 centimeters. The tubes are 1.5, 2, 2.5, and 3 cm in length. Each holder is mounted in an adjustable optical holder with the front side as close to the shield as possible. Care is taken to insure that all four holders line up collinearly with the source and detector. The inside of the aluminum tube is polished to insure that internal scattering is minimized and the one-dimensional assumptions are valid.

To run a test, the source is allowed to heat up and reach steady state for at least 2 minutes. During this time, the detector and foam samples must be protected from the radiation. After reaching steady state, the foam samples are tested in sequence for at least 30 seconds each. Data is taken at 10 hertz and recorded by a computer. This allows for a fine resolution in the data points. After all foam thicknesses have been tested, the last holder is removed from the testing area and an incident radiation value is recorded. This value is used to normalize the data and determine the degree of extinction achieved with each thickness of foam.

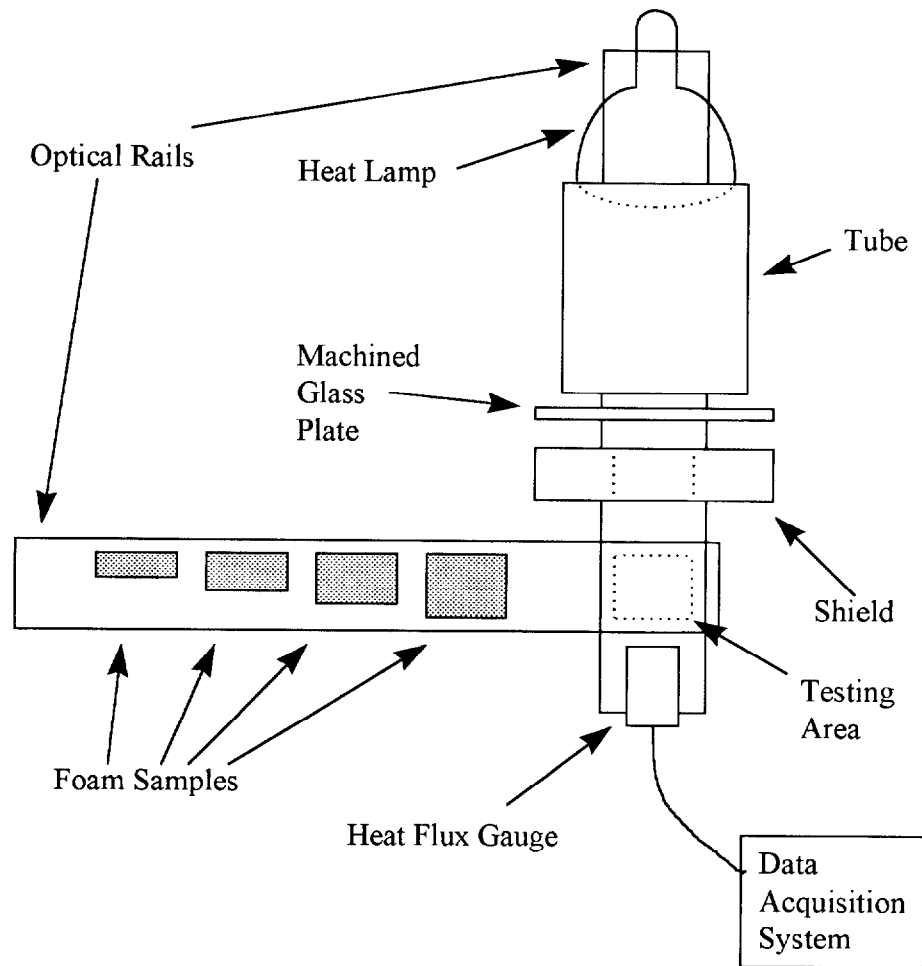


**Figure 23** Diagram of Radiation Absorption Test Rig

### Testing Procedure

To insure that the radiation absorption is measured properly, a rigid protocol of events is needed. The initial or startup conditions must be monitored before testing, strict test procedures must be upheld, and careful analysis of the data must be completed

### initial conditions

For the radiation absorption test, the room temperature and initial radiation are measured. The room temperature for these tests were all between 16 and 20° C. Additionally, the initial radiation as read from the flux gauge before turning on the source was consistently below  $1\text{E-}7$  volts or  $2\text{E-}5$  W/cm<sup>2</sup>.

## **Data Gathering**

The testing procedure for the radiation absorption has three stages. The first stage is checking the initial conditions, setting up the data acquisition system, and making the foam concentrate. The second stage is to turn on the light source to warm up, start the foam generator and make the actual foam, measure the expansion ratio of the foam, and fill the foam holders. The third stage is to line up the foam holders and test the different thicknesses.

In stage one, if the initial conditions are met, the data system is set up and the foam concentrate is mixed and poured into the generator. In the second stage, the light is turned on at least two minutes before testing, the foam generation starts, and at least two foam weights are taken to determine the expansion ratio of the foam. Additionally, the foam holders are filled with the foam and scraped off with a thin piece of plexiglass to insure the uniform thickness of the sample. In the final stage, the foam holders are lined up on the foam staging track and sequentially translated through the test area. Each sample must be tested for at least 30 seconds, but preferably less than 60 seconds. Time notations should be made on a data sheet to reflect when each sample is placed in the testing area and taken out of the testing area. Furthermore, the samples must be tested in the order that they were filled. This minimizes any differences in exposure to ambient conditions. If the samples are tested again, within five minutes, the data shows less than a 10% change. At the end of the fourth sample, a measurement of the incident radiation is made without any sample between the light source and the heat flux gauge.

## **Data Analysis**

The first step in the analysis is to import the data into a spreadsheet and plot it. A representative plot of the data as it is taken is shown in Figure 24. The plot shows the testing periods as constant energy portions between tall spikes. The radiation spikes between samples represent the incident radiation that is allowed to pass through the testing area after one sample is removed and before it is replaced with the next sample. This also provides a clear break in the data between one sample and the next. There should be four distinct areas on the plot that show the periods of time when each of the respective samples is being tested. To get a good estimate of the radiation transmitted through the foam, an average value for the heat flux must be taken over the longest stretch of stable behavior for each sample. Once the average values have been calculated, they are normalized with respect to the incident radiation. These quantities are now used in equation (5) with the related thickness from the test.

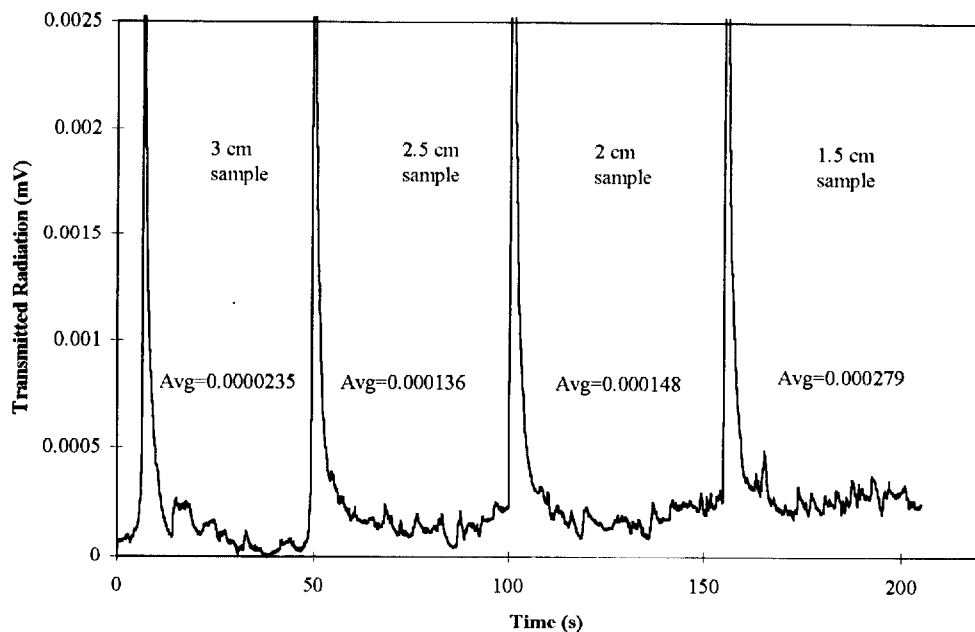


**Figure 24** Sample radiation absorption experimental data

After examining the results from equation (5), the points for thicknesses of 1.5, 2, and 2.5 cm appear to be linear, as expected. The values from a thickness of 3 cm are consistently not on the line with the other data. The accuracy of the data acquisition system at such a low level of radiation is in question. The data at 3 cm is therefore left out of the linear regressions for the foam samples.

After all the regressions for each foam are carried through, comparisons are made between foam samples. Through statistical evaluation, it is determined that the transformed slopes, or absorption coefficients, are statistically the same within a foam brand, regardless of expansion ratio. The data on a semi-log plot is therefore regressed with a fixed slope for the data gathered with the same foam brand.

### 3.3 Thermal Diffusivity

Much like the radiation absorption testing, many factors must be accounted for when measuring the thermal diffusivity of a fire protection foam.

#### Thermal Diffusivity Test Rig

##### theoretical basis

The basis for this test rig lies in the intended analysis. The analysis will numerically solve the constant property conduction equation for a semi-infinite plate to determine the

temperature profile between known boundary conditions.

$$\partial^2 T / \partial x^2 = 1/a \partial T / \partial t \quad (6)$$

Equation (6) is the conduction equation in one dimension with no heat generation. It contains the quantities of temperature (T), time (t), and thermal diffusivity (a). The initial condition is a constant temperature throughout the foam given by an average of the temperatures measured at three locations within the foam at the beginning of the test. The boundary conditions will be defined by two time varying temperature profiles measured at different depths within the foam during the test. This can be solved numerically to determine the expected value of the temperature at any location between the boundary conditions

To use equation (6) for the numerical solution, temperatures are taken at three depths within the foam over a period of time. During the test, one-dimensional heating takes place on the foam and the temperature traces are all recorded. The highest and lowest temperature traces (closest and furthest from the heat source) are used as the boundary conditions for the temperature profile between them. By design, the third temperature history is taken at the central location between the outside boundary conditions. The constant property conduction equation (6), is solved numerically for the initial and boundary conditions and a defined value for the thermal diffusivity, a. The temperature history at the central location, generated by the numerical model and boundary conditions, is compared with the actual temperature history measured at the central location. The numerical solution that most closely matches the actual data represents the experimental thermal diffusivity.

### **Special Considerations**

The first consideration for measuring the thermal diffusivity is achieving a one dimensional heat flux at the surface of the foam. To achieve this, a lab scale Bunsen burner was chosen to supply heat to a 6 inch tall aluminum cylindrical block with a diameter of 7 inches. Insulation was attached to the outside of the block, leaving the top and bottom faces exposed. The Bunsen burner is placed beneath the center of the block, while the foam to be tested is placed on the top surface. The high thermal conductivity of the aluminum block heats up and provides a near isothermal condition at the foam surface. This results in a one-dimensional heat flux near the center of the foam region. This is represented in Figure 25.

The second major consideration is measuring the temperature inside the foam without disturbing the foam while it is being tested. To achieve this, six type-T thermocouples are suspended down over the aluminum block on two 1/16 inch plexiglass rods. Three thermocouples are attached to each rod such that when suspended over the block each rod has a thermocouple at 1, 2, and 3 cm from the surface of the block. The



thermocouples are coaxial on each rod. The two rods are placed approximately 2 cm apart near the center of the block. If the temperature traces from the thermocouples on separate rods, but at identical heights, read the same temperature, then the assumption of a semi-infinite one-dimensional heat flux condition is verified. With this instrumentation setup, the two data sets can be averaged at each height.

## Design and Setup

The test apparatus is built for strength and durability. A diagram of the test setup is shown in figure 26. Steel channels are used to construct a platform with venting from the sides to exhaust the gas burner fumes. A marinite sheet with a 6.5 inch hole is placed on the top surface of the platform. Marinite is used because it does not conduct heat appreciably even at high temperatures. The aluminum block rests on the marinite sheet centered over the hole and exposed to a Bunsen burner from below. Additional insulation is placed around the 7 inch diameter aluminum block to minimize heat loss to the surroundings. The block is 6 inches in height to allow for adequate diffusion of heat across the face and achieve the desired one-dimensional heat flux at the top surface. A lab scale Bunsen burner is placed below the aluminum block to create the homogeneous heat flux through the block. The six thermocouples as described above are suspended down from an aluminum bar on parallel plexiglass rods to measure the temperature inside the foam at positions of 1, 2, and 3 cm from the surface of the aluminum block.

To run a test, foam is placed on the top surface of the block and the Bunsen burner is lit. The temperature inside the foam is measured by the six thermocouples and recorded

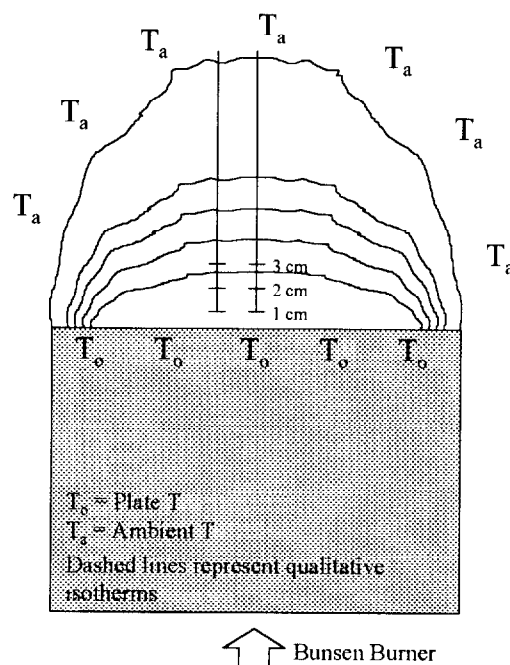


**Figure 25** One Dimensional Heat Transfer

at 20 hertz by the computer. The data is averaged and the 1 and 3 cm depth temperatures are used as boundary conditions in the constant property conduction equation. For a given value of the thermal diffusivity, the numerical solution provides a temperature history at the central thermocouple location. The value of thermal diffusivity is determined by matching the best numerically derived temperature history with the actual thermocouple data.

## Testing Procedures

To insure the integrity of the results, again, the initial conditions, test procedure and analysis for the thermal diffusivity must be carefully designed.

### Initial conditions

The only initial conditions for this test are related to temperatures. The room temperature must be between 16 and 20° C. Furthermore, the foam concentrate must be made with cold water from the tap, approximately 13 ° C. The initial temperature of the aluminum block must be in equilibrium with the room temperature.

### Test Procedure

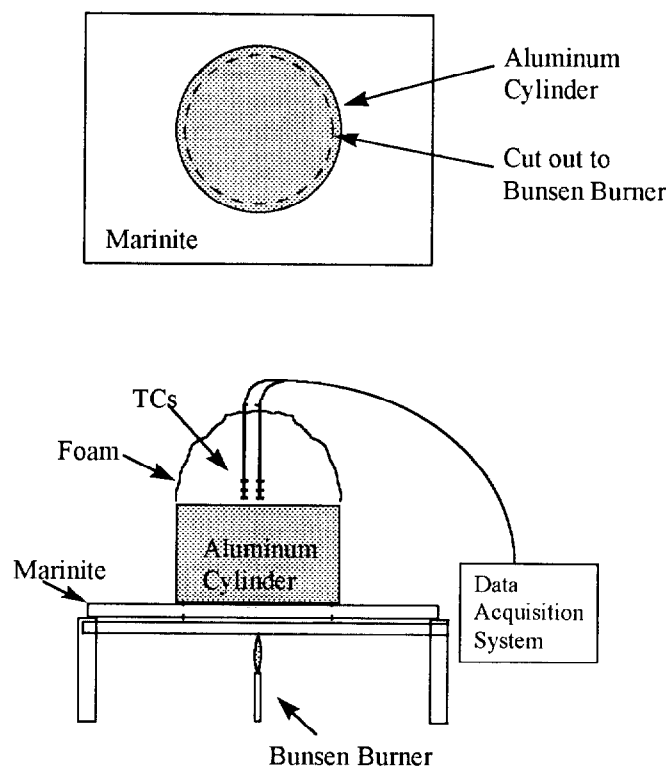


**Figure 26** Diagram of Thermal Diffusivity Test Rig

There are three stages to the testing procedure for thermal diffusivity. The first stage is to check the initial conditions, check the heights of the thermocouples, set up the data acquisition system, and prepare the foam concentrate. The second stage is to generate the foam and measure the expansion ratio. The third stage is to pour at least 10 centimeters of foam on top of the aluminum block, light the Bunsen burner, and begin taking data.

## Data Analysis

To analyze the data, two FORTRAN programs were written. The first program reduces the data from twenty hertz to one hertz by a simple averaging routine. This was done to help eliminate any small scale noise from the data acquisition system. The program, can be found in Appendix D. Once the data is reduced, it can be plotted easily. Plotting the data at this stage is necessary in order to determine the heated portion of the test.

The aluminum block takes approximately three minutes to heat up and provide the uniform temperature boundary condition that is necessary. Also, the foam exhibits an evaporative cooling effect throughout the foam during the first two or three minutes of the testing. This happens because the air-steam mixture trapped inside the bubbles of foam has not reached saturation at the onset of the test. To achieve saturation, the air must absorb moisture, and therefore, energy from the liquid, causing an overall cooling effect throughout the volume of the foam.

Once the data is plotted, it is easy to determine where the heating begins. The lowest point on the plot is taken as the starting point. From the graph, the time at which this occurs is recorded and the reduced data is truncated prior to this time. This can be seen graphically in Figure 27. Now, with a data file filled with average temperatures from three thermocouples during a one-dimensional heating, the data is read into the second program.

The second program is written to numerically solve the constant property conduction equation (6). This program reads in data, line by line, and solves the conduction equation by a Crank-Nicolson method with 101 nodes. A diagram showing the locations of the nodes can be seen in Figure 28. The program which solves the equation by the Crank Nicolson method can be found in Appendix D. From the diagram, the value for the temperature at node 51 is representative of the 2 cm thermocouple. The Crank Nicolson approach creates a tridiagonal matrix with the boundary conditions, and results in a system of linear algebraic equations which can be solved simultaneously. The program is used to solve for the temperature at node 51 (representative of 2 cm) for seven different values of thermal diffusivity. These seven values are  $1 \text{ E-}7$ ,  $2 \text{ E-}7$ ,  $5 \text{ E-}7$ ,  $1 \text{ E-}6$ ,  $2 \text{ E-}6$ ,  $5 \text{ E-}6$ ,  $1 \text{ E-}5 \text{ m}^2/\text{s}$ . These values span the range between the thermal diffusivity of water and air, the primary constituents of foams. The values calculated, as well as the actual

recorded data are sent to a final output file. This file is read into a spreadsheet, plotted, and the closest fit to the actual data at the 2 cm thermocouple is taken as the thermal diffusivity for that foam sample.

### 3.4 Database of Foam Properties and Evaluation

The following pages show the final reduced data from all of the basic foam characterizing tests that were completed. There are two sections, the first describes the values for the radiation absorption modeling of each foam, while the second shows the thermal diffusivity for each of the foams tested. Within each section, the data is organized by first showing a testing matrix that was completed, then describing the determined characteristics for each individual foam product.

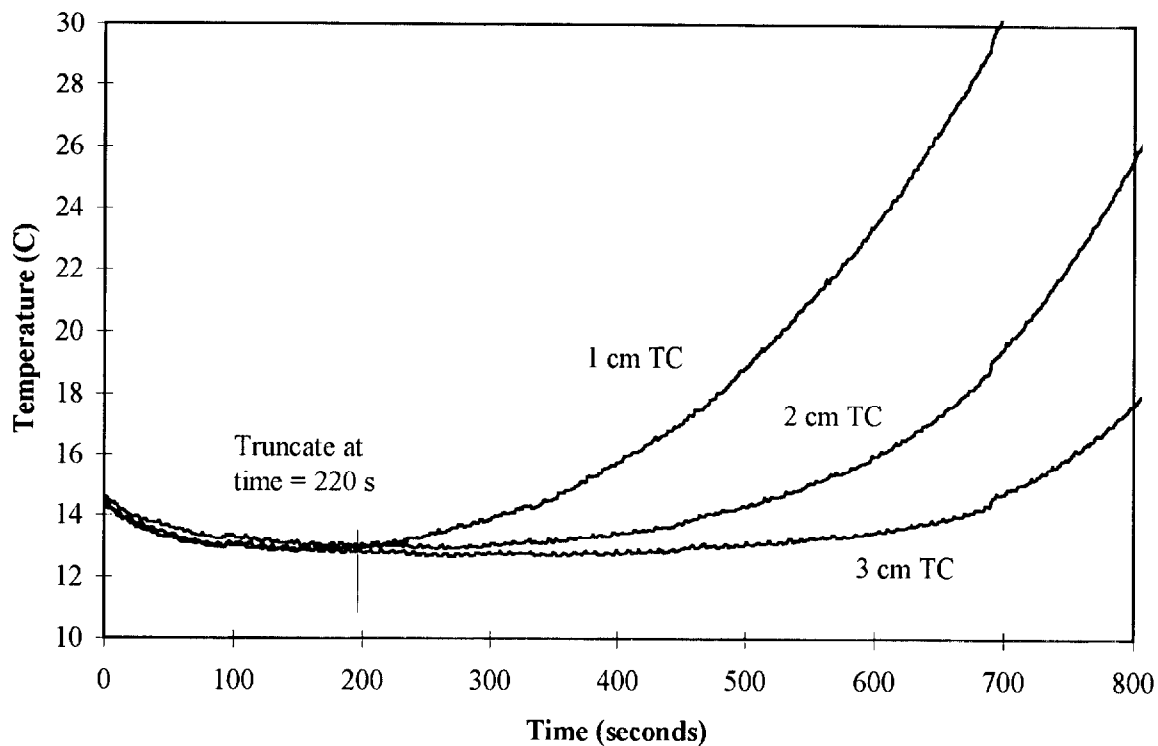


**Figure 27** Truncation of Diffusivity Data

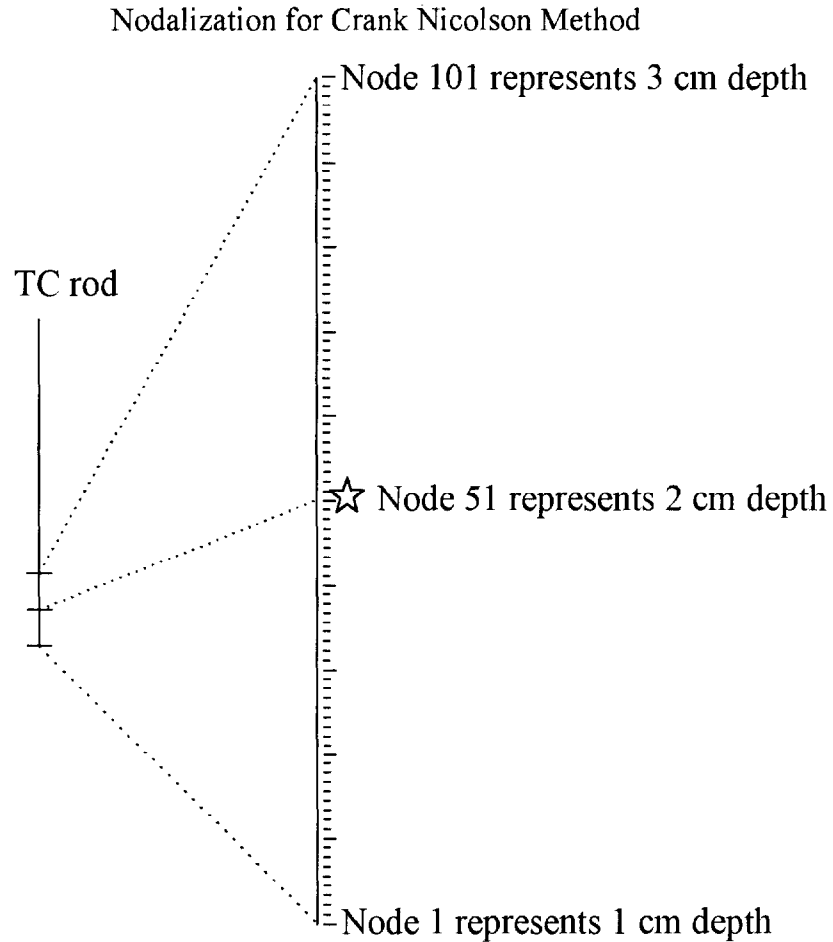


**Figure 28** Diagram of Crank Nicolson Node Assignment

### Radiation Absorption

The radiation absorption quantities that were determined from the experiments include a value for the radiation absorption coefficient and a measure of the reflectivity and scattering for each foam. The value for the reflectivity and scattering is best shown as a percentage of incident light. Therefore, a quantity RSC is given by,

$$RSC = I_{RSC} / I_o * 100 \quad (7)$$

The value of RSC represents the total energy that is not absorbed nor transmitted by the foam.

## Test Matrix

The following table shows the test matrix that was completed for the radiation absorption modeling. The numbers in the chart refer to the number of experiments that were completed at the given parameters. A designation of “untestable” refers to a foam that is too wet to stay in the test holders long enough to complete a test.

Table 5 Radiation Absorption Test Matrix

Radiation Absorption	XP=15	XP=20	XP=25	XP=30
Foam A	untestable	3	3	0
Foam B	untestable	2	2	0
Foam C	untestable	untestable	2	2
Foam D	untestable	untestable	2	2
Foam E	3	4	4	1

## Foam E

After examining all the data from the twelve runs with protein based foam, it was determined that within the bulk of the foam, up to an expansion ratio of 30, the radiation absorption is constant. The slopes of the regression curves are nearly identical and show no significant trend with expansion ratio. This is shown in Figure 29. In the graph, the slopes have been converted into the radiation absorption coefficients as evaluated from equation (5). The calculated values of the radiation absorption are plotted against their expansion ratio, and an average value for  $a$  is computed from all the protein based foam runs. By simple statistical methods, the average radiation absorption coefficient is  $0.51 \text{ cm}^{-1}$  with a standard deviation of  $0.20 \text{ cm}^{-1}$ .

Using the constant value for the absorption, a relative measure of the reflection and scattering can be characterized by extrapolating to the limit of zero thickness. Protein based foam exhibits a small variation in the reflected and scattered ( $I_{\text{SRC}}$ ) energy with expansion ratio. The graph in Figure 30, shows the percentage (RSC) of light reflected and scattered by the surface of the foam as a function of the expansion ratio for protein based foam. As is shown, the reflection goes down as the expansion ratio increases.

In Appendix B, the data and regressions are plotted by expansion ratio for each of the protein based foam samples tested. The data is plotted on a  $\text{LOG}_{10}$  scale.

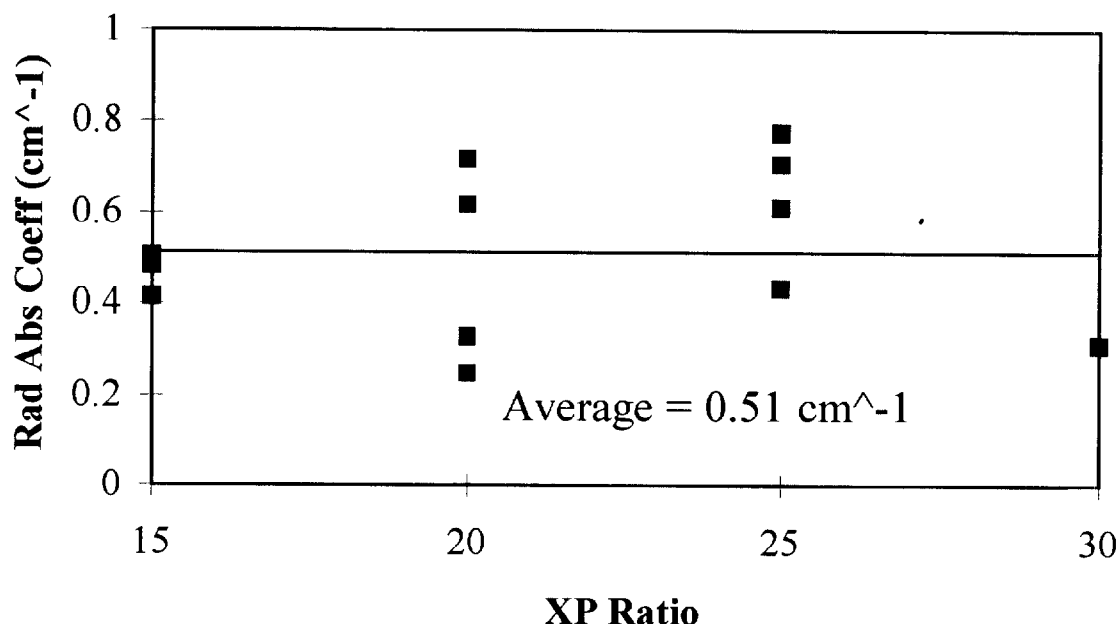


**Figure 29** Radiation Absorption Coefficient. v.s. XP for Foam E

### **Foam A**

Foam A was tested for expansion ratios of 20 and 25. As is the case for protein based foam, foam A shows a constant radiation absorption within the central thickness, or bulk, of the foam. The radiation absorption coefficient is 0.65 cm<sup>-1</sup>. Foam A also behaves much like protein based foam in that its RSC energy decreases as the expansion ratio increases. For an expansion ratio of 20, the RSC is 94.5%, while for an expansion of 25, it is only 92.8%. The regressions and data are plotted in Figure 31.

### **Foam B**

Beginning with Foam B, a different behavior is seen in the remaining synthetic foams. Although the radiation absorption in the bulk is constant over expansion ratios, the reflected portion of the energy is also held constant over the expansion ratios tested. For Foam B, the radiation absorption coefficient is 0.65 cm<sup>-1</sup> for expansion ratios between 20 and 25. The RSC, however, is 90.4% for the same range of expansion ratios. The data and regression can be seen in Figure 32.

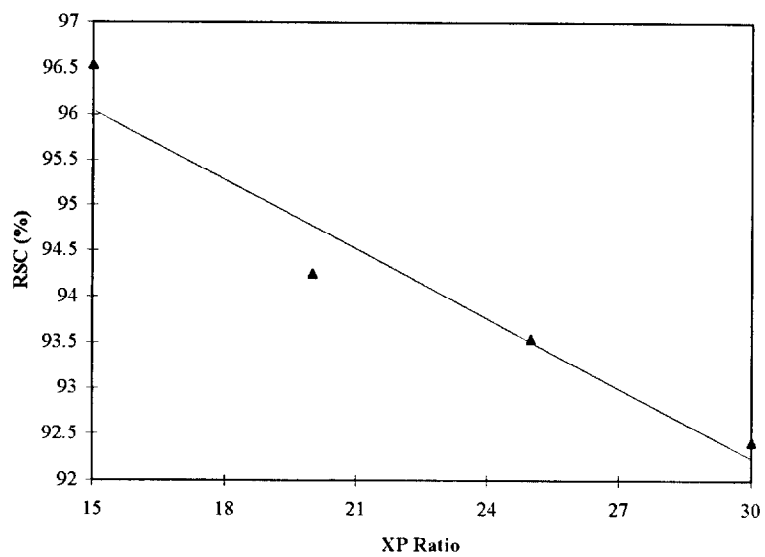


**Figure 30** Reflection and Scattering from Protein based Foam

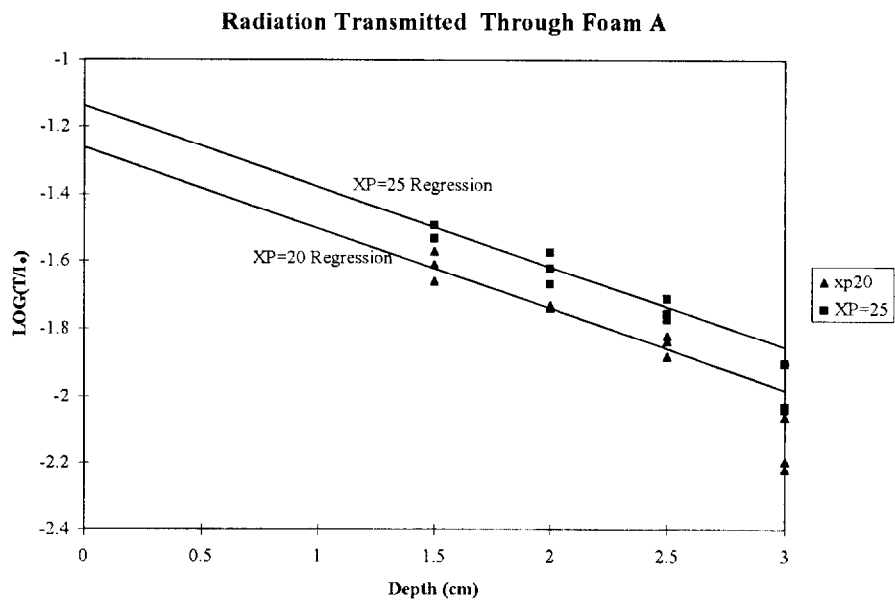


**Figure 31** Radiation Absorption Through Foam A



### **Foam C**

Foam C exhibits a radiation absorption coefficient of  $0.72 \text{ cm}^{-1}$ . This is constant for expansion ratios of 25 to 30. The reflection and scattered energy (RSC) is 84% for Foam C between the expansion ratios of 25 and 30. The data and regression can be seen in Figure 33.

### **Foam D**

Foam D shows a radiation absorption coefficient of  $0.84 \text{ cm}^{-1}$ . This is constant for expansion ratios of 25 to 30. The constant reflection and scattering energy (RSC) is 79%. The data and regression can be seen in Figure 34.

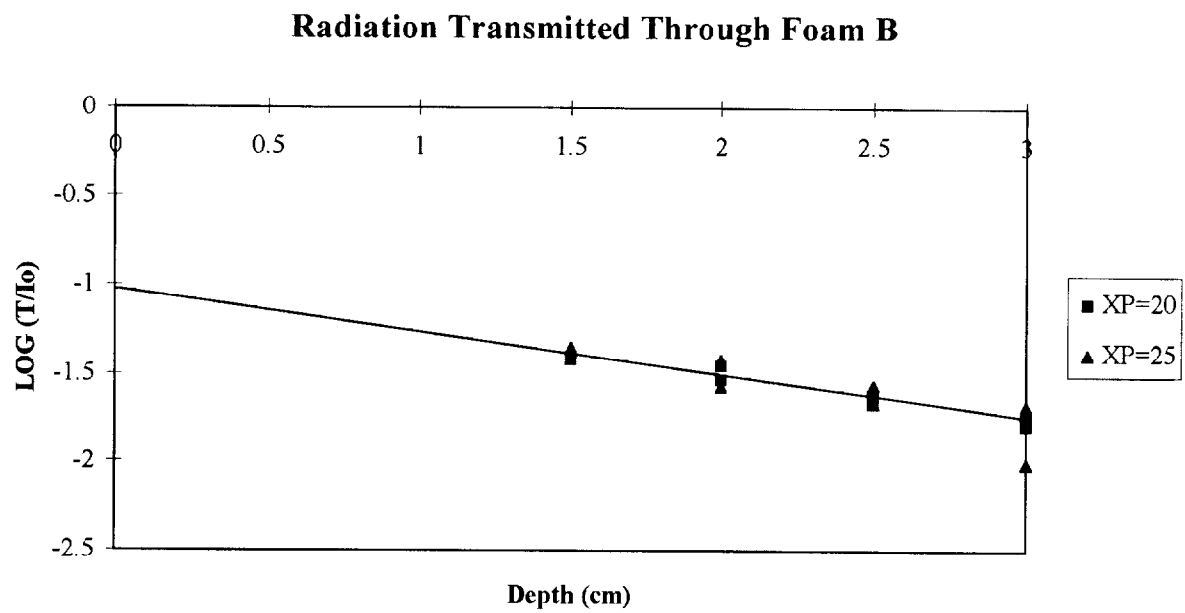


**Figure 32** Radiation Absorption Through Foam B

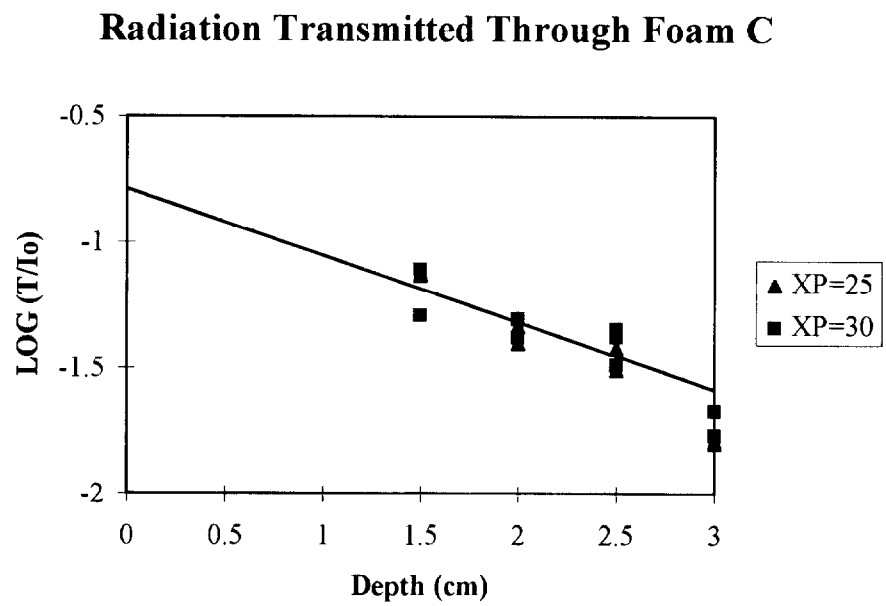


**Figure 33** Radiation Absorption Through Foam C

### Radiation Transmitted Through Foam D

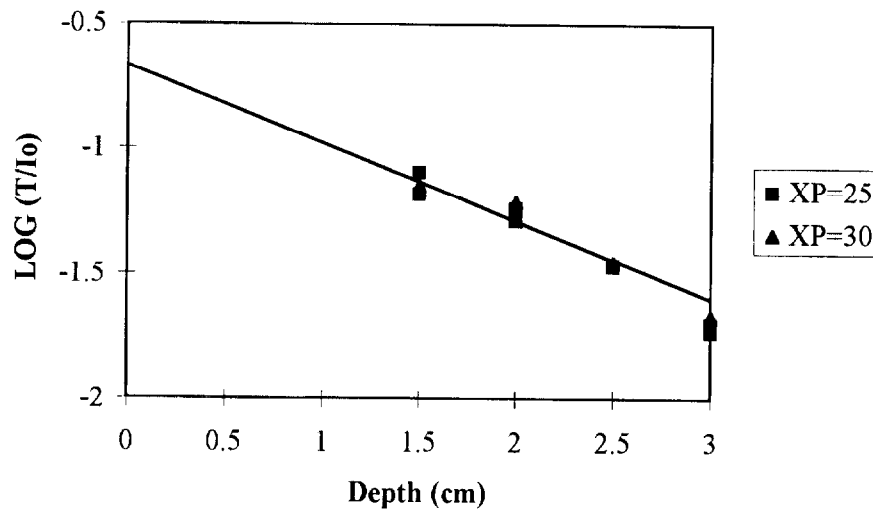


**Figure 34** Radiation Absorption Through Foam D

### Thermal Diffusivity

The thermal diffusivity is measured for 20 foam samples. The thermal diffusivity is determined from the plots of each experiment's temperature history. The plots can be found in Appendix C for all samples tested.

### Test Matrix

Table 6 shows the test matrix for the thermal diffusivity. The tests were completed only on foams that could be tested for their radiation absorption coefficient.

**Table 6** Thermal Diffusivity Test Matrix

Thermal Diffusivity	XP = 15	XP = 20	XP = 25	XP = 30
Foam A	untestable	1	1	0
Foam B	untestable	2	2	0
Foam C	untestable	untestable	2	3
Foam D	untestable	untestable	2	1
Foam E	2	2	2	0

## Overall Thermal Diffusivity Results

All five of the fire protection foams tested exhibited the same thermal diffusivity. This includes all the tested expansion ratios for each foam. An overall thermal diffusivity of  $5 \times 10^{-7} \text{ m}^2/\text{s}$  is measured for all foams and for all tested expansion ratios. Plots for each of the 20 experiments including the numerical solutions for the three nearest diffusivities can be found in Appendix C. The value of  $a$  must be evaluated as an asymptote at the beginning of the graph because the foam expands and changes as it is heated.

## Importance of Properties

The energy absorption of a fire protection foam is related to both the radiation absorption coefficient and the  $I_{\text{RSC}}$  energy. If a foam can reflect or scatter more energy, then it will not have to absorb as much in its bulk. In the field of fire protection, it is necessary to consider the case of a thick layer of foam. The layer is thick enough such that no radiation is passed through it ( $I_t=0$ ). The question now becomes how long will the foam last and protect the surface it covers. The portion of the incident energy that is not reflected must be absorbed within the foam. If the reflection and scattering can be increased, less energy is absorbed by the foam and it will last longer. If a foam initially reflects 92%, but is somehow improved to reflect 93%, the absorbed energy in the bulk of the foam goes from 8% to 7%, an improvement of 12 %.

The thermal diffusivity is apparently unchanged between foam concentrates or through the manipulation of the expansion ratio. This is likely based on the fact that the foam concentrates are primarily composed of water. The thermal conductivity effects through any foam product are likely to be similar.

## Evaluation and Comparison of Standard Foams

One important issue in evaluating foams is the ease of application and use. Fire protection foams are not static, but rather change and evaporate continuously. Their application, therefore must coincide closely with the impending fire for maximum protection.

In addition to timely application, all of the foams are sensitive to their expansion ratio. If the expansion ratio goes too low or too high, the foams cease to be effective. A low expansion ratio foam does not stick well to vertical surfaces, since it flows too much. On the other hand, a high expansion ratio foam may blow away in the wind currents created by the fire. In this case, the foam is so light it may be carried off in the updrafts. It is therefore very important that the foams be produced at the correct expansion ratio. It is noted that this ratio changes with the various products.

## **Most Durable Foams**

After testing all five foams, protein based foam is the most durable of the foams tested. The protein based foam shows an ability to stick to vertical surfaces (aluminum and iron) throughout tested expansion ratios. All four of the synthetic foams do not perform well at one or more of the expansion ratios. The synthetic foams do not have the same cohesive structure as their protein based counterpart. At low expansion ratios, below 25, the foam structures are not strong enough to stick to vertical surfaces. Even at higher expansion ratios, they have a tendency to flow off a surface rather than stick to it. This inability to stick at low expansion ratios was a major disadvantage for this test series.

#### 4. SUMMARY AND CONCLUSIONS

A foam generating system has been designed and built. A consistent foam output is generated by this system and various measurements are performed on the foams. In total five different foams have been tested. The measurements considered a range of expansion ratios. For the most part thermal properties of the foams are not a strong function of the expansion ratio. However, the foams effectiveness (i.e. cohesiveness and ) is sensitive to the expansion ratio. A low expansion ratio foam does not stick well to vertical surfaces, since its viscosity is too low. On the other hand, a high expansion ratio foam may blow away by the draft created by fire. It is therefore very important that the foams be produced at the correct expansion ratio. It is noted that this ratio changes with the various products. After testing all five foams, protein based foam is, by far, the best performer as fire protection agent.

The foam structure is characterized by its bubble size. The data shows decreasing bubble sizes from 1000 micron to 300 micron as the expansion ratio increases from 10 to 35. The generation pressure influences also the bubble size since foam generated at lower operating pressure exhibits larger variation in bubble sizes, and foam generated at higher operating pressure exhibits more uniform bubble sizes.

The thermal expansion coefficient for the protein foams ranges from  $3.84\text{E-}3$  to  $5.77\text{E-}3 \text{ K}^{-1}$  where these values correspond to expansion ratios of 27 and 14 respectively. As the foam responds to the heat and expands, the air inside the higher expansion ratio foam bubble will expand and further thin the bubble wall, which will break when it exceeds the surface tension. The lower expansion ratio foam forms thicker liquid walls between the bubbles than the higher expansion ratio foam, and this allows the air inside the lower expansion ratio foam to expand further before overstretching the bubble walls and breaking them.

The radiation absorption coefficient for fire protection foams ranges from  $0.51$  to  $0.84 \text{ cm}^{-1}$ . This is a measure of a foams ability to absorb radiation through the bulk of the foam. However, the results must be considered in combination with the reflective and scattering energy measurements that are coupled to them in application. As the reflection and scattering increase, the absorption decreases, as there is less energy that must be diminished. The ultimate goal is not to have a foam that reflects and scatters the best, or absorbs the best, but one that has the best combination of these factors. Such a foam will protect a structure from thermal energy the best. Therefore, the quantities given here must be used carefully, and used in conjunction with one another, to accurately describe a foam's performance.

The thermal diffusivity for all foams, at all tested expansion ratios, is  $5 \text{ E-}7 \text{ m}^2/\text{s}$ . This shows that the conductive effects of a hot surface through any of these fire protection foams will be comparable. This is, therefore, a poor metric for the performance differential

between foams.

Future research should focus on the role of thermal expansion in fire protection foams. The thermal expansion of foams may provide insight into the complex recombination of bubbles. In addition, research must focus on higher heat flux testing of foams for their thermal behavior under more extreme conditions. This information is key to understanding the microscopic properties that result in the desired macroscopic characteristics of the fire protection foams.

## **APPENDIX A**

### **Selected Photographs of Foam Used in the Analysis**



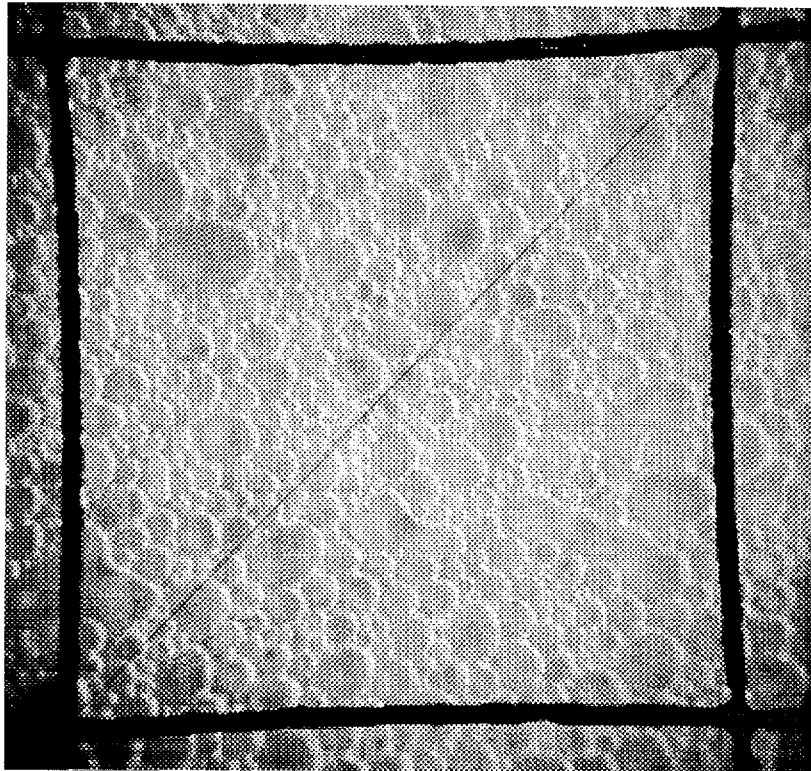


**Figure 1**      Pressure: 15 Psig      Expansion Ratio: 14

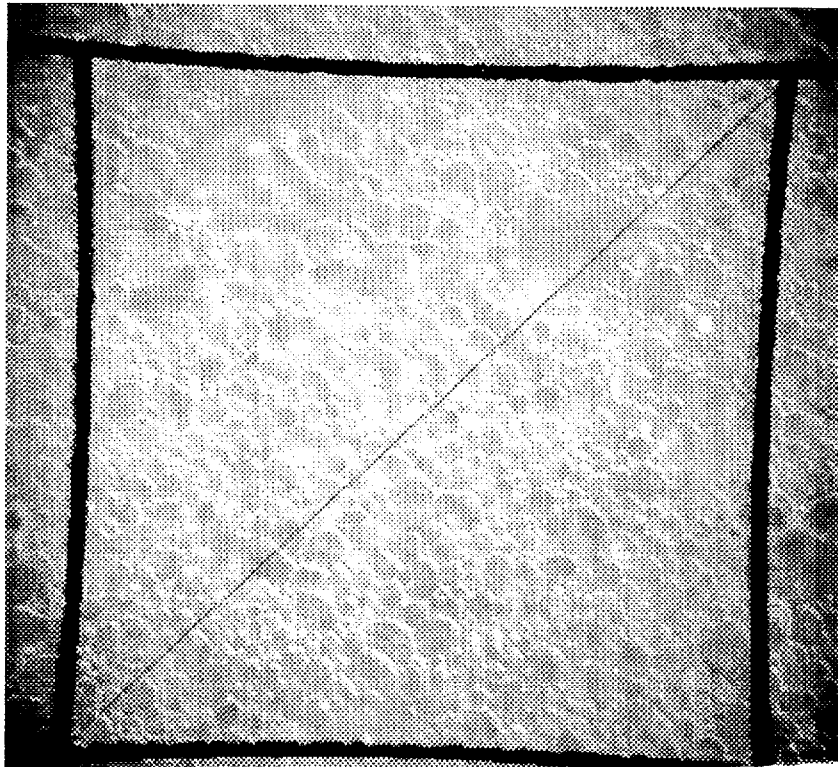


**Figure 2**      Pressure: 15 Psig      Expansion Ratio: 20

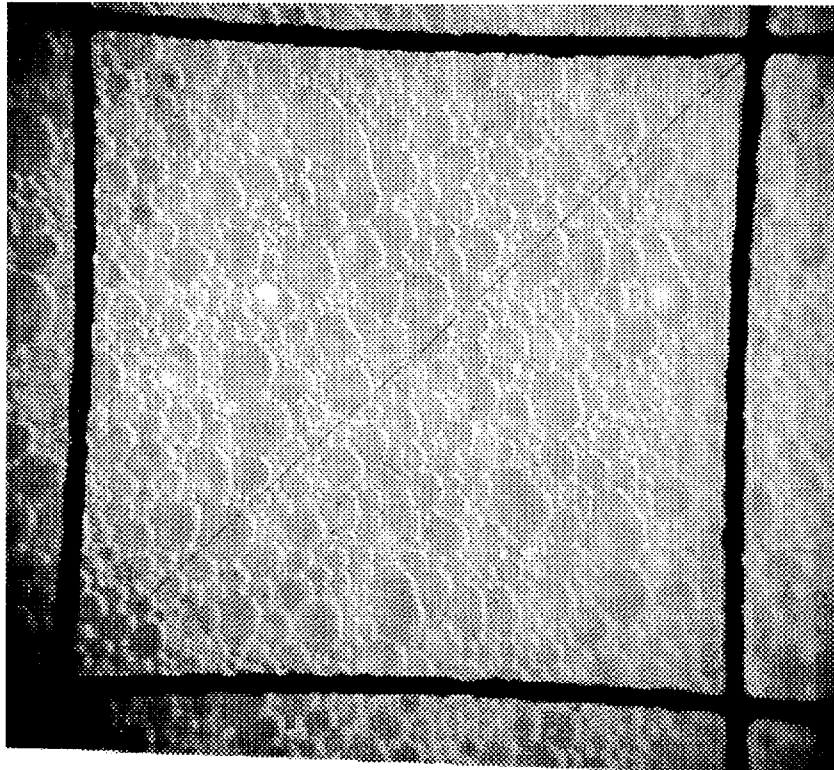


**Figure 3**      Pressure: 15 Psig      Expansion Ratio: 27



**Figure 4**      Pressure: 15 Psig      Expansion Ratio: 33

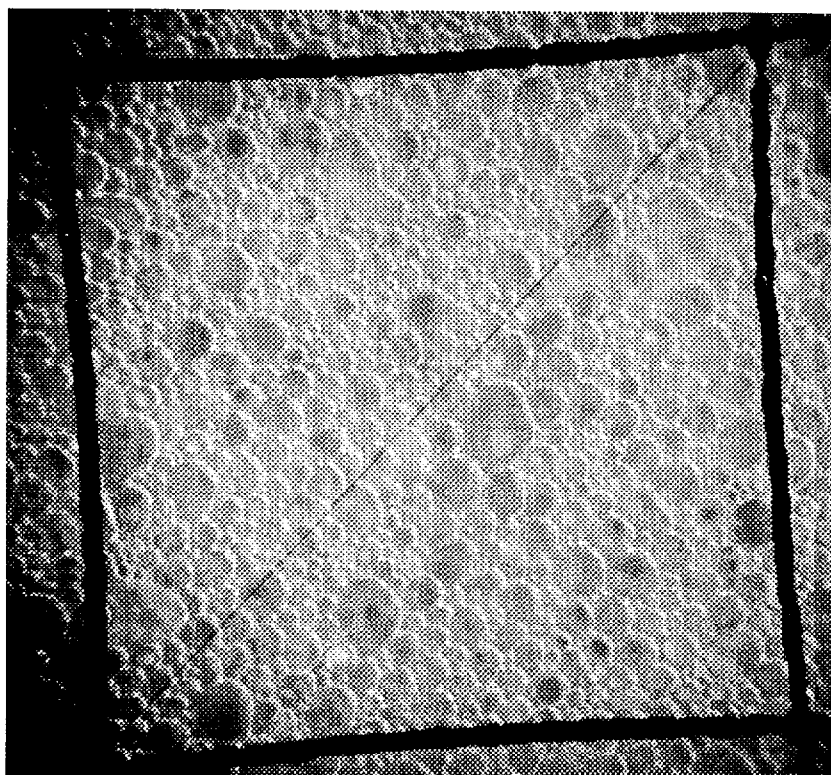


**Figure 5**      Pressure: 20 Psig      Expansion Ratio: 14

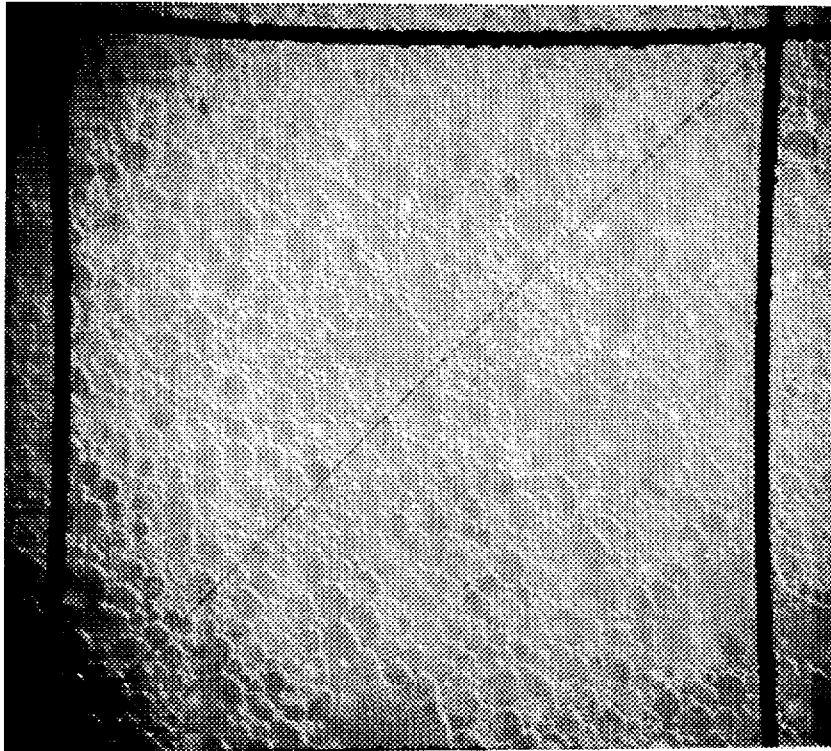


**Figure 6**      Pressure: 20 Psig      Expansion Ratio: 20

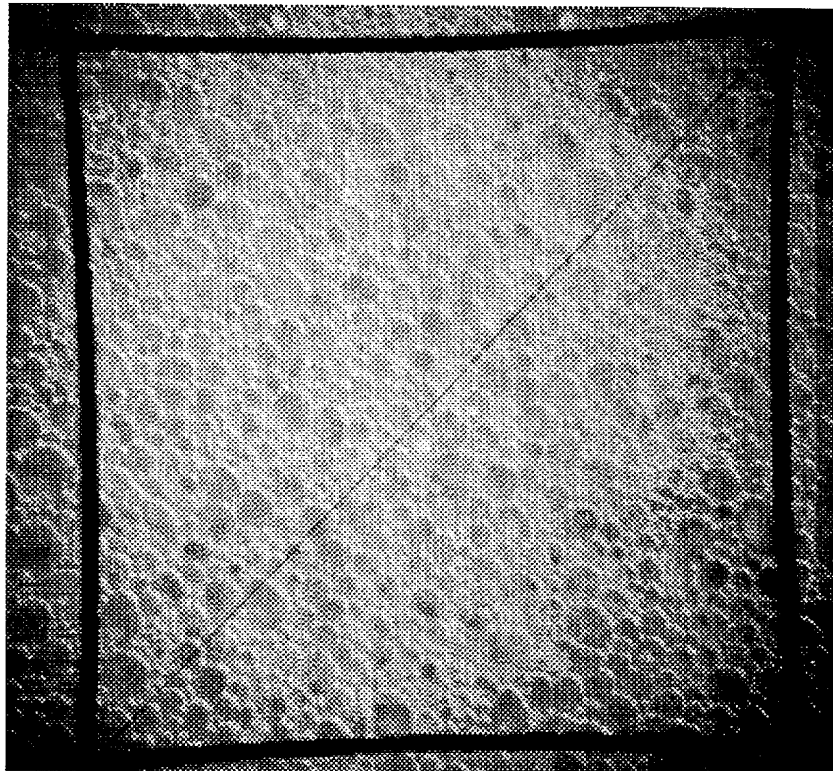


**Figure 7**      Pressure: 20 Psig      Expansion Ratio: 27

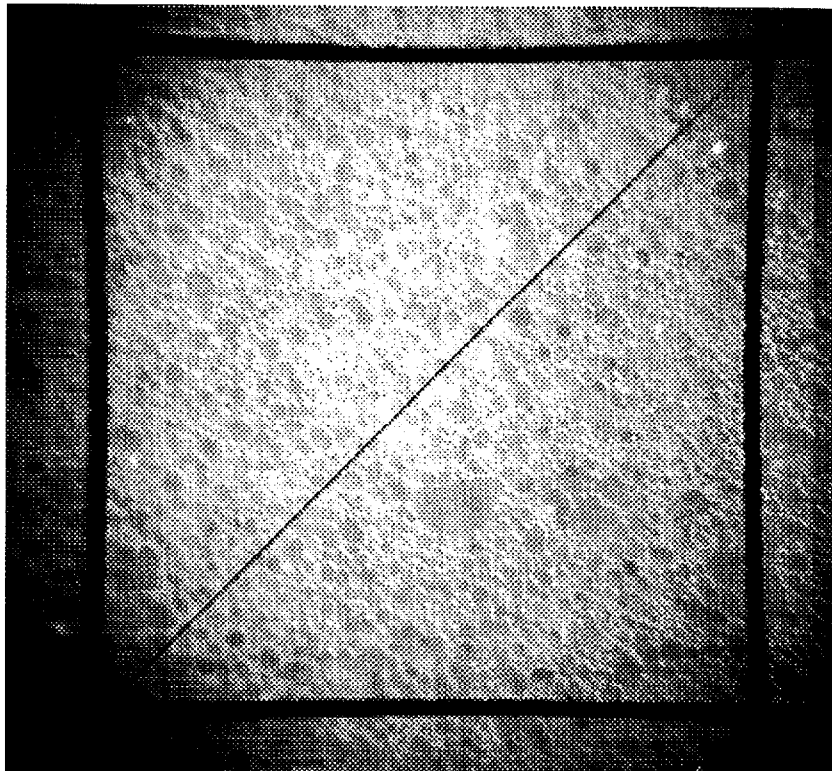


**Figure 8**      Pressure: 20 Psig      Expansion Ratio: 33



**APPENDIX B**  
Radiation Absorption Data

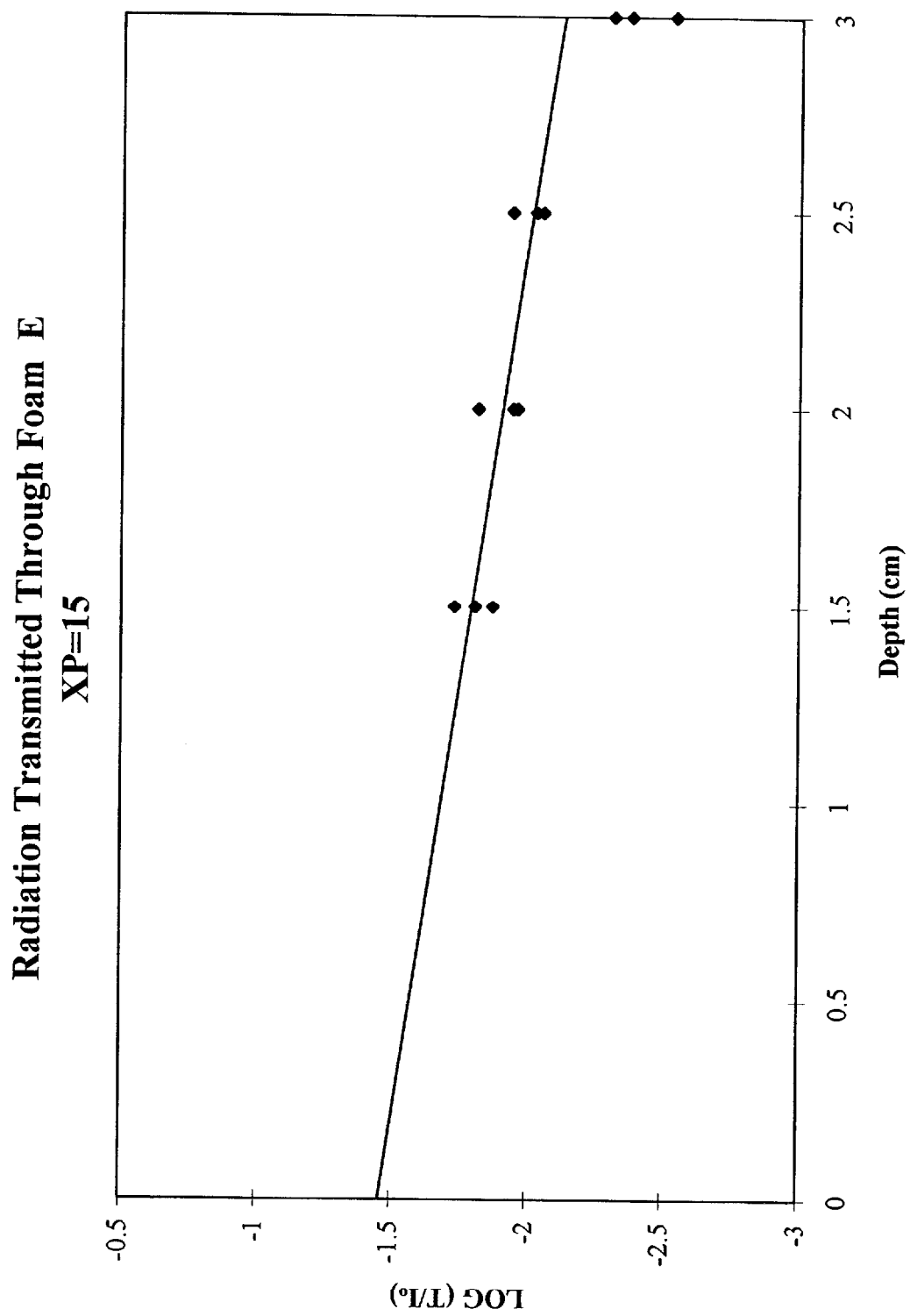


Figure B1 Radiation Absorption Through Foam E, XP=15

# **Radiation Transmitted Through Foam E** **XP=20**

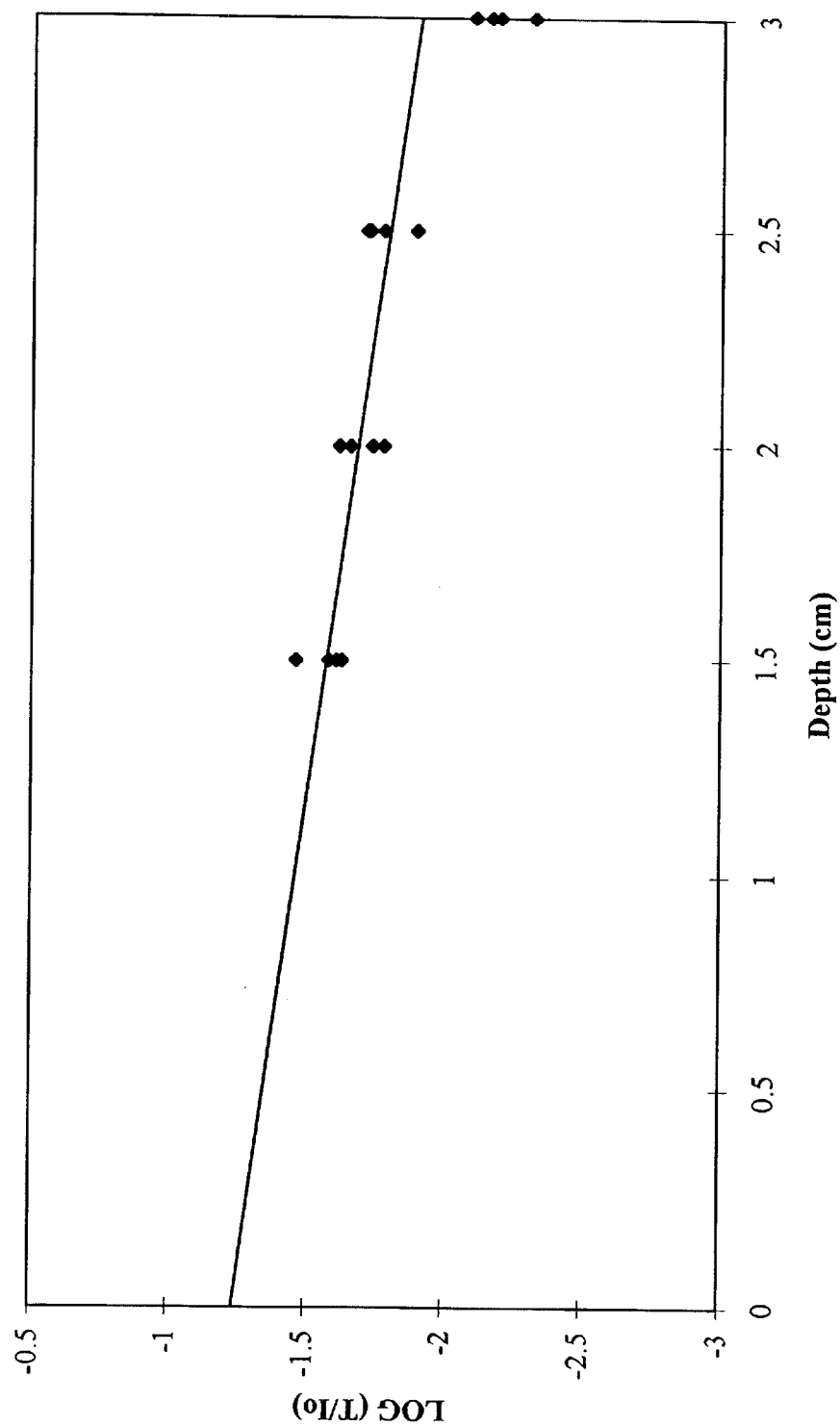


Figure B2 Radiation Absorption Through Foam E, XP=20

# Radiation Transmitted Through Foam E XP=25

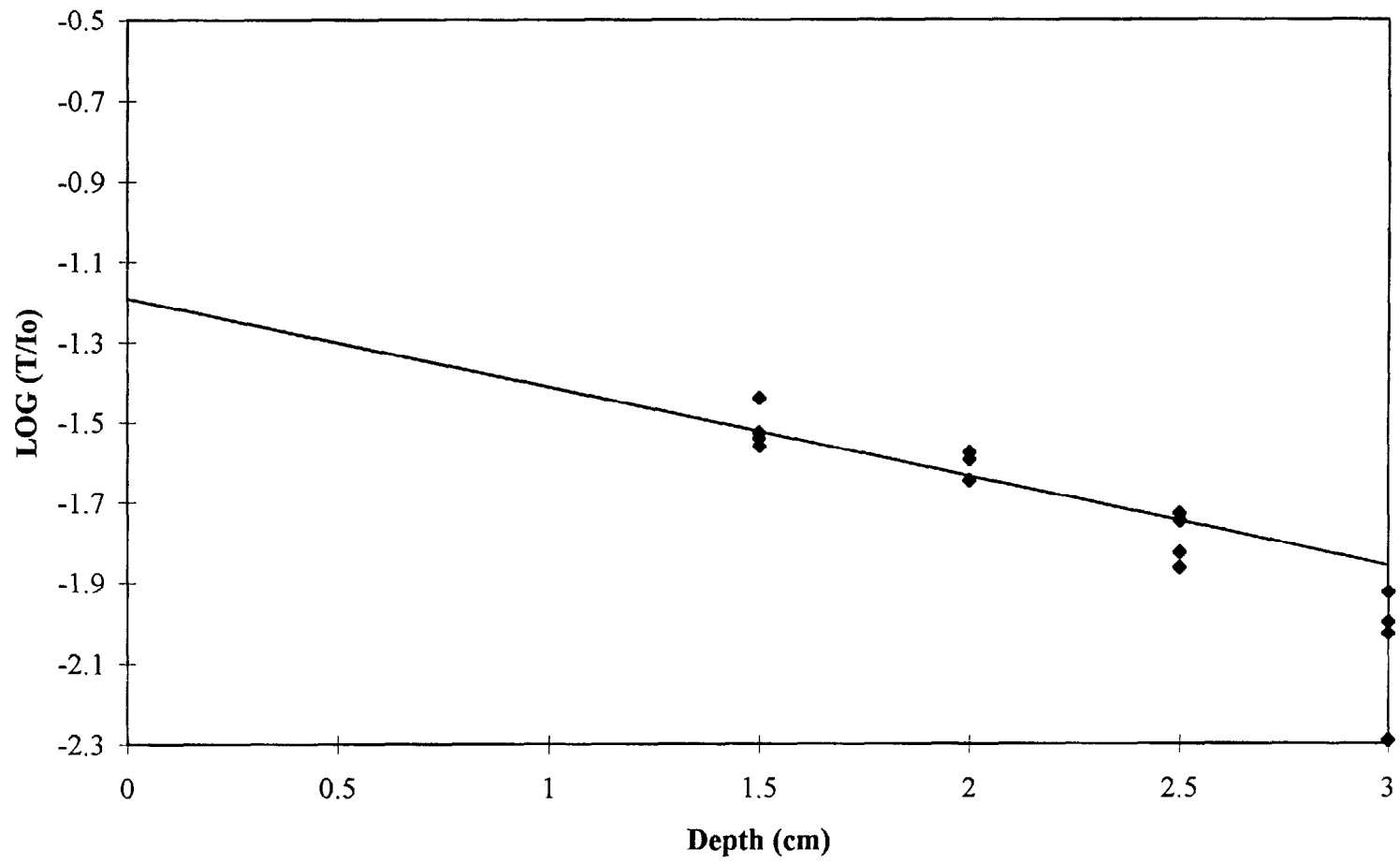
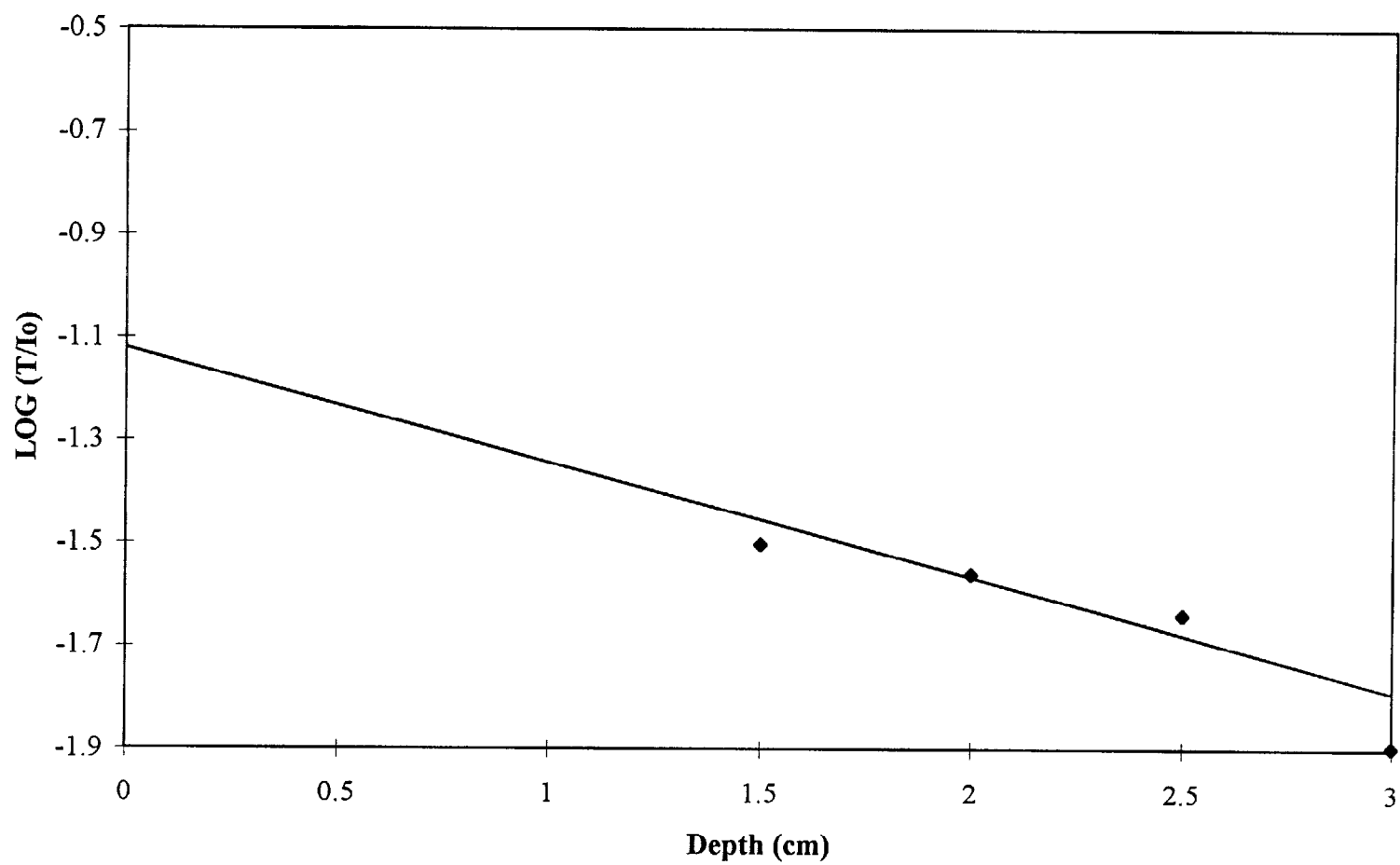


Figure B3 Radiation Absorption Through Foam E, XP=25

# Radiation Transmitted Through Foam E XP=30

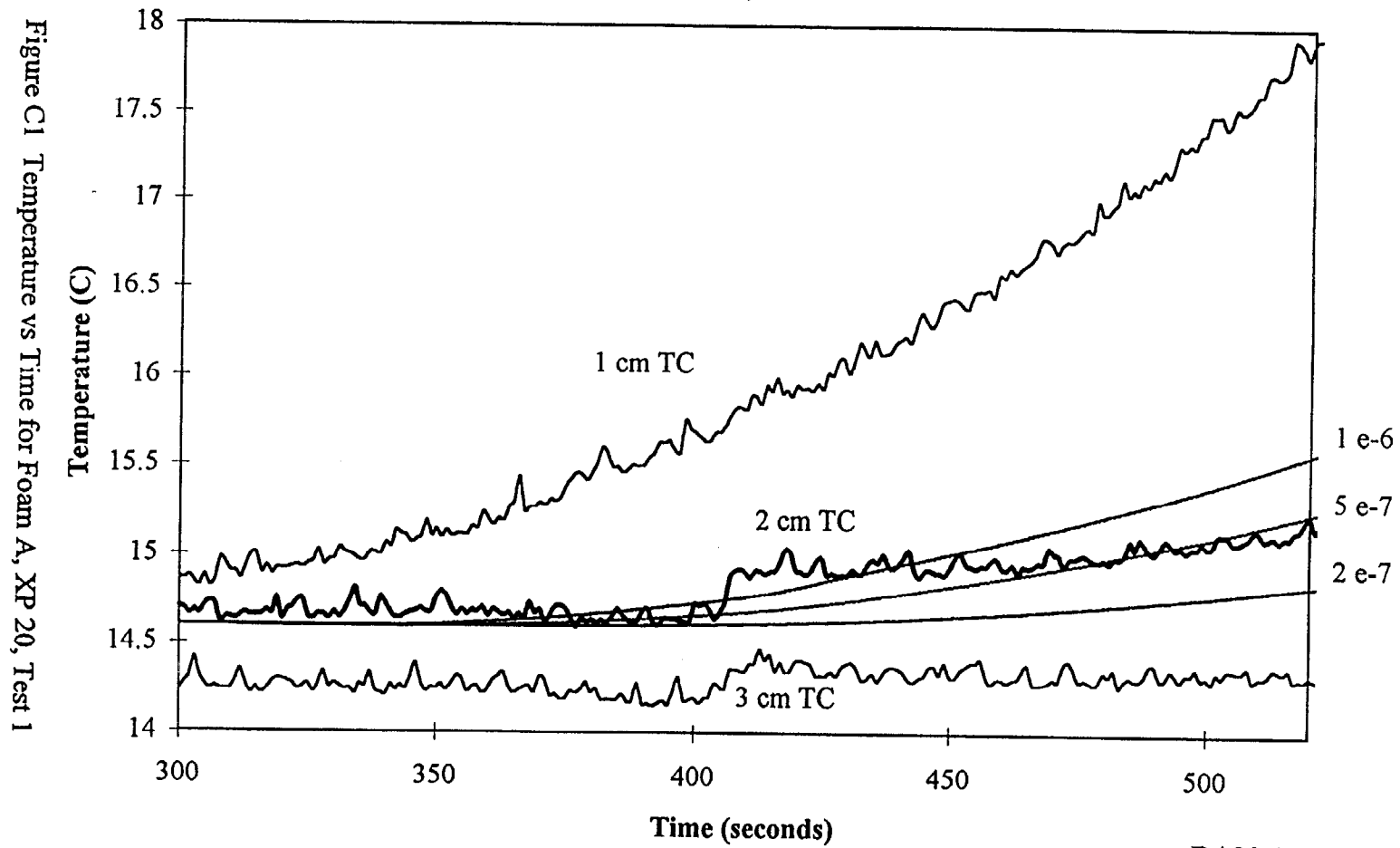
Figure B4 Radiation Absorption Through Foam E, XP=30



## **APPENDIX C**

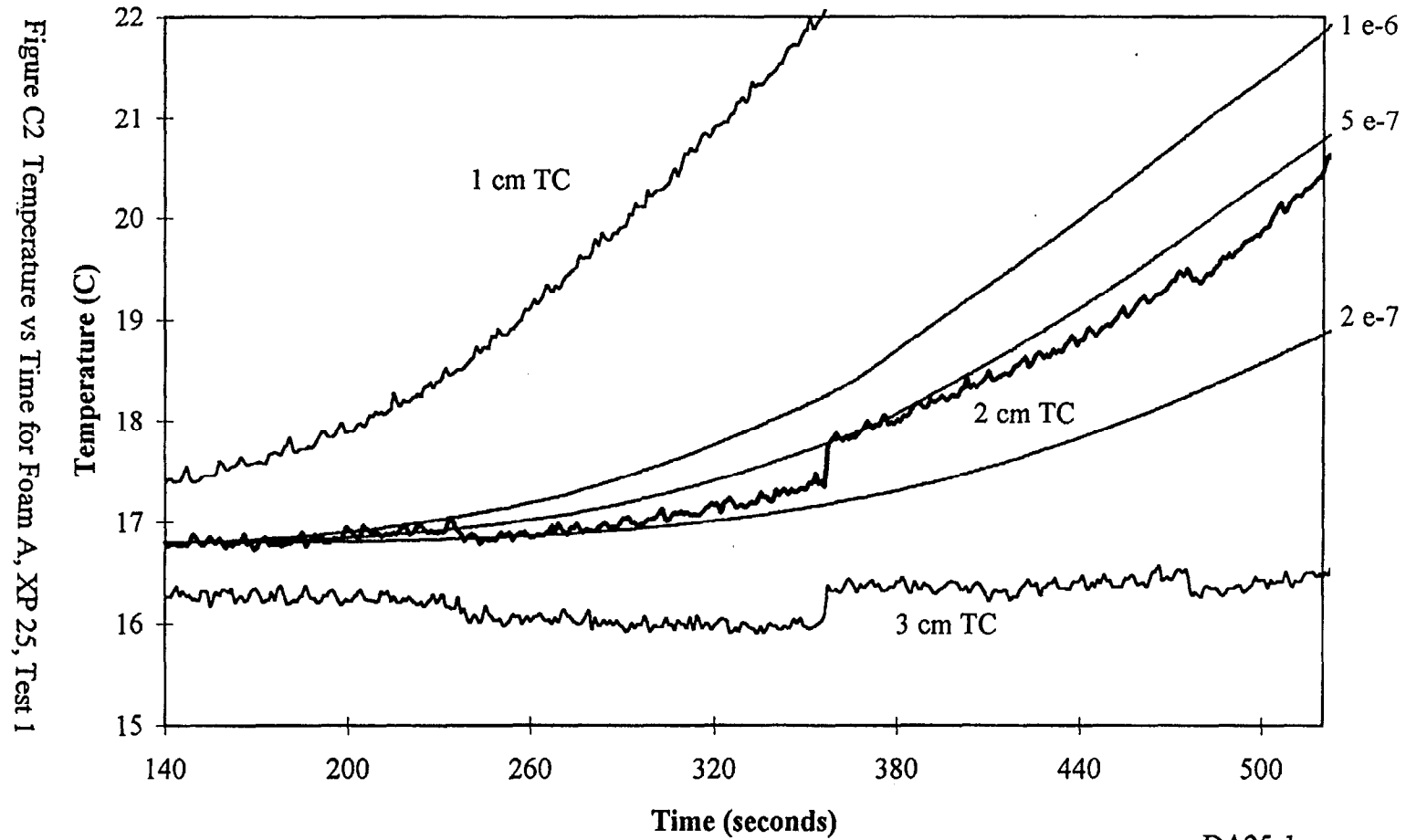
### **Thermal Diffusivity Data**

# Temperature vs Time for Foam A XP=20, Test 1



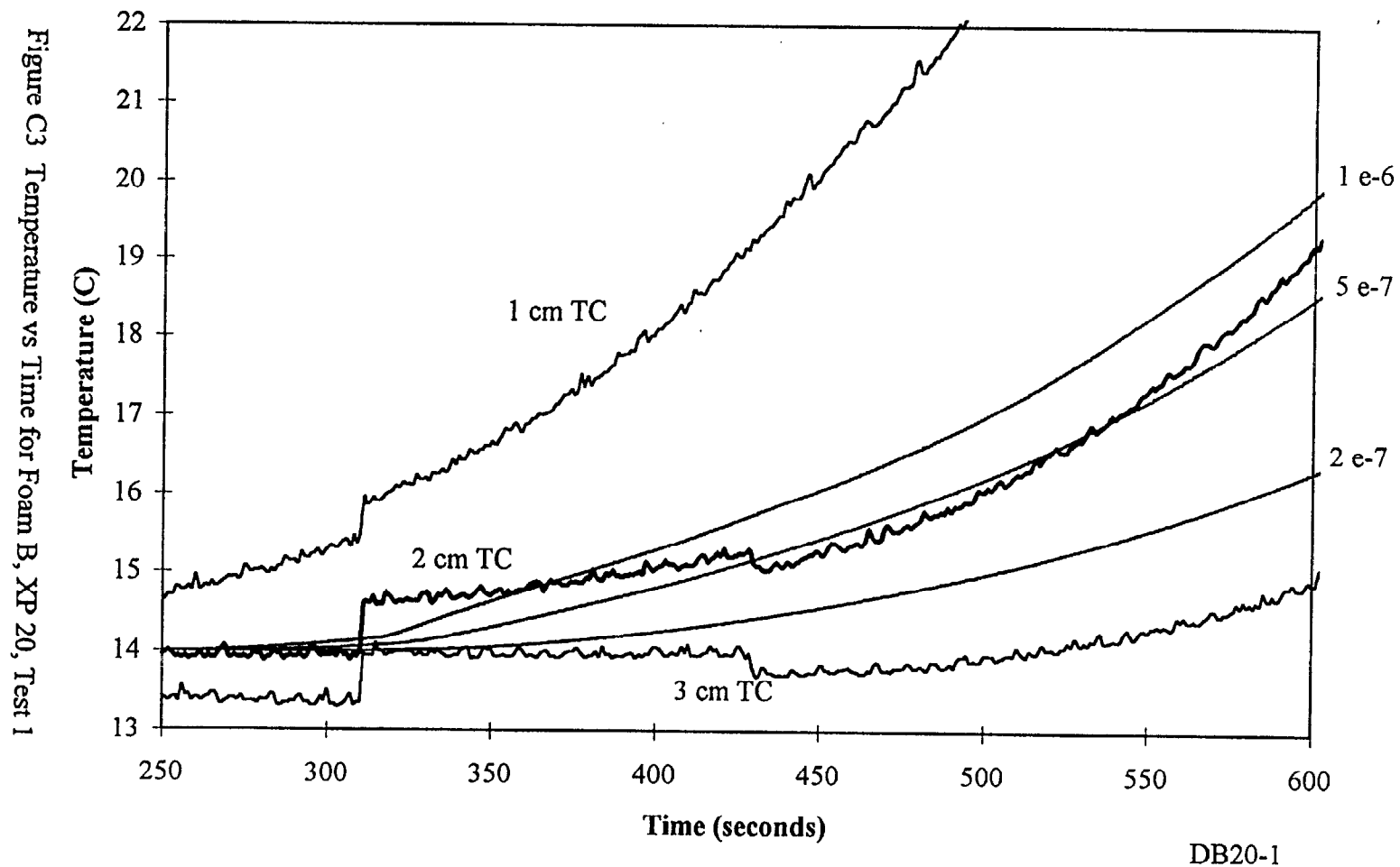
DA20-1

# Temperature vs Time for Foam A XP=25, Test 1

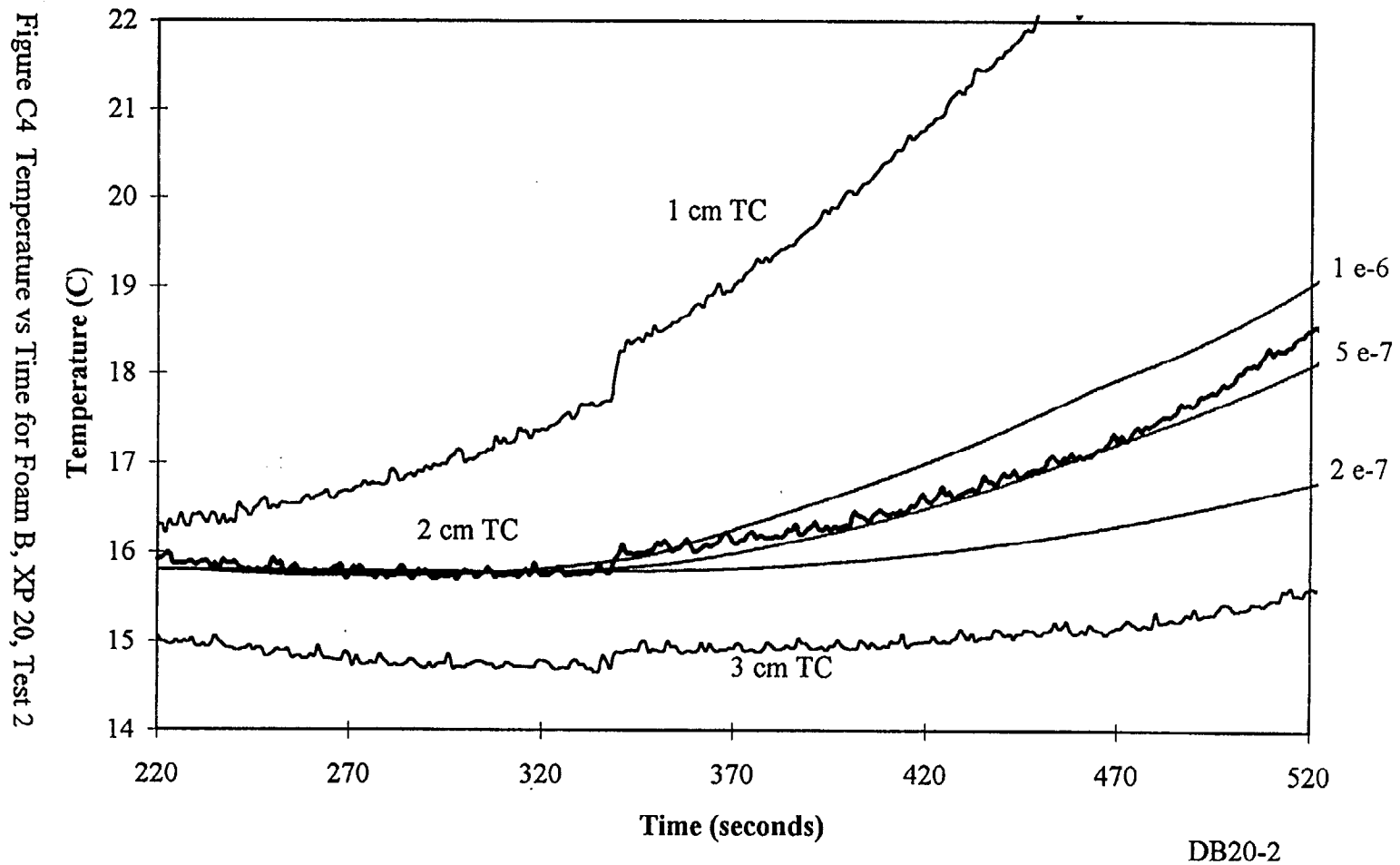




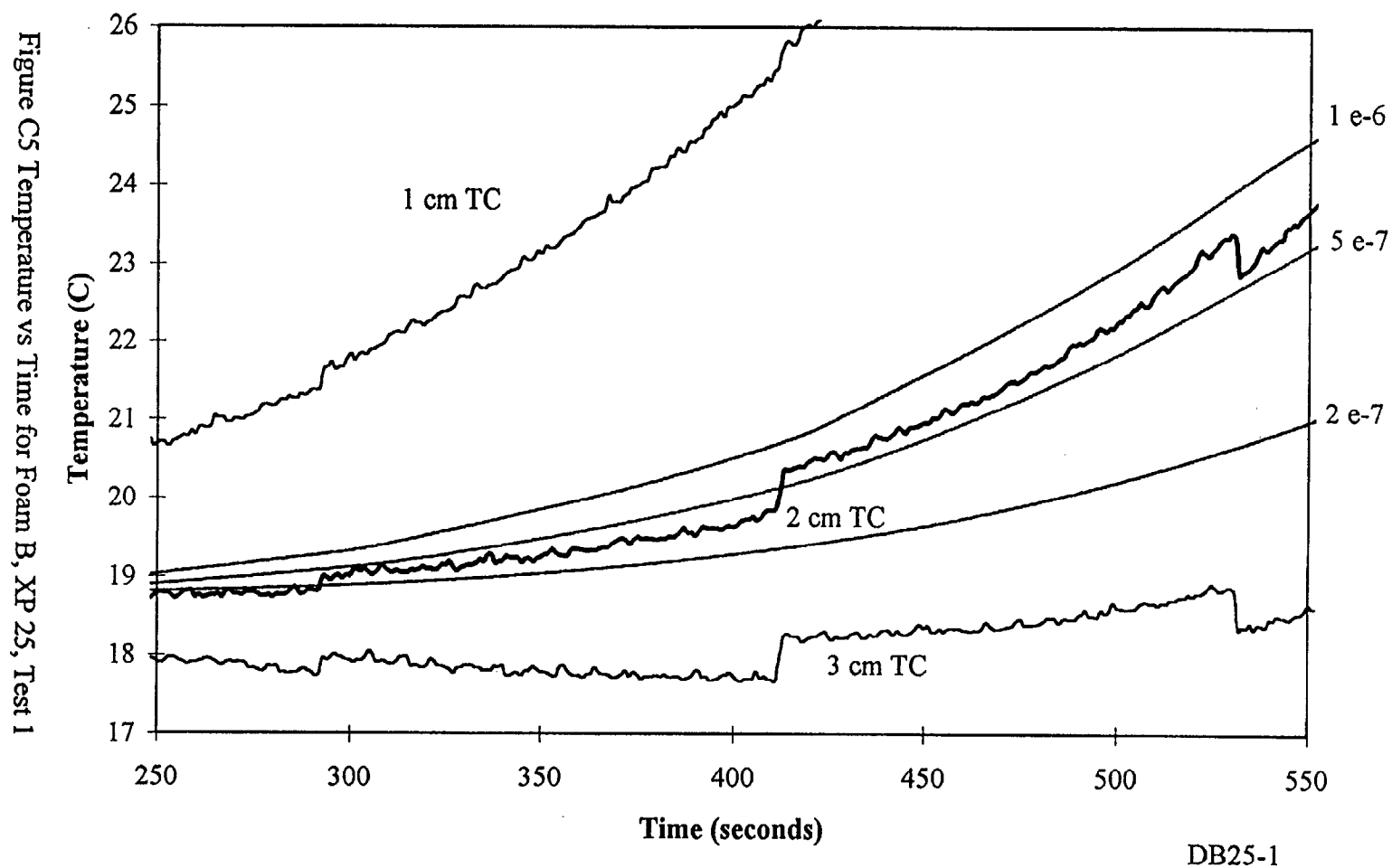
### Temperature vs Time for Foam B XP=20, Test 1



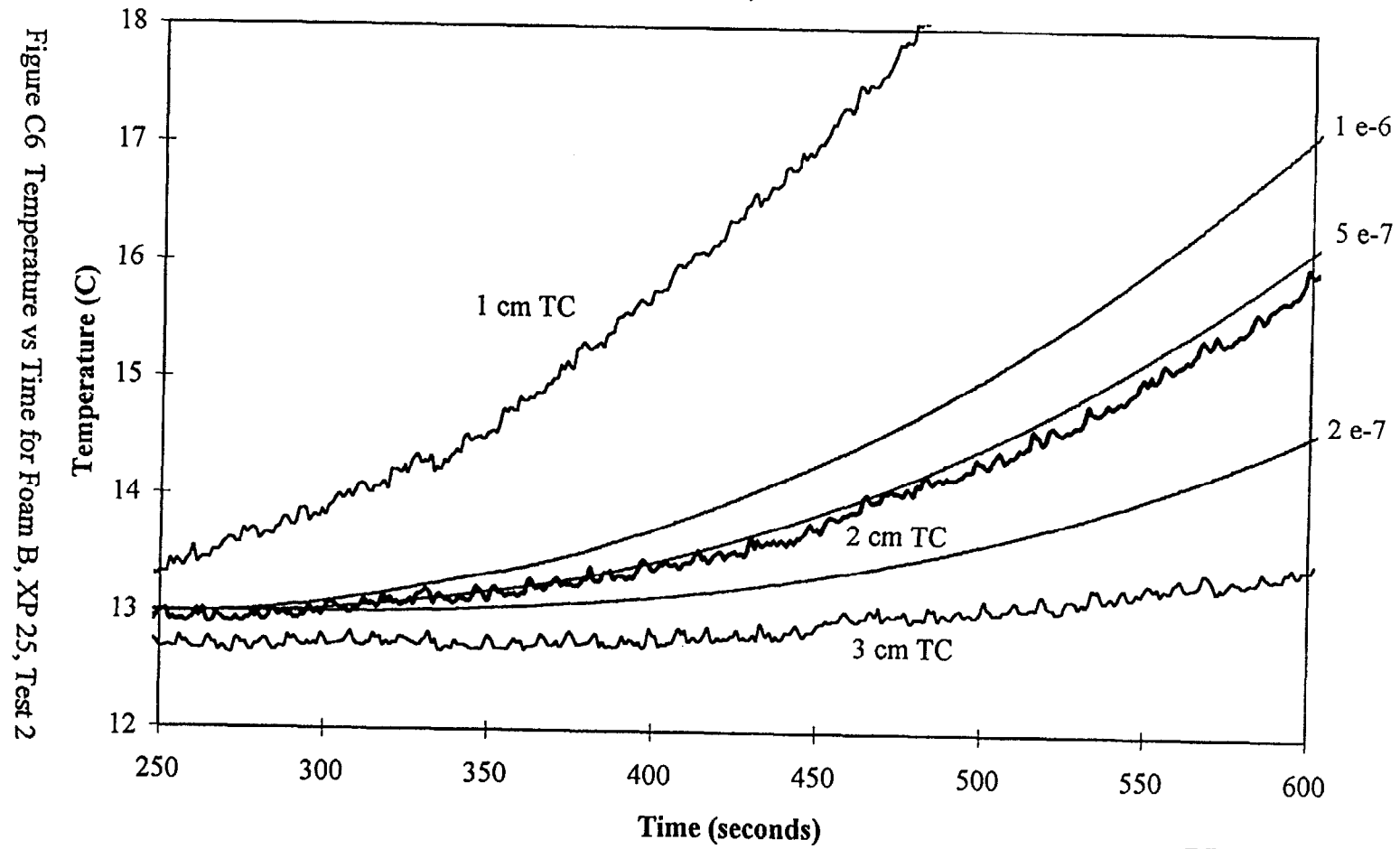
# Temperature vs Time for Foam B XP=20, Test 2



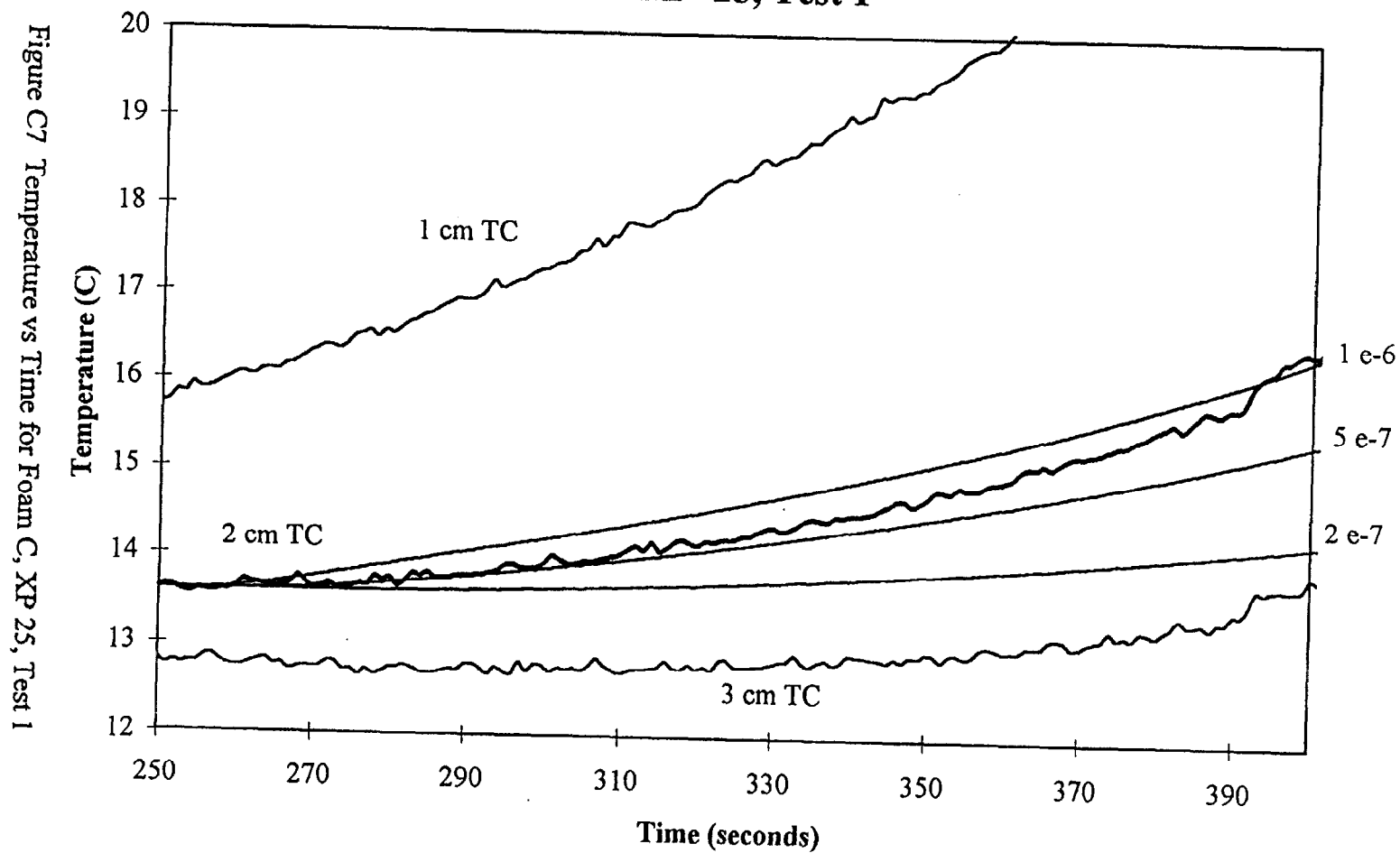
# Temperature vs Time for Foam B XP=25, Test 1



# Temperature vs Time for Foam B XP=25, Test 2

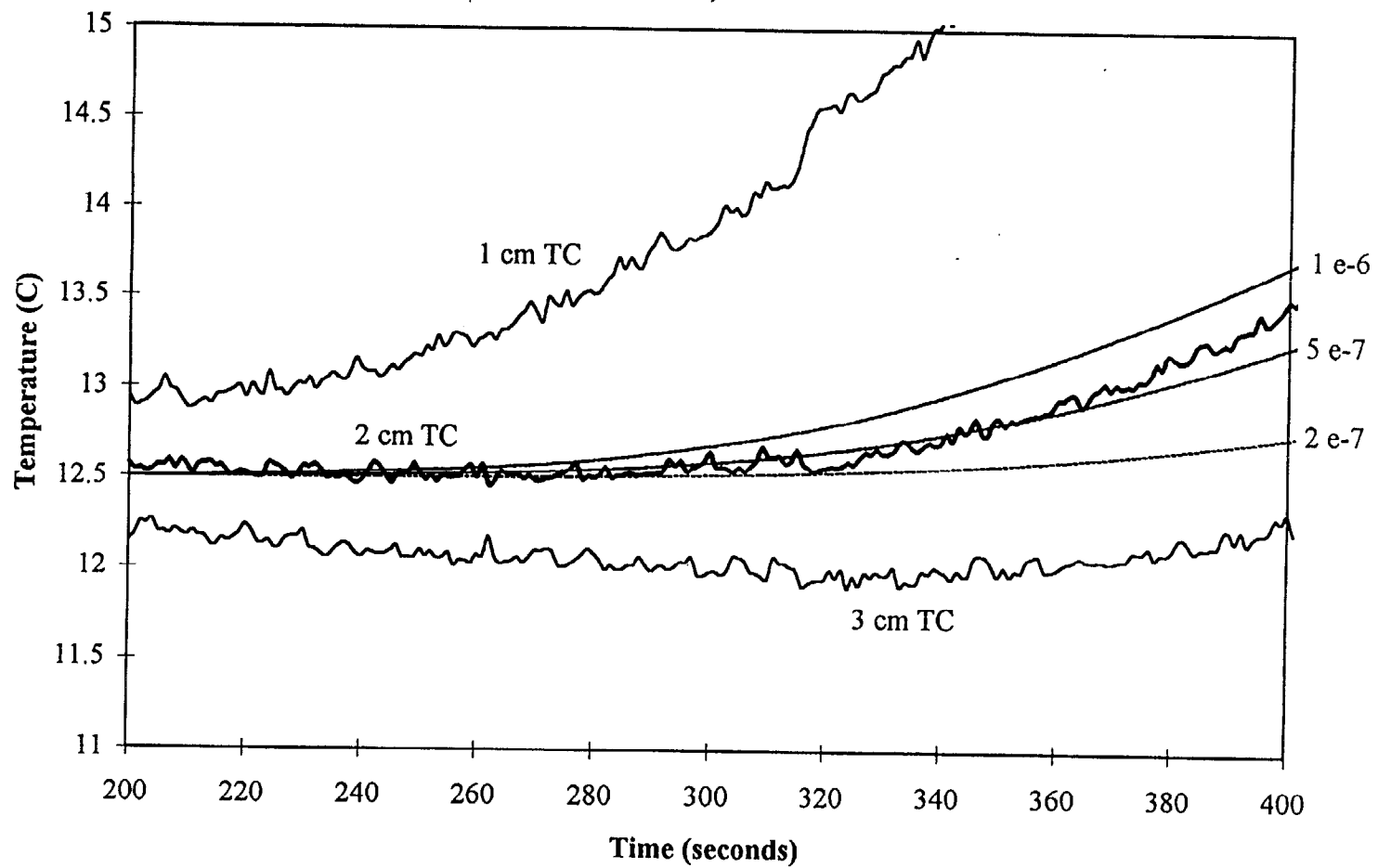


# Temperature vs Time for Foam C XP=25, Test 1



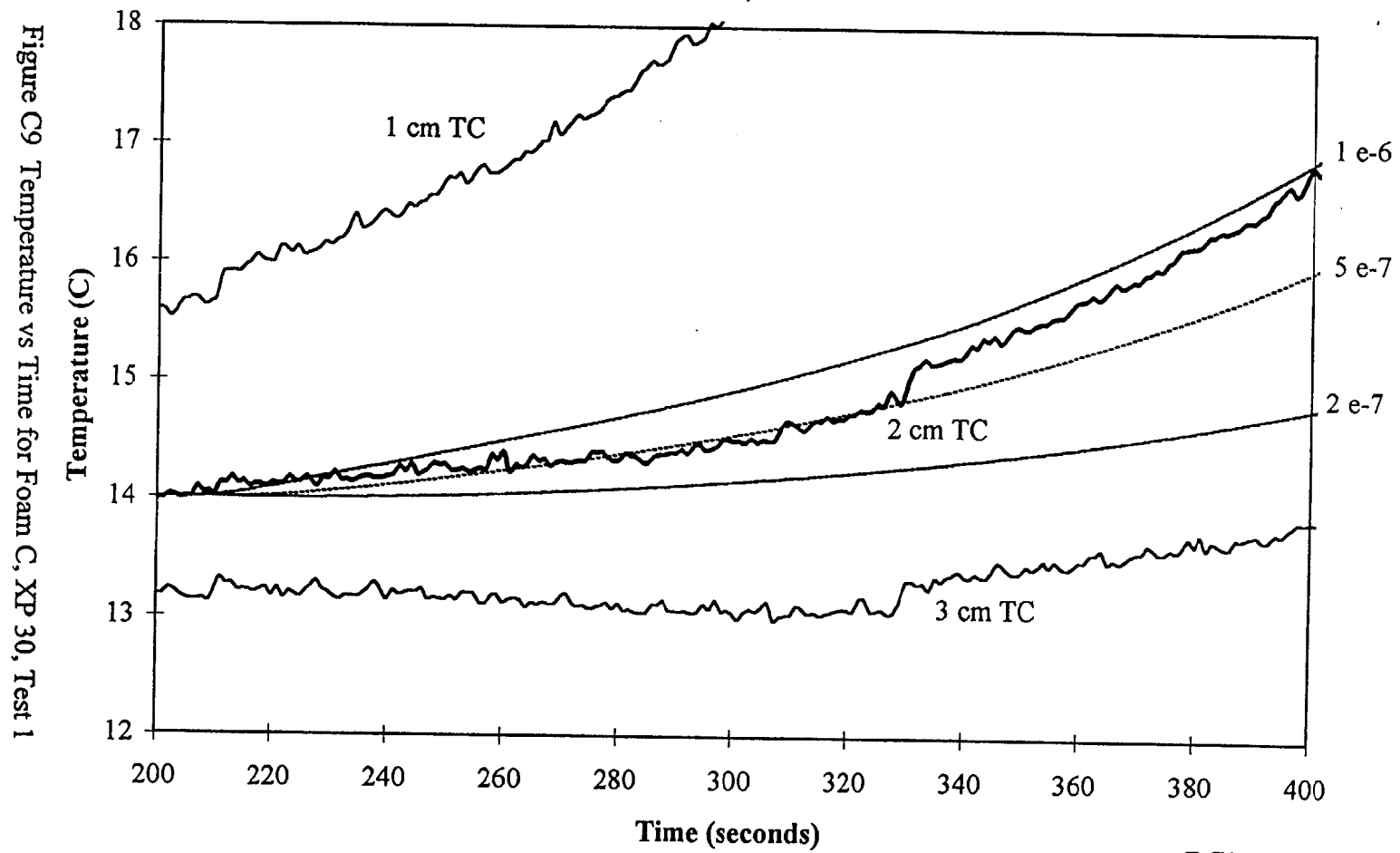
# Temperature vs Time for Foam C XP=25, Test 2

Figure C8 Temperature vs Time for Foam C, XP 25, Test 2



DC25-2

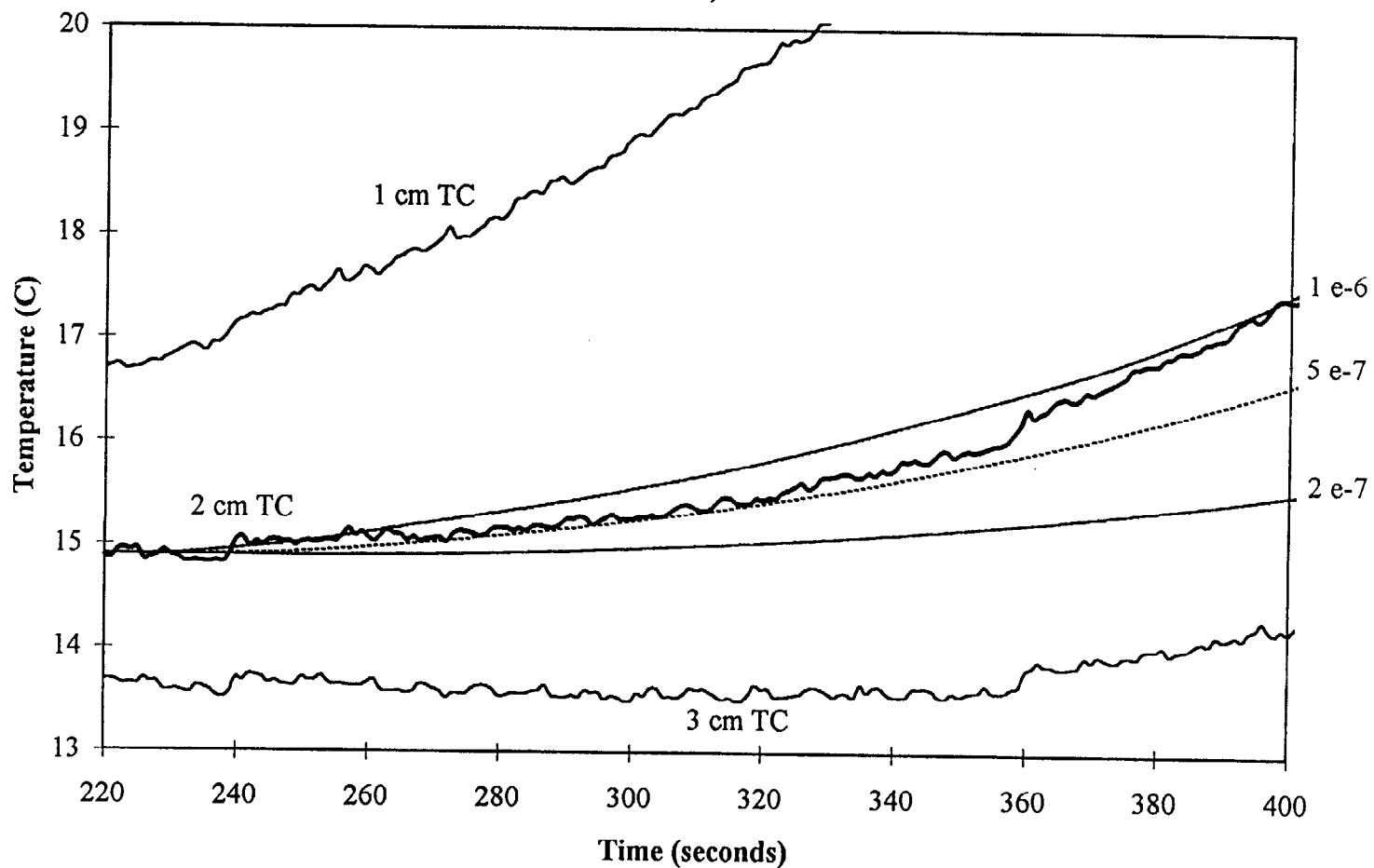
# Temperature vs Time for Foam C XP=30, Test 1



DC30-1

# Temperature vs Time for Foam C XP=30, Test 2

Figure C10 Temperature vs Time for Foam C, XP 30, Test 2

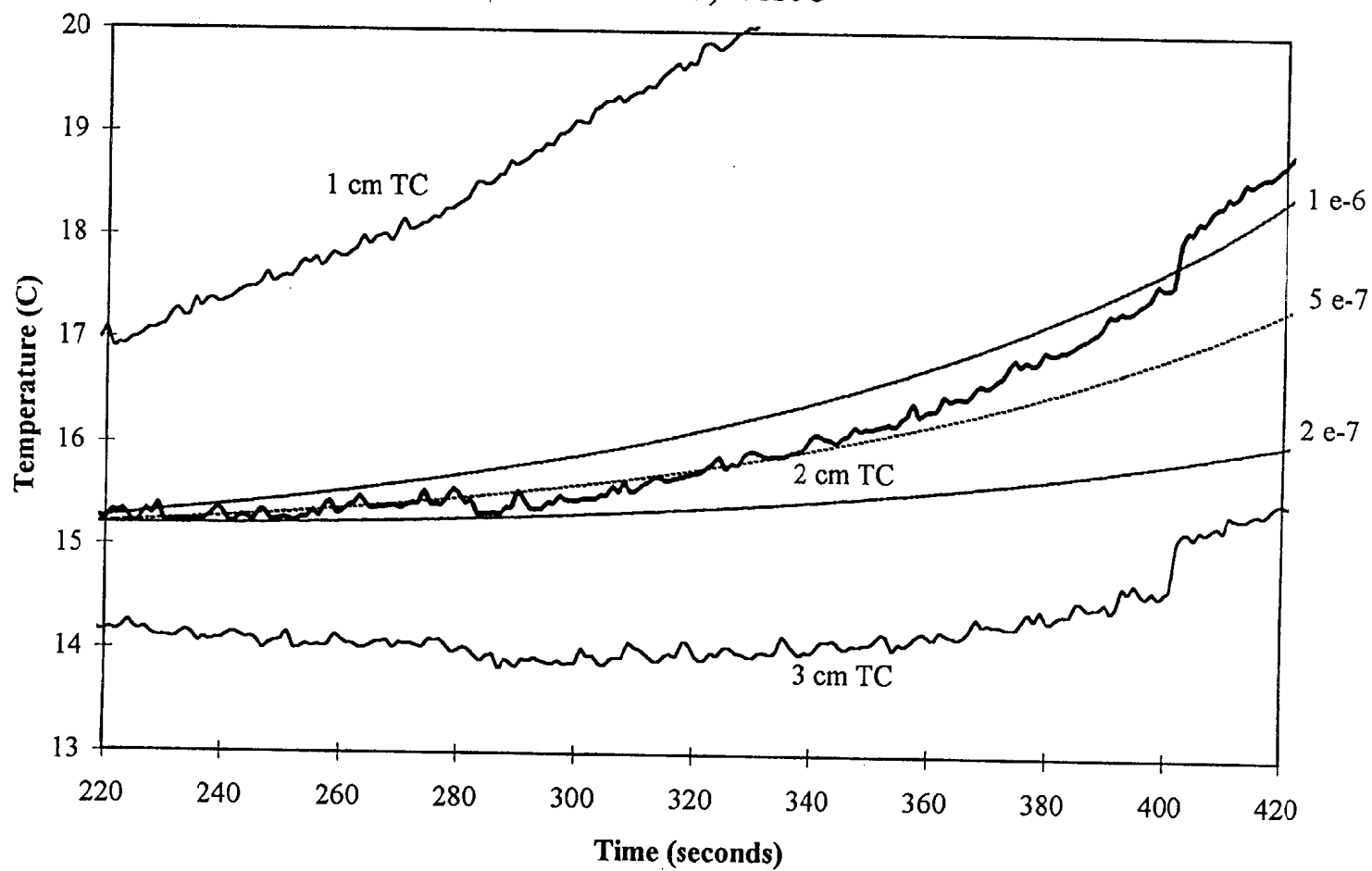


DC30-2



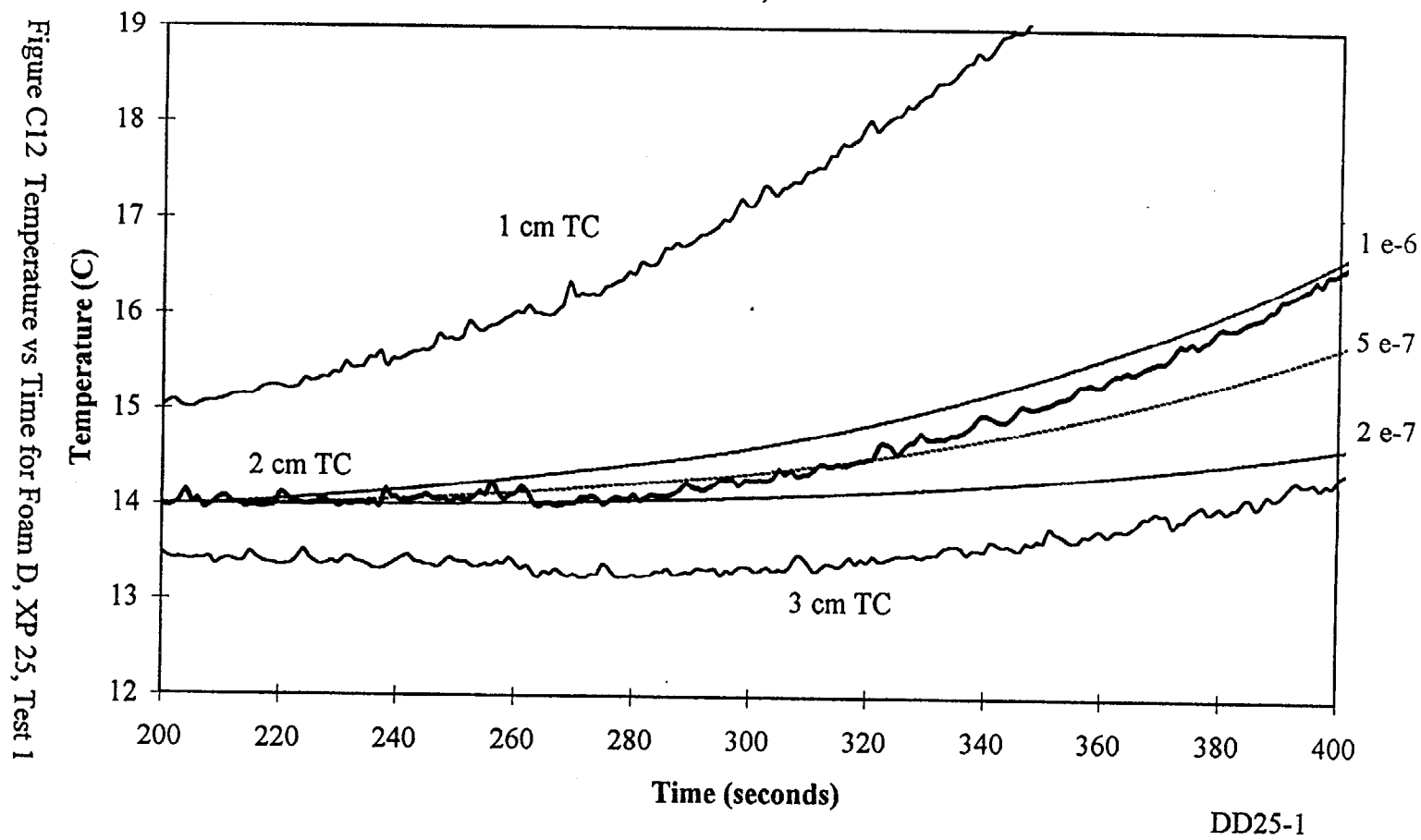
# Temperature vs Time for Foam C XP=30, Test 3

Figure C11 Temperature vs Time for Foam C, XP 30, Test 3

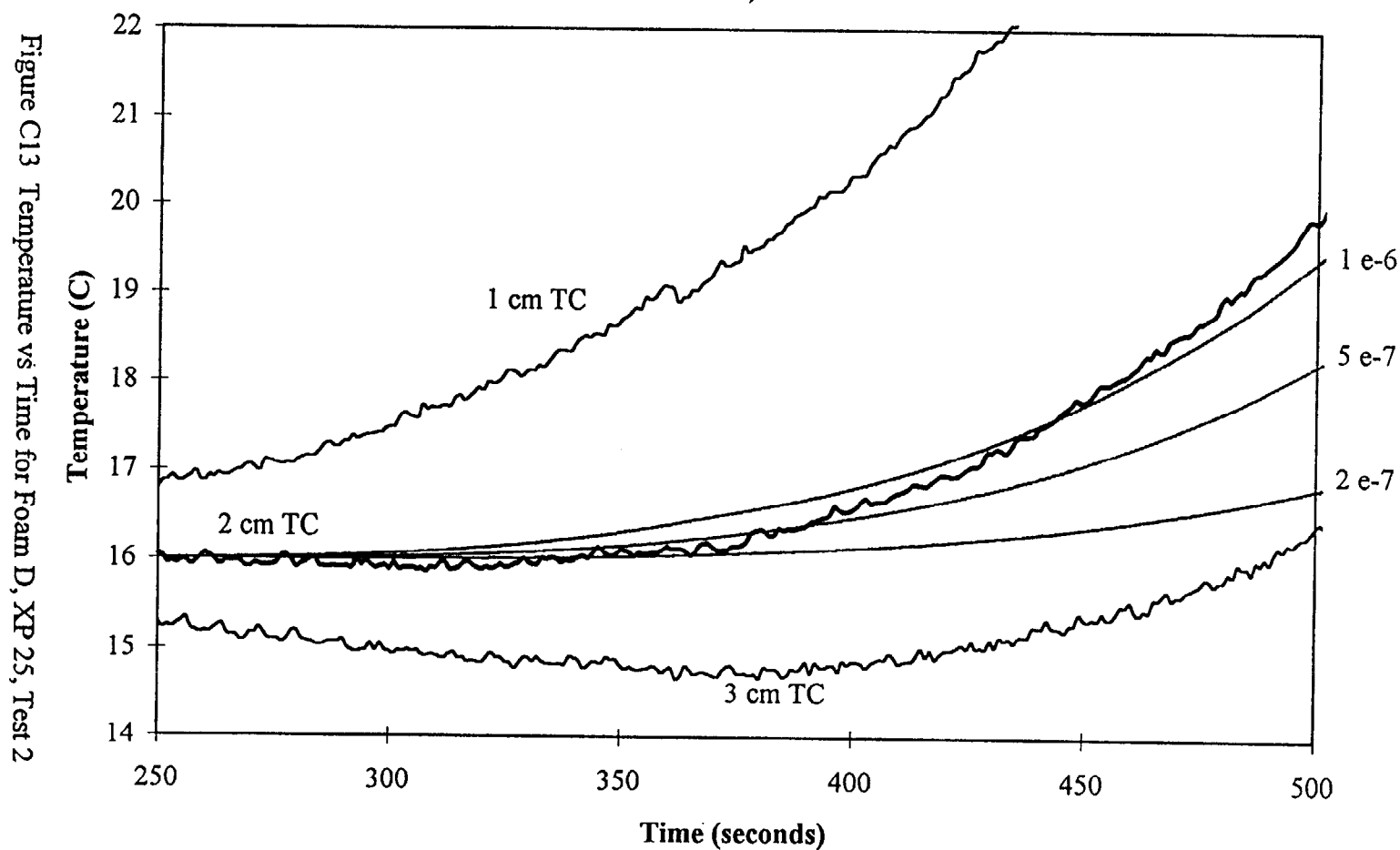


DC30-3

# Temperature vs Time for Foam D XP=25, Test 1



# Temperature vs Time for Foam D XP=25, Test 2



DD25-2

# Temperature vs Time for Foam D XP=30, Test 1

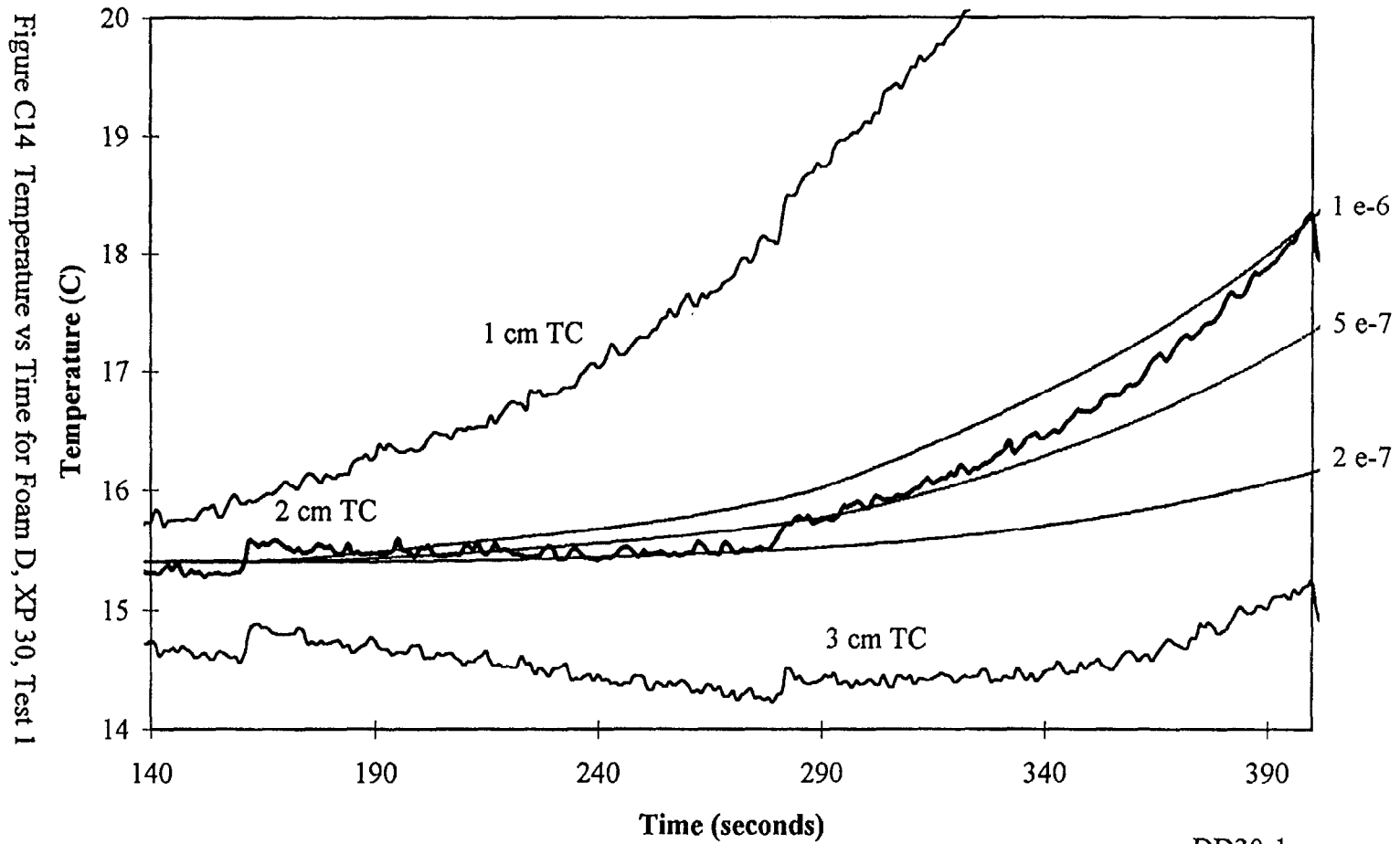


Figure C15 Temperature vs Time for Foam E, XP=15, Test 1

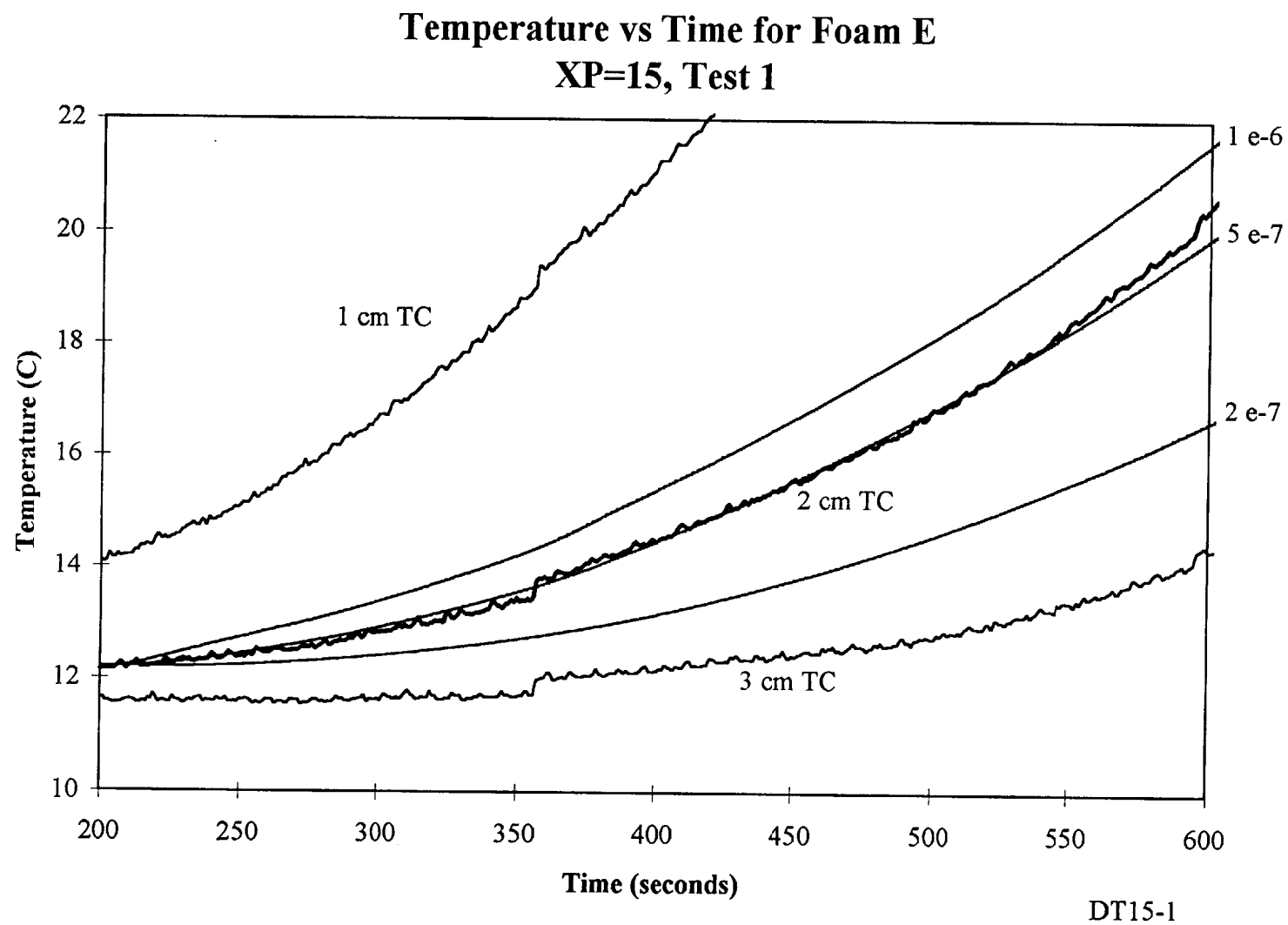
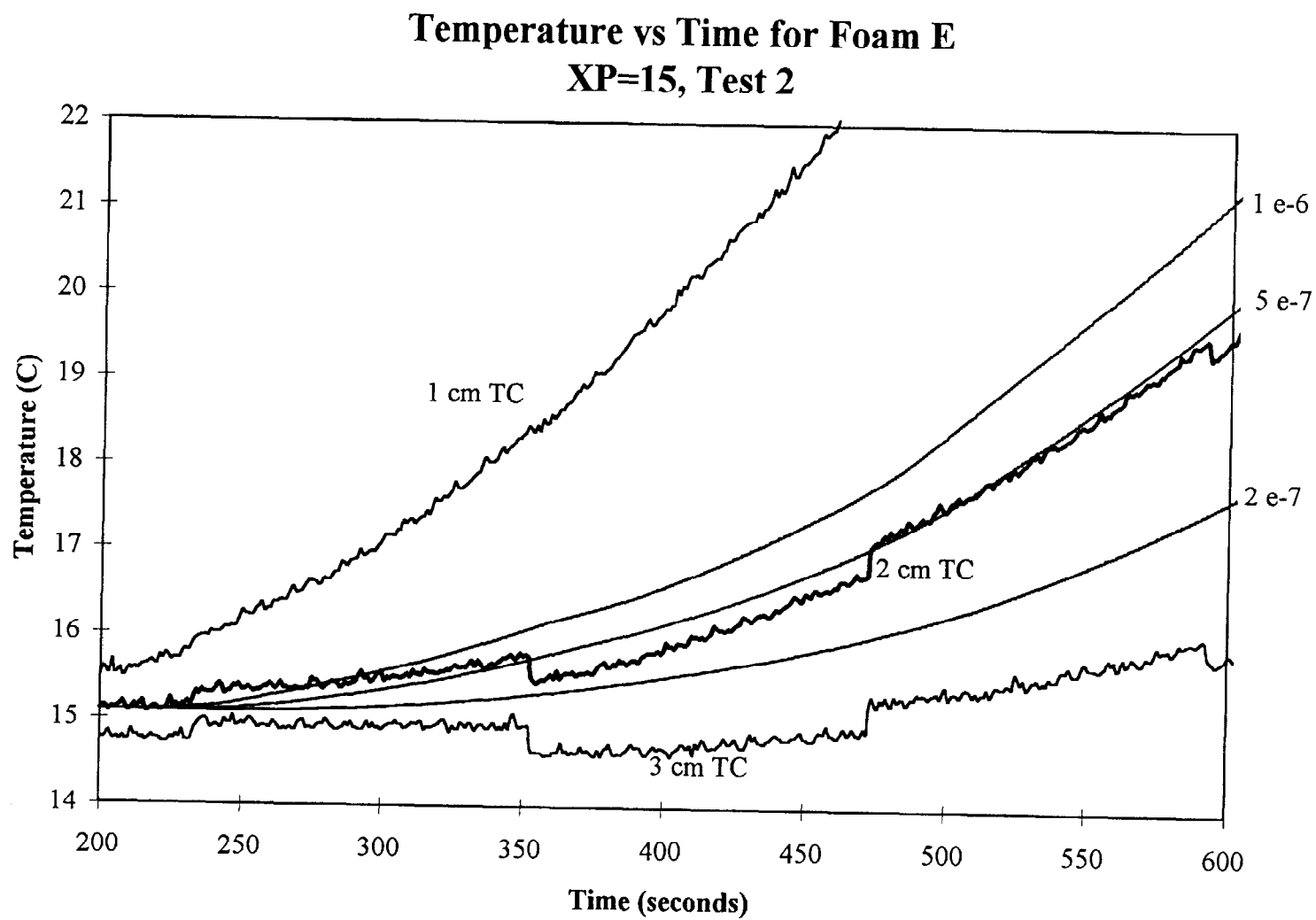


Figure C16 Temperature vs Time for Foam E, XP=15, Test 2



DT15-2

Figure C17 Temperature vs Time for Foam E, XP=20, Test 1

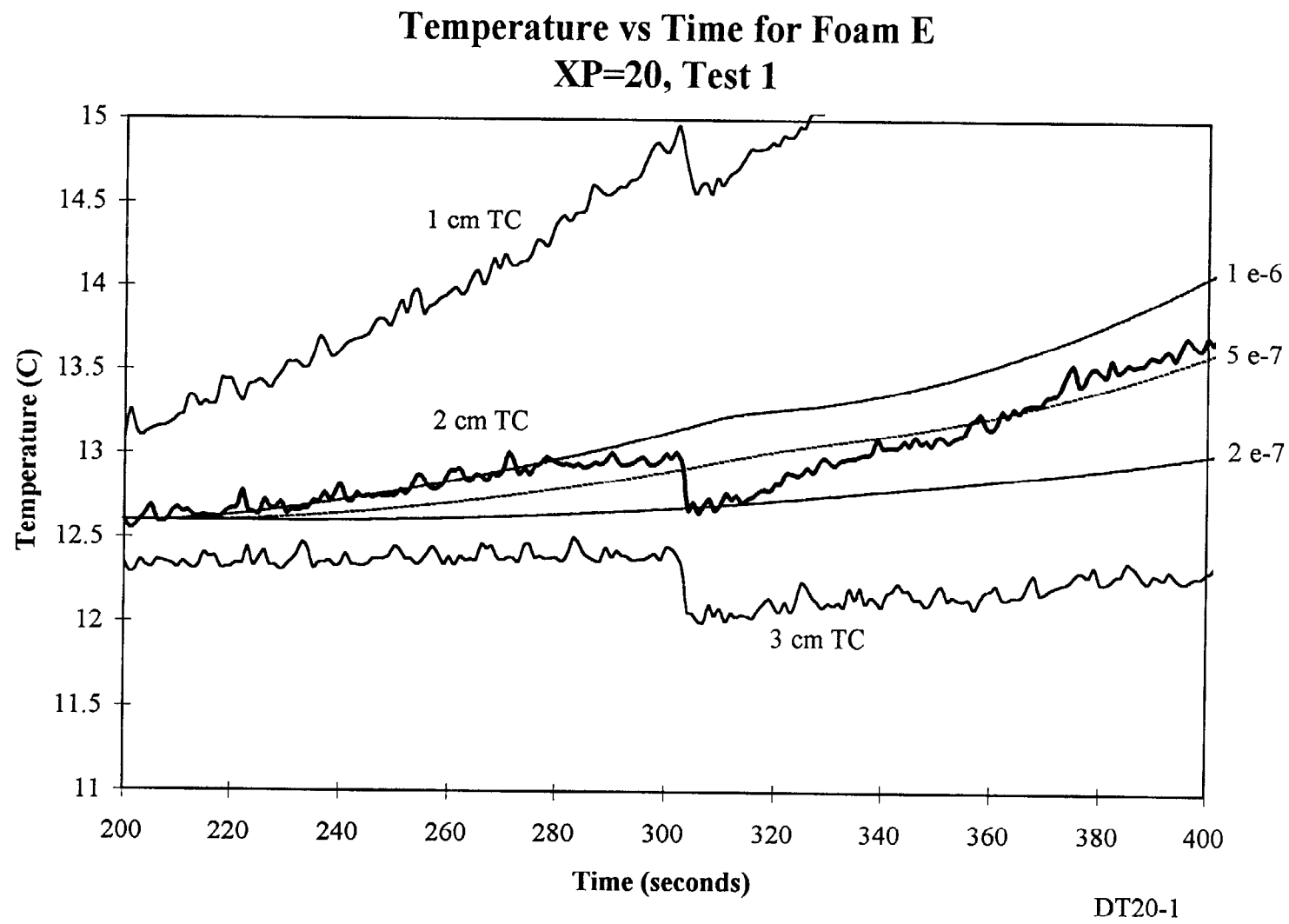


Figure C18 Temperature vs Time for Foam E, XP=20, Test 2

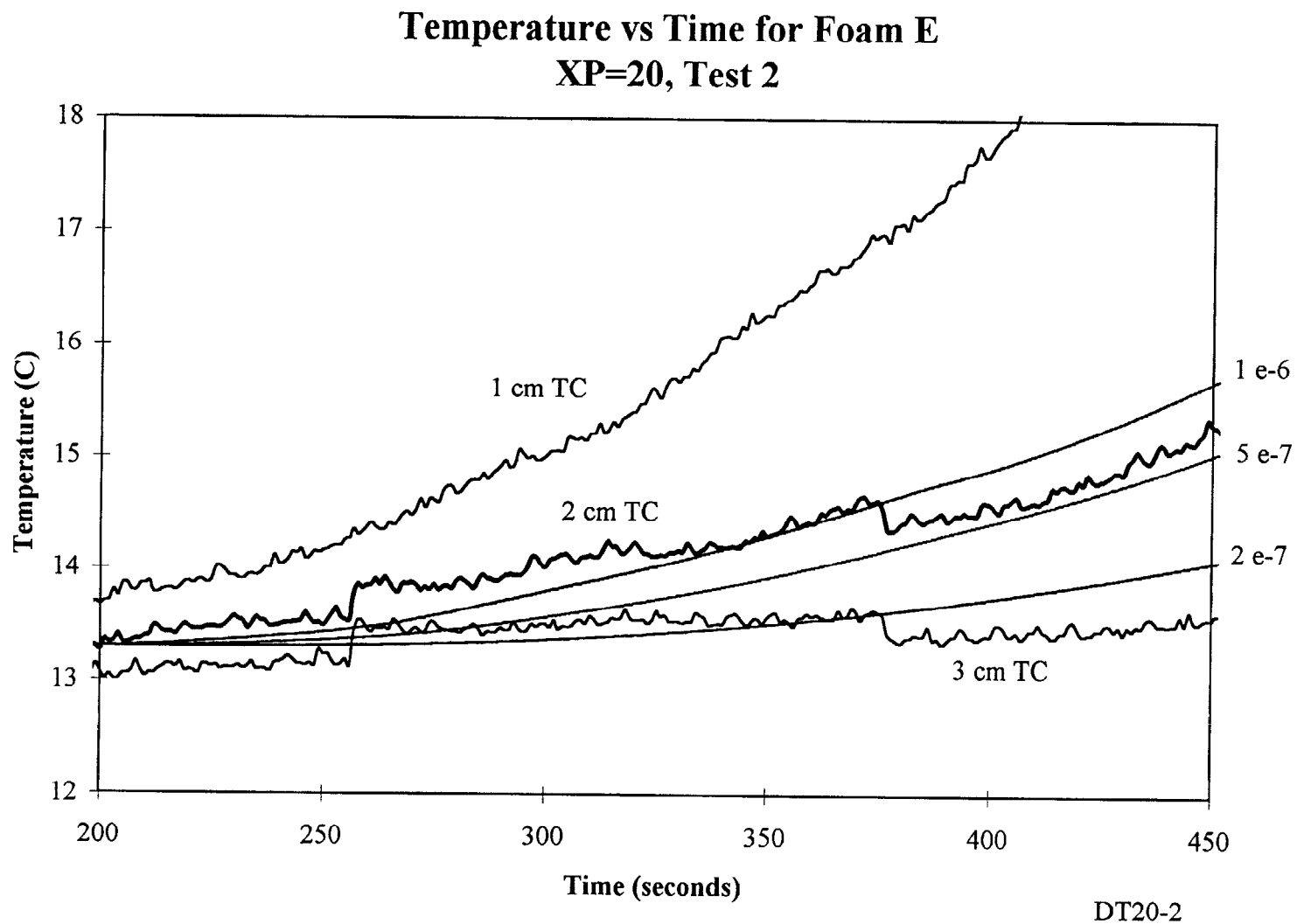




Figure C19 Temperature vs Time for Foam E, XP=25, Test 1

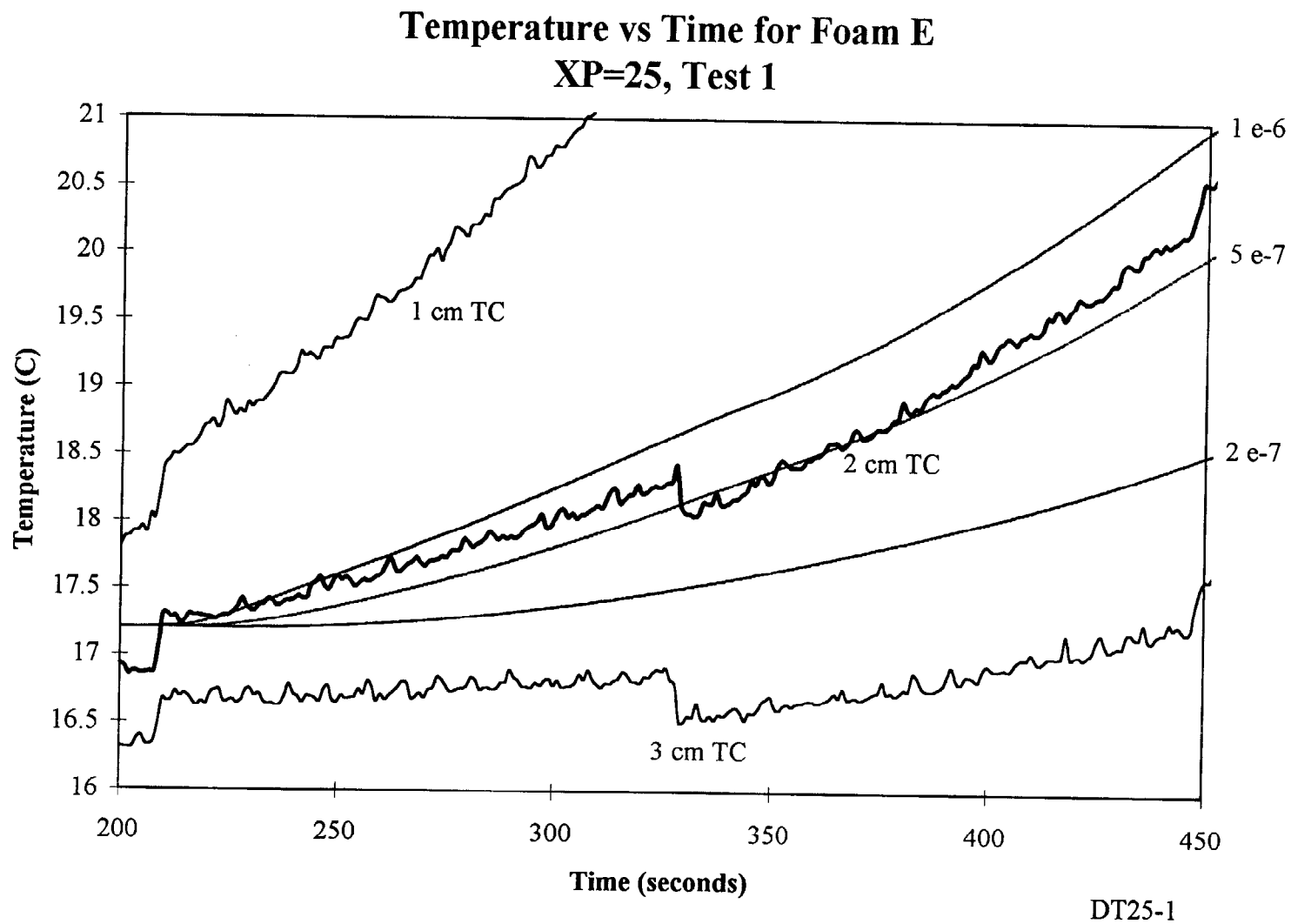
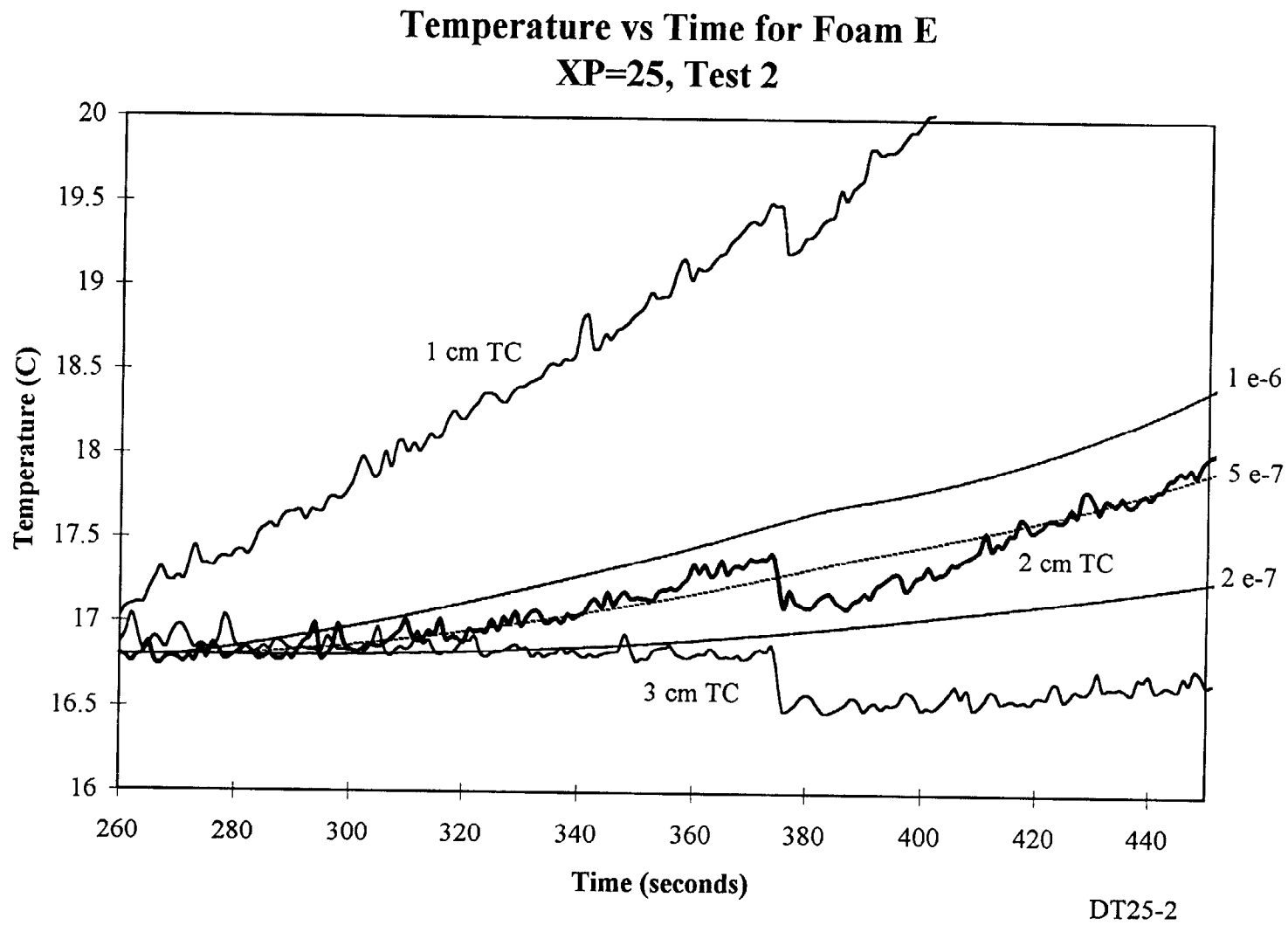


Figure C20 Temperature vs Time for Foam E, XP=25, Test 2



## **APPENDIX D**

### Fortan Programs

## REDUCTION OF DATA PROGRAM

### PROGRAM REDUCE

- c Fortran Program REDUCE.FOR
- c This program is intended to reduce the file size and average the
- c thermocouple data for the thermal diffusivity test. The initial
- c data file has seven columns of data, the first column is the time,
- c while the last six are thermocouple readings. The first and fourth,
- c second and fifth, and third and sixth thermocouple are at the same
- c height in the experiment therefore will be averaged.
- c Variables used:
- c LINE1 :First line of data in file not needed
- c INFILE :Input file with data
- c OUTFILE :Output file for reduced data
- c DATA1..6 :Actual data values read from infile for columns 1..6
- c SUM1..3 :Cumulative sum of data from infile
- c AVG1..3 :Final average of data over 2N data points
- c TIME :Time during test
- c N :Number of data points to average per thermocouple
- c COUNT :Status number for how many data points have been summed

```
CHARACTER*1 LINE1(108)
CHARACTER*20 INFILE, OUTFILE
CHARACTER*1 DATE1(9),TIME1(8)
REAL*8 DATA1,DATA2,DATA3,DATA4,DATA5,DATA6
REAL*8 AVG1,AVG2,AVG3
REAL*8 SUM1,SUM2,SUM3
REAL*8 TIME
INTEGER N,COUNT
```

- c Main Program body begins
- c Open data file, open new output file for reduced data
- PRINT \*, 'ENTER NAME OF DATA FILE'
- READ '(A)', INFILE
- OPEN (UNIT=15, FILE=INFILE, STATUS='OLD')
- PRINT \*, 'ENTER NAME OF OUTPUT FILE'
- READ '(A)', OUTFILE
- OPEN (UNIT=16, FILE=OUTFILE, STATUS='NEW')
- c Read in the first line of text preceeding actual data

READ (15,910) LINE1

c Set constants and time counter

EOF = 1

N=20

TIME=0

c Begin Loop for reduction of data

5 IF (EOF .GE. 1) THEN

COUNT = 0

SUM1=0

SUM2=0

SUM3=0

10 IF (COUNT .LT. N) THEN

READ (15,920,END=999) DATE1,TIME1,DATA1,DATA2,

2 DATA3,DATA4,DATA5,DATA6

SUM1=SUM1+DATA1+DATA4

SUM2=SUM2+DATA2+DATA5

SUM3=SUM3+DATA3+DATA6

COUNT=COUNT+1

IF (COUNT .eq. (N/2)) TIME=TIME+1

GO TO 10

END IF

AVG1=SUM1/(2\*N)

AVG2=SUM2/(2\*N)

AVG3=SUM3/(2\*N)

WRITE (16,930) TIME, AVG1, AVG2, AVG3

GO TO 5

END IF

c Format Lines

910 FORMAT (108A )

920 FORMAT (9A,1X,8A,1X,6(F8.5,1X))

930 FORMAT (F10.5,2X,F8.5,2X,F8.5,2X,F8.5)

950 FORMAT (6(2X,F8.5))

999 CONTINUE

END

## NUMERICAL SOLUTION TO CONDUCTION EQUATION

### Program DIFFUSE

- c Foam temperature history calculations based on one dimensional
- c heat flux on a semi-infinite plate.
- c n number of nodes
- c u\*in input data to Crank Nicholson
- c u\*out output data from Crank Nicholson
- c infile input file specification
- c outfile output file specification
- c alpha\* Values chosen to investigate thermal diffusivity
- c tinit Initial temperature of foam
- c dt Time step
- c dx Spatial step for nodes= 2cm / #nodes

### PARAMETER (n=101)

```
implicit double precision (a-h,o-z)
double precision uin(1000),uout(1000)
double precision u2in(1000),u2out(1000)
double precision u3in(1000),u3out(1000)
double precision u4in(1000),u4out(1000)
double precision u5in(1000),u5out(1000)
double precision u6in(1000),u6out(1000)
double precision u7in(1000),u7out(1000)
character *20, OUTFILE,INFILE
```

- c The body of the main program

```
alpha1=1.e-7
alpha2=2.e-7
alpha3=5.e-7
alpha4=10.e-7
alpha5=2.e-6
alpha6=5.e-6
alpha7=10.e-6
```

```
PRINT *, 'ENTER NAME OF INPUT FILE'
READ '(A)', INFILE
PRINT *, 'ENTER NAME OF OUTPUT FILE'
READ '(A)', OUTFILE
write(*,*) 'Enter the initial temperature '
read(*,*) Tinit
```

```
dt=1.  
dx=0.02/n
```

```
a1=alpha1/(dx*dx)  
a2=alpha2/(dx*dx)  
a3=alpha3/(dx*dx)  
a4=alpha4/(dx*dx)  
a5=alpha5/(dx*dx)  
a6=alpha6/(dx*dx)  
a7=alpha7/(dx*dx)
```

```
print*, "Alpha = ", a1, "to", a7  
print*, "Alpha1*dt = ", a1*dt
```

- c Set the initial temperatures throughout foam  
do 25 i=1,n  
  uin(i)=Tinit  
  u2in(i)=Tinit  
  u3in(i)=Tinit  
  u4in(i)=Tinit  
  u5in(i)=Tinit  
  u6in(i)=Tinit  
  u7in(i)=Tinit  
25 continue
- c Open files for data input and output  
  OPEN (UNIT=17, FILE=OUTFILE, STATUS='unknown')  
  OPEN (UNIT=16, FILE=INFILE, STATUS='old')
- c Read line by line the data from the infile  
  910 continue  
    read(16,904,end=999) time,Bleft,Bmid,Bright
- c Local output monitoring  
  print\*, time,Bleft,Bright
- c Boundary Conditions for the numerical model  
  uin(1)=Bleft  
  uin(n)=Bright  
  u2in(1)=Bleft  
  u2in(n)=Bright

```

u3in(1)=Bleft
u3in(n)=Bright
u4in(1)=Bleft
u4in(n)=Bright
u5in(1)=Bleft
u5in(n)=Bright
u6in(1)=Bleft
u6in(n)=Bright
u7in(1)=Bleft
u7in(n)=Bright

```

- c Call Crank Nicholson program for each of the different alphas
 

```

call cnstd(dt,n,a1,uin,uout)
call cnstd(dt,n,a2,u2in,u2out)
call cnstd(dt,n,a3,u3in,u3out)
call cnstd(dt,n,a4,u4in,u4out)
call cnstd(dt,n,a5,u5in,u5out)
call cnstd(dt,n,a6,u6in,u6out)
call cnstd(dt,n,a7,u7in,u7out)

```
- c central node is number 51
 

```

nx=51

```
- c Write to file output
 

```

write(17,905) time,Bleft,Bright,Bmid,uin(nx),u2in(nx),u3in(nx),
2u4in(nx),u5in(nx),u6in(nx),u7in(nx)

```
- c Update temperature history
 

```

do 20 i=1,n
uin(i)=uout(i)
u2in(i)=u2out(i)
u3in(i)=u3out(i)
u4in(i)=u4out(i)
u5in(i)=u5out(i)
u6in(i)=u6out(i)
u7in(i)=u7out(i)
20 continue

```
- c Repeat loop for next time step
 

```

goto 910

```
- c Format Lines
 

```

901 format(F4.1,6(F8.3))

```



```
902 format(F4.1)
903 format(F5.1,6(F8.3))
904 format(F8.5,3(2X,F8.5))
905 format(F10.5,10(2X,F10.5))
907 format(4A8,7(2X,F10.5))
999 continue
    close (unit=16)
    close (unit=17)
end
```

## CRANK NICOLSON SOLVER

```
subroutine cnstd(dt,n,a,uin,uout)
```

```
c  subroutine that contains the Crank-Nicolson algorithm (with second
c  order accuracy for spatial derivatives on a uniform grid)

c  dt   = time interval
c  n    = # of grid points (max. = NM)
c  a    = coefficient of RHS of discretized equation
c  uin  = velocity vector at time t
c  uout = velocity vector at time t+dt
c  tridag = subroutine that solves a tridiagonal matrix problem
```

```
PARAMETER (NM=500)
```

```
implicit double precision (a-h,o-z)
```

```
double precision ald(NM),acen(NM),aud(NM),q(NM)
```

```
double precision u(NM),uin(NM),uout(NM)
```

```
alpha=a*dt
```

```
do 10 i=2,n-1
```

```
    ald(i-1)=-alpha/2.
```

```
    acen(i-1)=1.+alpha
```

```
    aud(i-1)=-alpha/2.
```

```
    q(i-1)=alpha/2.*uin(i-1)-(alpha-1.)*uin(i)+alpha/2.*uin(i+1)
```

```
    if (i.eq.2) then
```

```
        q(1)=q(1)+alpha/2*uin(i)
```

```
    else if (i.eq.n-1) then
```

```
        q(n-2)= q(n-2)+alpha/2*uin(i)
```

```
    endif
```

```
10 continue
```

```
call tridag(ald,acen,aud,q,u,n-2)
```

```
uout(1)=uin(1)
```

```
do 20 i=2,n-1
```

```
    uout(i)=u(i-1)
```

```
20 continue
```

```
uout(n)=uin(n)
```

```
return
```

```
end
```

## TRI-DIAGONAL SOLVER SUBROUTINE

```
subroutine tridag(a,b,c,r,u,n)
```

- c Subroutine that inverts the linear system  $A b = c$ , where A is a
- c square, tridiagonal matrix
  
- c  $n$  = # of grid points (max. = NM)
- c  $a$  = vector of under-diagonal terms of matrix A
- c  $b$  = vector of diagonal terms of matrix A
- c  $c$  = vector of over-diagonal terms of matrix A
- c  $q$  = vector of known terms (RHS of lin. sys.)
- c  $u$  = vector of unknowns

```
parameter (NM=2000)
implicit double precision(a-h,o-z)
double precision a(n),b(n),c(n),u(n),r(n)
double precision bet,gam(NM)
integer j,n
```

```
if(b(1).eq.0.) pause 'tridag: rewrite eqns'
bet=b(1)
u(1)=r(1)/bet
do 11 j=2,n
    gam(j)=c(j-1)/bet
    bet=b(j)-a(j)*gam(j)
    if(bet.eq.0) pause 'tridag: error'
    u(j)=(r(j)-a(j)*u(j-1))/bet
11 continue
do 12 j=n-1,1,-1
    u(j)=u(j)-gam(j+1)*u(j+1)
12 continue

return
end
```

## REFERENCES

1. Cote A. And Bugbee, P., Principles of Fire protection, National Fire Protection Association, ST-1, 1988.
2. Fire-fighting Foams and Foam Systems, National Fire Protection Association SPP-44, 1977.
3. Kraynik, A.M. and Reinelt, D.A., Simple Shearing Flow of a 3 D Foam, National Institute of Standards and Technology, Gaithersburg, MD, 1992.
4. Wilder, I., A New Kit for Field Testing of Protein Foam, Fire Journal, January 1970.
5. Chubb National Foam literature, National Foams Environmental Products, Exton, PA, 1995.
6. Ladwig, T.H., Industrial Fire Prevention and Protection, Van Nostrand Reinhold, New York, 1991.
7. Tuve, R.L., Principles of Fire Protection Chemistry, National Fire Protection Association, Boston, MA, 1976.
8. Incropera, F.P. and DeWitt, D.P., Fundamentals of Heat and Mass Transfer, 3rd., John Wiley and Sons, New York, 1981.
9. Valve specification for Metering Valve MFV#6, Cole Palmer Instrument Co., Vernon Hills, IL, 1996.
10. Van Wylen, G.J. And Sonntag, R.E., Fundamentals of Classical Thermodynamics, 3rd., English/SI Version, John Wiley and Sons, New York, 1986.
11. Press, W.H., Flannery, B.P., Teukolsky, S.A., and Vetterling W.T., Numerical Recipes -- The Art of Scientific Computing (FORTRAN version), Cambridge, New York, 1990.
12. Kennedy, W.L., An IBM 650 Computer Program for Determining the Thermal Diffusivity of Finite-Length Samples, United States Atomic Energy Commission Research and Development Report, Ames Laboratory at Iowa State University of Science and Technology, 1960.
13. Jaluria Y. And Torrance K.E., Computational Heat Transfer, Hemisphere Publishing Corporation, Washington, 1986.

14. Strauss, W.A., Partial Differential Equations -- An Introduction, John Wiley and Sons, New York, 1992.
15. Scheuer, J.T. [et. Al.], Coaxial Plasma Thruster -- Performance of a Quasi-Steady, Multi megawatt, Coaxial Plasma Thruster, NASA Publication NAS1.26:195311, 1994.
16. Dhal, M.D., Aeroacoustics of Supersonic Coaxial Jets Noise Reduction, NASA Publication NAS1.15:106782, 1994.
17. Stoker, J.J. Water Waves -- The Mathematical Theory with Application, Interscience Publishers Inc., New York, 1957.
18. Zaller, M. M., and Klem M.D., Coaxial Injector Spray Characterization Using Water/Air as Stimulants, Liquid Propellant Rockets - Fuel Systems, NASA Publication NAS1.15:105322, 1991.
19. Schmidt, S.R. and Launsby, R.G., Understanding Industrial Designed Experiments, 3rd., Air Academy Press, Colorado, 1991.
20. DeVor, R.E., Chang, T., and Sutherland, J.W., Statistical Quality Design and Control -- Contemporary Concepts and Methods, Macmillan Publishing Company, New York 1992.
21. National Foam, Field Catalog, *Introduction to Foam*, 1987.
22. Wilson, A. J., *Foams: Physics, Chemistry and Structure*, Springer Verlag, New York, 1989.
23. Colletti, D. J., "Quantifying the Effects of Class A Foam in Structure Firefighting: The Salem Tests," *Fire Engineering*, Vol 146, No2, February 1993, pp 41-44.
24. NFPA Publication SPP-44, Fire-fighting foams and other systems.
25. Rochna, R. R., "Foam on the Range," *Fire Chief*, Vol 38, No 6, June 1994, pp 34-38.
26. Boyd, C., "Fire Protection Foam in a Radiative Environment," Ph.D. Dissertation, University of Maryland, 1996.
27. Siegel, R, and J. R. Howell. *Thermal Radiation Heat Transfer*, 3rd Edition, Hemisphere Publishing Corporation, USA, 1992.

- 28 Gopalnarayanan, S., et al., "Issue and Techniques Associated with the Measurement of Properties of Fire Protection Foams," NISTIR 5904, October 1996, U.S. Department of Commerce, NIST, Gaithersburg, MD.
- 29 Wang, S. H., "Generation and Characterization of a Fire Protection Foam," M.S Thesis, University of Maryland, 1997.

NIST-114  
(REV. 11-94)  
ADMAN 4.09

U.S. DEPARTMENT OF COMMERCE  
NATIONAL INSTITUTE OF STANDARDS AND TECHNOLOGY

(ERB USE ONLY)	
ERB CONTROL NUMBER	DIVISION
PUBLICATION REPORT NUMBER	CATEGORY CODE
NIST-GCR-98-742	
PUBLICATION DATE	NUMBER PRINTED PAGES
March 1998	

## MANUSCRIPT REVIEW AND APPROVAL

INSTRUCTIONS: ATTACH ORIGINAL OF THIS FORM TO ONE (1) COPY OF MANUSCRIPT AND SEND TO THE SECRETARY, APPROPRIATE EDITORIAL REVIEW BOARD.

TITLE AND SUBTITLE (CITE IN FULL)

Fire Protection Foam Thermal Physical Properties

CONTRACT OR GRANT NUMBER

60NANBD0073

TYPE OF REPORT AND/OR PERIOD COVERED

June 1996 - July 1997

AUTHOR(S) (LAST NAME, FIRST INITIAL, SECOND INITIAL)

Tafreshi, A.M., di Marzo, M., Floyd, R. and Wang, S.  
University of Maryland  
Department of Mechanical Engineering  
College Park, MD 20742

PERFORMING ORGANIZATION (CHECK (X) ONE BLOCK)

- ☒ NIST/GAITHERSBURG  
☐ NIST/BOULDER  
☐ JILA/BOULDER

LABORATORY AND DIVISION NAMES (FIRST NIST AUTHOR ONLY)

SPONSORING ORGANIZATION NAME AND COMPLETE ADDRESS (STREET, CITY, STATE, ZIP)

U.S. Department of Commerce  
National Institute of Standards and Technology  
Gaithersburg, MD 20899

PROPOSED FOR NIST PUBLICATION

- |   |  |  |
|---|--|--|
| <input type="checkbox"/> JOURNAL OF RESEARCH (NIST JRES)    | <input type="checkbox"/> MONOGRAPH (NIST MN)                       | <input type="checkbox"/> LETTER CIRCULAR         |
| <input type="checkbox"/> J. PHYS. & CHEM. REF. DATA (JPCRD) | <input type="checkbox"/> NATL. STD. REF. DATA SERIES (NIST NSRDS)  | <input type="checkbox"/> BUILDING SCIENCE SERIES |
| <input type="checkbox"/> HANDBOOK (NIST HB)                 | <input type="checkbox"/> FEDERAL INF. PROCESS. STDS. (NIST FIPS)   | <input type="checkbox"/> PRODUCT STANDARDS       |
| <input type="checkbox"/> SPECIAL PUBLICATION (NIST SP)      | <input type="checkbox"/> LIST OF PUBLICATIONS (NIST LP)            | <input type="checkbox"/> OTHER <u>NIST-GCR</u>   |
| <input type="checkbox"/> TECHNICAL NOTE (NIST TN)           | <input type="checkbox"/> NIST INTERAGENCY/INTERNAL REPORT (NISTIR) |  |

PROPOSED FOR NON-NIST PUBLICATION (CITE FULLY)

☐ U.S.

☐ FOREIGN

PUBLISHING MEDIUM

- ☒ PAPER ☐ CD-ROM  
☐ DISKETTE (SPECIFY) \_\_\_\_\_  
☐ OTHER (SPECIFY) \_\_\_\_\_

SUPPLEMENTARY NOTES

ABSTRACT (A 2000-CHARACTER OR LESS FACTUAL SUMMARY OF MOST SIGNIFICANT INFORMATION. IF DOCUMENT INCLUDES A SIGNIFICANT BIBLIOGRAPHY OR LITERATURE SURVEY, CITE IT HERE. SPELL OUT ACRONYMS ON FIRST REFERENCE.) (CONTINUE ON SEPARATE PAGE, IF NECESSARY.)

This report describes the research performed during the period of June 1996 - July 1997 under a joint research program between the Mechanical Engineering Department of the University of Maryland at College Park and the Building and Fire Research Laboratory of the National Institute of Standards and Technology. The research was conducted in the laboratories of the BFRL by Mr. Robert Floyd and Ms. Shirley Wang, Graduate Research Assistants of the ME Department at the time, under the supervision of Drs. Marino Di Marzo and Ali Tafreshi (ME Dept.-UMCP). This reports summaries result of the masters thesis of Mr. Floyd and Ms. Wang Which were defended in 1997.

KEY WORDS (MAXIMUM OF 9; 28 CHARACTERS AND SPACES EACH; SEPARATE WITH SEMICOLONS; ALPHABETIC ORDER; CAPITALIZE ONLY PROPER NAMES)

compressed air foam; fire fighting foam; fire protection; fire tests; thermal properties

AVAILABILITY

- ☒ UNLIMITED ☐ FOR OFFICIAL DISTRIBUTION - DO NOT RELEASE TO NTIS  
☐ ORDER FROM SUPERINTENDENT OF DOCUMENTS, U.S. GPO, WASHINGTON, DC 20402  
☒ ORDER FROM NTIS, SPRINGFIELD, VA 22161

NOTE TO AUTHOR(S): IF YOU DO NOT WISH THIS MANUSCRIPT ANNOUNCED BEFORE PUBLICATION, PLEASE CHECK HERE.

☐

ELECTRONIC INFORMS